SELECTION AND CHARACTERIZATION OF D-ENANTIOMERIC PEPTIDE LIGANDS FOR POLYGLUTAMINE PROTEINS WITH THERAPEUTIC POTENTIAL FOR POLYGLUTAMINE MISFOLDING DISEASES

Inaugural-Dissertation

zur Erlangung des Doktorgrades
der Mathematisch-Naturwissenschaftlichen Fakultät
der Heinrich-Heine-Universität Düsseldorf

vorgelegt von

Pauline Elisabeth Kolkwitz
aus Berlin

Düsseldorf, März 2022

aus dem Institut für Physikalische Biologie
der Heinrich-Heine-Universität Düsseldorf

Gedruckt mit der Genehmigung der
Mathematisch-Naturwissenschaftlichen Fakultät der
Heinrich-Heine-Universität Düsseldorf

Berichterstatter:
1. Prof. Dr. Dieter Willbold
2. Prof. Dr. Henrike Heise

Tag der mündlichen Prüfung: 05.04.2022

ABSTRACT

A variety of neurodegenerative diseases is caused by protein misfolding. Such misfolding can be triggered by an elongated polyglutamine tract. The elongated polyglutamine tract destabilizes the protein and causes the usually intrinsically disordered protein part to refold into beta-sheet rich structures. Those structures favor amyloid aggregation. During the aggregation process, toxic structures form, inducing cell death and thereby neurodegeneration.

Different types of neurons and brain regions are affected in the nine heritable polyglutamine diseases, depending on the mutated protein. For instance, an elongated polyglutamine tract in the androgen receptor causes spinal bulbar muscular atrophy (SBMA), in which the spinal cells of the anterior horn of lateral ventricle and therefore the motor neurons degenerate.

To this day, there is no causative therapy for the nine polyglutamine misfolding diseases available. A therapeutic agent that stabilizes the native structure of the polyglutamine protein through binding the polyglutamine tract would be a promising approach. To find such polyglutamine ligands, a mirror image phage display was performed. In this method a D-enantiomeric target is presented to a phage library with randomized peptides fused into their capsid protein. Thereby, this method enables to identify D-enantiomeric peptide ligands of L-enantiomeric polyglutamine proteins. In contrast to L-enantiomeric peptide therapeutics, D-enantiomeric peptide compounds are metabolically more stable and less immunogenic.

In this study mirror image phage display selections were performed with a D-enantiomeric general polyglutamine target and a D-enantiomeric fragment of the androgen receptor containing a polyglutamine tract. Several D-enantiomeric peptide compounds were identified this way and tested with respect to their aggregation inhibiting properties in Thioflavin T (ThT) experiments.

QF2D-2, an all-D peptide compound that was selected on the androgen receptor fragment, decelerated the aggregation of the androgen receptor fragment with an elongated polyglutamine tract, even under seeding conditions. QF2D-2 also bound to the general polyglutamine protein in surface plasmon resonance (SPR) measurements and even decelerated its aggregation. QF2D-2 could be a D-enantiomeric peptide drug candidate for SBMA therapy or even all nine polyglutamine misfolding diseases.

5

KURZFASSUNG

Verschiedene neurodegenerative Erkrankungen werden durch Proteinfehlfaltung verursacht. Eine mögliche Ursache für solche Fehlfaltungen ist ein verlängerter Polyglutamintrakt, der die Struktur des Proteins destabilisiert, sodass sich der, üblicherweise intrinsisch ungefaltete, polyglutaminhaltige Teil des Proteins in betafaltblattreiche Strukturen umfaltet. Dies begünstigt amyloide Aggregation. Im Zuge dessen bilden sich toxische Strukturen, die zur Neurodegeneration führen. Welche Nervenzellen degenerieren ist abhängig vom mutierten Protein, so führt beispielsweise ein verlängerter Polyglutamintrakt im Androgenrezeptor zur spinobulbären Muskelatrophie (SBMA) bei der die spinalen Vorderhornzellen degenerieren, was zum Abbau der Motorneuronen führt.

Bis heute ist keine ursächliche Therapie für die neun Polyglutaminfehlfaltungs-erkrankungen verfügbar. Ein vielversprechender Ansatz für eine wirksame Therapie ist die Stabilisierung der nativen Polyglutaminstruktur mit Liganden des Polyglutamin-traktes. Um solche Liganden zu finden, wurde eine Mirror- Image- Phage- Display-Selektion durchgeführt. Bei dieser Methode wird ein D-enantiomeres Zielprotein einer Phagenbibliothek präsentiert, in deren Hüllprotein randomisierte Peptide eingebaut werden. So können D-enantiomere Peptidliganden für Polyglutaminproteine gefunden werden. Im Gegensatz zu L-enantiomeren Peptidtherapeutika, sind D-Peptide metabolisch deutlich stabiler und weniger immunogen.

In dieser Studie wurden Mirror- Image- Phage- Display- Selektionen auf einem universellen D-enantiomeren Polyglutamintarget und dem D-enantiomeren Fragment des Androgenrezeptors, das einen Polyglutamintrakt enthielt, durchgeführt. Auf diese Weise wurden verschiedene D-enantiomere Peptidkandidaten selektiert, die in Thioflavin T (ThT) Experimenten auf ihre Aggregationshemmenden Eigenschaften getestet wurden.

Das auf dem Androgenrezeptorfragment selektierte D-Peptid QF2D-2 verzögerte die Aggregation des Androgenrezeptorfragments mit verlängertem Polyglutamintrakt, auch unter geseedeten Bedingungen und zeigte sogar in Aggregations- und Surface plasmon resonance (SPR)-Bindungsstudien mit dem universellen Polyglutaminprotein einen Effekt. QF2D-2 könnte ein D-enantiomerer Peptidwirkstoffkandidat für SBMA oder im Optimalfall alle neun Polyglutaminfehlfaltungserkrankungen sein.

SBMA- spinal bulbar muscular atrophy

ThT- Thioflavin T

SPR- Surface plasmon resonance

FRAXA- Fragile X syndrome

FXTAS- Fragile X-Associated Tremor/Ataxia Syndrome

PolyQ- polyglutamine

EGF- epidermal growth factor

ATP- adenosine triphosphate

SOD1- Superoxide dismutase 1

Q- Glutamine

ssNMR- solid state nuclear magnetic resonance

GST- glutathione S-transferase

PolyP- polyproline

YFP- yellow fluorescent protein

AD- Alzheimer's disease

PD- Morbus Parkinson

HD- Huntington's chorea

ALS- Amyotrophic lateral sclerosis

RNA- ribonucleic acid

SCA- spinocerebellar muscular atrophy

DRPLA- dentatorubral-pallidoluysian atrophy

ER- endoplasmic reticulum

DNA- desoxyribonucleic acid

LHRH- Luteinizing Hormone Releasing Hormone

siRNA- small interfering RNA

shRNA- small hairpin RNA

ssDNA- single stranded DNA

TFA- Trifluoroacetic acid

HFIP- Hexafluoroisopropanol

PBS- phosphate buffered saline

TBS- Tris buffered saline

CM- carboxymethylated dextran

FC- Flow cell

TBS-T Tris buffered saline with Tween20

CD- Circular dichroism

NaAc- sodium acetate

TS- Target selection

ES- Empty selection

DC- Direct control

NGS- Next generation sequencing

TSAT- Target sequence analysis tool

mHTT- Mutant huntingtin

ASO- antisense oligonucleotide

1. INTRODUCTION

1.1. TRINUCLEOTIDE REPEAT DISORDERS

Several genetic disorders belong to the trinucleotide repeat disorders which are characterized by the expansion of a trinucleotide repeat over a certain threshold. This destabilizes the protein and interferes with its physiological function. The affected trinucleotide repeats are prone to be elongated during the meiosis, leading to highly variable phenotypes and severities, depending on the repeat length. The disease's phenotype depends on the affected protein, ranging from X-linked mental retardation syndromes like Fragile X syndrome (FRAXA) to neurodegenerative diseases such as Fragile X-Associated Ataxia Syndrome (FXTAS). Nine out of the sixteen known trinucleotide repeat disorders are caused by the expansion of a polyglutamine region, referred to as polyglutamine diseases [1]. This thesis is focused on these polyglutamine diseases.

1.2. GLUTAMINE

Glutamine is an amino acid which is encoded by the CAG or CAA triplet [2]. It is commonly abbreviated as Gln or Q [3]. Glutamine is a not very reactive, polar amino acid that does not ionize [4]. The amide groups are labile at extremely low pH and if they are exposed to heat [4]. The N-term can become cyclic in a spontaneous way. If glutamine is deamidated it will become glutamate [4].

Several proteins contain sections with a number of consecutive glutamines. These proteins are referred to as "polyglutamine proteins" or "polyQ proteins". Interestingly, polyglutamine proteins are unique to eukaryotic cells where they make up 0.1 % of all proteins. In contrast polyglutamine proteins cannot be found among prokaryotes or archaea [2].

About 10.5% of the slime mold *D. discoideum's* proteins contain a polyglutamine tract, which makes it the living being with the most polyglutamine proteins. The human proteome contains more than 60 polyglutamine proteins, which corresponds to 0.34% of it [2, 5].

Another common amino acid that forms poly amino acid tracts is alanine. Polyglutamine and polyalanine tracts share some common features. Both are often coiled coil regions or helices [6, 7]. It was found that coiled-coil regions often continued C-terminally of the polyglutamine tract, whereas an alpha-helix is often found N-terminally of the polyglutamine tract [7]. It follows that the polyglutamine tract containing part of the protein is usually unstructured [7]. It is postulated that the polyglutamine tract is promoting or stabilizing protein-protein interactions [2, 8]. To do so, the coiled-coil polyglutamine section extends its neighboring coiled-coil region to promote the interaction with other unstructured proteins [2]. This is supported by the finding that polyglutamine proteins do have more interaction partners than an average protein [2].

Polyglutamine proteins are known to be important for transcriptional regulation and are therefore often located in the nucleus [9-11]. Among the interaction partners are many nuclear proteins associated to hormone receptors, epidermal growth factors (EGFs), zinc finger proteins, adenosine triphosphatase (ATPase) associated proteins, ubiquitin and MH1 domains [2].

Polyglutamine proteins like huntingtin are also involved in stress induced autophagy [12]. It is known that polyglutamine proteins interact with beclin1 and affect the proteasome and autophagy system [13].

Polyglutamine sections are often structurally instable as water is a poor solvent for them [7, 14]. If polyglutamine is dissolved in aqueous buffer it forms collapsed structures [14].

Polyglutamine proteins can be cellular sensors for pH, temperature or stress and thereby modulate transcription through altered interaction with transcription factors. Alternations of the polyglutamine tract and its shift to aggregation can also be a transcription modulator [15].

1.4. PROTEIN FOLDING

Proteins need to be folded into their native structures to fulfil their physiological function. This takes place in aqueous surrounding or lipids [4]. The folding of a protein is induced by the intramolecular interaction of its amino acid residues. These can be covalent interactions between cysteines, repulsion effects due to electron orbitals that cannot overlap, electrostatic interactions that can be short- or long ranged depending on the strength of the repulsion or attraction, van-der-waals interactions, hydrophobic interactions and hydrogen bonds [4]. All these interactions affect the position of the single amino acid residues finding there energetically optimal position via a trial and error process [16]. The native conformation of the protein is favored in this process because it usually is the energetically most advantageous conformation [16].

In aqueous solutions the folding process is promoted by the collapse of hydrophobic amino acid residues into the inside of the molecule, secondary structures and covalent bonds are formed and the native conformation is accomplished via intermediate states [17].

In cells these intermediates can be stabilized by chaperones, which assist many proteins in order to fold correctly [17-20]. Chaperones shield hydrophobic amino acid residues that would be exposed in the unfolded state or during the folding process until they are hidden in the folded protein [21, 22]. So the folding depends on the environment which can differ between different cellular compartments [16]. *In vivo* the protein folding can start before the translation is finished [17].

1.5. PROTEIN AGGREGATION

As discussed before, protein folding is a complex process. Various factors can influence the folding or misfolding of a protein, such as the contact with interaction partners [23]. But the possible interactions are limited by external factors [24].

For many proteins more than just one conformation is possible and there are alternative conformations that might also be native or can be considered as misfolded. These misfolded proteins might be prone to aggregation [25]. Therefore, folding and aggregation of proteins are often considered to be competing mechanisms [26]. Aggregating proteins are strikingly often natively unstructured proteins or protein parts that refold into beta sheets [8, 27, 28]. It is thought that covalent binding might be involved in some aggregation processes, but the exact mechanism is still unidentified [29]. It is known that regions with a lot of hydrophobic amino acid residues, few polarity and an enhanced tendency to form beta sheets tend to aggregate with a higher frequency [27].

The aggregation process is usually divided in three distinct phases. The first one is the lag phase. The lag phase is the time needed until the primary nucleation process, namely the accumulation of monomers into small, soluble oligomers takes place [30]. These oligomers can accumulate into larger aggregates [31]. So the lag phase marks the transition from physiological to non- physiological conformation and is followed by a phase of rapid growth [31]. The growth phase is determined by fibril growth through monomer recruitment and secondary nucleation [30]. During the secondary nucleation, proteins bind to the fibril surface. They can form local clusters that adapt to the fibril structure. When these structures reach a sufficient size, they can dissociate from the fibril and function as a new, growing fibril [24]. Another example of secondary nucleation is the fragmentation of larger aggregates that keep growing afterwards [32]. This increase in fibril quantity stops when the equilibrium between growth and dissociation is reached or if monomer depletion limits further exponential growth, both options are referred to as the steady state phase. It follows that the fibril formation process can be divided into 1. nucleation 2. elongation and 3. equilibrium [30]. The first step is a slow process, whereas the second is comparatively fast. If the amount of formed aggregates is monitored and plotted it can be fitted with a sigmoidal fit [30].

The most popular aggregate structure is the amyloid fibril. Common features of amyloid fibrils are a cross-beta sheet as quartary structure and insolubility [33, 34]. Amyloid conformagtions can be promoted by a prion-like mechanism [35, 36]. But the ability to aggregate and seed strongly depends on the external conditions like pH, salt concentration and temperature [37-40]. The aggregate's morphology is also highly dependent on the amyloid protein [41].

As an example, Matsumoto at al [41] found that mutant superoxide dismutase 1 (SOD1) forms distinct, porous aggregates through which other proteins can diffuse into the center of the aggregate. In contrast to that, polyglutamine proteins formed intracellular, cytoplasmic and nuclear aggregates with a dense core and a surface that can interact with chaperones and recruits other proteins like transcription factors [41]. In contrast to other aggregates, those formed by polyglutamine proteins are not completely soluble in formic acid. The bigger aggregates dissociate into oligomers but those do not dissociate into monomers [29].

1.5.1.1. Aggregation of polyglutamine proteins

Polyglutamine proteins are intrinsically disordered due to their homopolimery and their polar sidechains [42]. In a bigger protein context like huntingtin or ataxin-3, polyglutamine tracts can exist in different conformations [43, 44].

Pure polyglutamine proteins

Disaggregated polyglutamine proteins consisting of a pure polyglutamine chain not longer than 44 Qs are initially in the random coil conformation at neutral pH [45], since the random coil conformation is the preferred state of the polyglutamine monomer. But if the polyglutamine protein is incubated at 37° C for some time it refolds into beta-sheets [45]. As mentioned before, water is a poor solvent for polyglutamine proteins [42]. Due to that they form collapsed structures in aqueous buffers although glutamine is a polar amino acid. In fact water is such a poor solvent for polyglutamine proteins that pure polyglutamine chains with more than 15 glutamines are insoluble in aqueous buffers [45, 46]. If the glutamine chain is flanked by highly polar lysines, it

becomes soluble in water [45]. The collapse of polyglutamine proteins in aqueous solutions is promoted by intrabackbone interactions [14, 42]. With increasing glutamine number the compactness of the peptide increases as well [47]. Backbone-backbone interactions become more probable, which are known to be typical interactions in beta-sheets. Polyglutamine proteins form a beta hairpin this way. The glutamine sidechains strongly interact with the side chains of other glutamines, which promotes the formation of oligomers and later aggregates [48].

Aggregation mechanisms of polyglutamine proteins

Prior to fibril formation, the polyglutamine protein monomers form intermediary oligomers that accumulate into larger aggregates [49-51]. The fibrils then keep growing via monomer recruitment [31, 52]. In order to be recruited, the monomer must form a beta-hairpin before it can be annexed by the fibril [48]. Interestingly, small, distinct aggregates recruit more effectively than bigger ones [45].

Polyglutamine proteins can aggregate in different ways. Not only amyloid fibrils can form during the aggregation process, amorphous aggregates, smaller spherical structures and off-pathway oligomers were also observed [49, 53-58]. Analogous to the aggregation of other amyloid proteins, the polyglutamine induced aggregation can be divided into three phases. The lag phase marks the thermodynamically unfavorable transition from native to non-native conformation and is therefore the slowest and rate limiting step. It is followed by a phase of rapid growth due to the elongation of the formed fibrils [31]. At some point equilibrium between monomer and soluble polymers is reached [55, 59, 60].

Polyglutamine monomers organize into oligomers with heterogeneous structures [61, 62]. Soluble, linear aggregates without a distinct secondary structure have been described [60], as well as monomers that form spherical oligomers evolving into protofibrils that later become fibrils with rough ends [56]. Oligomers can be highly variable in size. Sizes ranging from dimer up to oligomers composed of several hundreds of monomers have been observed [49, 63-65]. Vitalis et al [66] observed polyglutamine proteins to form unstructured dimers at the start of the aggregation process. The

aggregate morphology and characteristics are dependent on the temperature and the concentration [45, 67], whereas the aggregation kinetics is dependent on the exact conformation of the monomer [66].

Polyglutamine fibrils

Most of the fibrils formed by polyglutamine proteins can be described as typical amyloid fibrils [53, 68]. They show ThT and congo red activity, typical features of amyloid fibrils [45, 69]. The amyloids form in a nucleated growth mechanism [70]. The critical nucleus's size depends on the length of the glutamine chain [52, 71]. Proteins with longer polyglutamine tracts form amyloid fibrils spontaneously. This cannot be observed for glutamine chains shorter than 20. But those can be involved in secondary nucleation mechanisms. Short Polyglutamine chains with flanking lysines with 25-32 Qs were described to form aggregates spontaneously with an elongated lag and elongation phase [45].

The beta structured aggregates are stabilized by hydrogen bonds between the glutamine sidechains. Chen et al [69] observed that polyglutamine proteins form amyloid fibrils with a high beta content. They observed two fibril types: a ribbon-like structure, or seldom, intertwined fibrils. Some experimental results indicate that the aggregate structure could be described as a "steric zipper". As an example, solid state nuclear magnetic resonance (ssNMR) measurements suggested that the fibril core may be composed of two structurally distinct interlocked beta-sheets, leading to an internal polymorphism, as it might contain differently structured monomers, which would mean that two distinct conformers coassemble in the fibril core [48].

Like other amyloid proteins, the fibrils formed by polyglutamine proteins are able to seed, even between different polyglutamine lengths [45, 72]. If the seed amount equals 5% of the monomer mass, the lag phase becomes undetectably short [45].

Iuchi et al [29] observed that the aggregates formed by polyglutamine proteins are insoluble in formic acid. They concluded that polyglutamine aggregates must be stabilized by covalent bonds. Possibly, the transglutaminase is involved in this process.

Aggregation of proteins containing polyglutamine tracts

The aggregation of polyglutamine proteins is highly dependent on the protein context in which the polyglutamine tract can be found and on the number of glutamines [49, 68, 73]. Folded proteins are not as prone to aggregation as unfolded ones, but if the glutamine tract is long enough they will also aggregate [73]. It is known that the polyglutamine tract is the driving force of the aggregation because even non-aggregating proteins can be impelled to aggregate by introducing a sufficiently long glutamine tract into the protein [73]. This also works in the opposite way, an aggregation prone polyglutamine tract can be stabilized by the addition of a large, folded protein like GST [68]. The regions flanking the polyglutamine tract have the highest impact on its aggregation behavior. A C-terminal polyP region reduces the aggregation propensity and impedes the aggregate stability [74]. Another example is the exchange of hydrophobic amino acid residues with charged ones in the N-terminal domain of the huntingtin protein. As this eliminates the inaccessibility of intermolecular sidechains, the formation of oligomers is no longer favored [75]. The flanking sequences are also known to affect the fibril's morphology [76, 77].

Since there are a lot of polyglutamines in the eukaryotic proteome, it can happen that amyloid fibrils form *in vivo* [68]. A commonly known example of an *in vivo* aggregating protein is huntingtin which readily aggregates if its polyglutamine tract exceeds 46 glutamines [78]. It has been described that huntingtin forms amyloid fibrils via alpha helix rich oligomers [55]. The fibril structure is similar to the one of pure polyglutamine fibrils [48]. It was observed in three dynamic states in cells: fast diffusion, dynamic clustering and stable aggregation [79]. The aggregation phases described before can also be observed *in vivo* as well as a fourth phase that is marked by the sequestration of large aggregates into inclusion bodies [78]. In cells, small oligomers are formed, prior to the large inclusion bodies. These inclusion bodies recruit polyglutamine proteins from the cytoplasm, heavily reducing the monomer concentration in the cell [78]. Several different aggregate species and monomers were found to exist *in vivo* at the same time, when *C. elegans* expressed different glutamine-chains fused with YFP [80].

The aggregation kinetic differs between different polyglutamine proteins. In contrast to huntingtin, the androgen receptor contains a domain that is prone to form amyloid fibrils. This domain interacts with the polyglutamine tract during the aggregation process [81].

The *in vivo* aggregation is also modulated by the interaction with other cellular proteins as was observed for the polyglutamine containing protein ataxin-1. The ataxin-1 aggregation is enhanced if it interacts with other coiled-coil proteins or if it cannot interact with the spliceosome, which is its physiological interaction partner [82, 83]. The polyglutamine tract of the androgen receptor can interact with the transglutaminase which promotes the formation of covalent bonds that stabilize the formed oligomers [29].

1.6. PROTEIN MISFOLDING DISEASES

Proteins that are latently instable can misfold and might be prone to aggregation. The formed aggregates can have a cytotoxic effect [84]. Several neurodegenerative diseases belong to those protein misfolding diseases, such as Alzheimer's disease (AD), Morbus Parkinson (PD), Huntington's chorea (HD), prion encephalopathies or Amyotrophic lateral sclerosis (ALS) [85-87]. Misfolding can be induced through mutation, as it is the case for polyglutamine diseases or familiar AD, or by the slow failure of the proteostasis, due to aging [20, 88-90]. Aggregation is a natural process that is usually prevented by the cellular quality control mechanisms that become more error-prone with increasing age [27].

Two disease mechanisms are possible as a consequence of protein misfolding: Loss of function and toxic gain of function [91-93]. The disease pathology of protein misfolding diseases usually exceeds what would be expected from a loss of function effect [94]. It is a commonly accepted and experimentally supported hypothesis that the misfolded proteins have a cytotoxic effect due to a toxic gain of function [95, 96]. This was shown for AD, PD, ALS, tauopathies, polyglutamine diseases and others [97-102]. The toxic species is still not fully unveiled, but the most probable candidates are soluble oligomers [62, 103-107]. Maybe because they have a reactive surface with exposed

hydrophobic amino acid residues and unpaired beta-strands [108]. Oligomers also have a bigger surface related to their size than fibrils, which makes them more reactive [109]. The hypothesis was also supported by the finding that drug candidates aiming to reduce the Abeta oligomer load, but not the amount of fibrils, lead to a cognitive improvement in the mouse model [110].

The toxic mechanism is still elusive, though. Oligomers were observed to impede the cell membrane [27] and interact with non-natural interaction partners [109, 111]. These interaction partners are mostly metastable proteins with intrinsically disordered regions and less complex amino acid sequences such as RNA binding proteins [109, 111-113].

It is discussed whether the formation of bigger aggregates and inclusion bodies might be a protective mechanism of the cell in order reduce the number of free oligomers [103], whilst others state that fibrils are involved in pathology because they sequester valuable proteins and release oligomers [84, 111].

The aggregates can prevent themselves from being degraded by the proteasome and autophagy systems and trap chaperones [114, 115] which impedes the cellular protein quality control system [84]. Chaperones were also shown to have a neuroprotective effect, as their knock-down increase the progress of HD and AD [20]. The chaperones bind toxic oligomers in order to promote aggregate formation and reduce the oligomer load [116].

As mentioned before, mutation can be the cause of protein misfolding and therefore also the cause of a protein misfolding disease. This is the case for polyglutamine diseases, belonging to the triplet repeat diseases. The protein's misfolding is triggered by an elongated glutamine tract. This happens because the glutamine coding CAG triplet is repeated too often [31, 117]. There is a critical glutamine number threshold for each polyglutamine disorder. If this threshold is exceeded, the affected protein misfolds which is connected to neurodegeneration [31, 118]. In the majority of polyglutamine diseases the respective proteins misfold if they contain more than 35-40 glutamines [118-121].

It is known that the elongated polyglutamine tract is the disease's origin. This is supported by the finding that the incertation of an elongated polyglutamine tract into a non-aggregating protein or the internalization of pure polyglutamine proteins leads to neurodegeneration as well [73, 122]. Today, nine heritable polyglutamine misfolding diseases are known, namely HD, SBMA or Kennedy's disease, spinocerebellar muscular atrophy 1 (SCA1), SCA2, SCA3 or Machado-Joseph disease, SCA6, SCA7, SCA12, SCA17 and dentatorubral-pallidoluysian atrophy (DRPLA) or Haw River syndrome [89, 118, 123-131]. All of these diseases are autosomal, dominant heritable diseases, except for SBMA which is x-linked chromosomal inherited [31, 132, 133]. SBMA is special among the polyglutamine misfolding diseases, not only because it is the only x-linked mutation but also because all other polyglutamine misfolding diseases are inevitably fatal [31].

To this day, no effective therapies are known [118].

The polyglutamine misfolding disease's pathologies differ depending on the affected protein. In HD, the huntingtin contains the elongated polyglutamine tract whereas SBMA is initiated by an elongated polyglutamine tract in the androgen receptor [89, 134]. If an elongated polyglutamine tract is internalized into a natively non-polyglutamine protein *in vivo*, the mice developed a neurodegenerative disease similar to the known polyglutamine diseases [135].

The autopsy of passed away patient's brains showed severe neurodegeneration and cells containing inclusion bodies [134, 136-138]. These inclusion bodies contained amyloid fibrils [68]. The disease's progression is promoted by a prion like mechanism as the misfolded polyglutamine proteins can penetrate other cells and seed aggregation there [72].

Some of the polyglutamine misfolding disease's symptoms can be explained by a loss of function mechanism. It was shown that the knockout of huntingtin in adult mice caused some of the symptoms [139] and also some symptoms of the SBMA are due to androgen insensitivity [140]. But a pure loss of function mechanism cannot explain the whole pathology [141, 142].

Analogous to other protein misfolding diseases, the oligomers are thought to be the toxic species in polyglutamine misfolding diseases. This hypothesis is supported by the fact that the inclusion body load does not correlate with neurodegeneration [143-145]. It is discussed whether the formation of inclusion bodies might be a protective mechanism of the cell to deal with toxic oligomers [103, 146]. The monomer is another possible toxic candidate if it would fold into a toxic conformation. But this seems unlikely as polyglutamine reactive antibodies recognize both polyglutamine proteins with normal and pathogenic glutamine number [31].

It was found that polyglutamine oligomers cause stress in the endoplasmic reticulum (ER) [147-149]. Another hint to toxic oligomers is the fact that DNA damage correlates with the oligomer and protofibril load [150].

The polyglutamine aggregates can interact with several different proteins. Preferred interaction partners are proteins with a high glutamine content interrupted by aromatic amino acids [79]. The oligomers often interact with transcription factors [151]. This interaction and the resulting impediment of the transcription regulation might be one of the toxic mechanisms in polyglutamine diseases which are still not fully understood [151, 152]. Another toxic mechanism might be the damage of nuclear DNA [64, 153], the internalization of other proteins into the aggregates which leads to loss of function effects concerning those proteins [61], interference with the protein quality control system and clearing mechanisms of the cell [154, 155], affection of the endocytosis and microtubule transport [156], impediment of the cell membrane [157, 158] and causation of mitochondrial dysfunction [124, 159].

21

The impediment of gene control systems like transcription factors and gene expression by mutant huntingtin was described by Li et al [79]. Huntingtin aggregates recruit FoxP2 for example, a transcription factor that is important for language development and control of movements in striatal neurons [79]. FoxP2 is also involved in the development of cortical-basal ganglia, which are typically damaged in HD patients [160, 161]. So it could be the case that the toxic gain of function is partially due to the loss of function of recruited transcription factors like FoxP2.

1.8. THERAPEUTIC APPROACHES FOR POLYGLUTAMINE DISEASES

Protein aggregation can be inhibited in different ways, for example by binding of free monomer, binding to monomers participating in primary or secondary nucleation, binding to oligomers to prevent secondary nucleation, binding to fibril ends or bigger aggregates in order to hamper fibril elongation or aggregate growth or binding to the fibril surface to prevent secondary nucleation through fibril fragmentation or surface catalyzed secondary nucleation [30]. The obvious target for the treatment of polyglutamine diseases is the elongated polyglutamine tract as it triggers the fatal misfolding event.

A binding partner of the natively folded polyglutamine tract might shift the equilibrium to the monomer side or raise the threshold of tolerated glutamines [162] by hampering the accumulation of monomers and stabilize the native conformation. So it is a promising approach to find binding partners for polyglutamine regions.

Some polyglutamine proteins, like ataxin-1, aggregate faster if they have contact with their coiled-coil interaction partners. Blocking these interactions might decrease the aggregation [82], which could also be realized by binding to the polyglutamine region. Several approaches targeted the polyglutamine tract. Polyglutamine binding antibodies like 1C2 were shown to inhibit the polyglutamine induced aggregation *in vitro* and *in vivo* [163-168]. Benzothiazoles seemed to be promising drug candidates as well. They inhibited the aggregation *in vitro* and *in vivo*, but failed in the mouse model due to metabolic instability or did not improve the disease phenotype [169].

Other studies targeted polymeric polyglutamine proteins, like oligomers. It was observed for the fibril binding congo red that disruption or prevention of oligomerization improved cell survival [170]. An alternative approach is the enhancement of aggregation in order to accelerate the formation of possibly protective inclusion bodies [171]. Epigallocatechingallate (EGCG) that can be extracted from green tea leaves, inhibited the aggregation of polyglutamine proteins *in vitro* and in vivo [172-174]. Its therapeutic effect is premised on the formation of off-pathway aggregates [173].

Since the disease phenotype is a complex mixture of effects due to loss of function and gain of function, there are also indirect ways to modulate disease onset and progression. It is one possibility to enhance the cell's protein quality control system, e.g. through activation of the proteasome or the autophagy systems [175-177], another to induce some chaperones pharmacologically, which can have a therapeutic effect [178, 179] or use natural osmolytes that work like chemical chaperones [180]. Trehalose activates the macro autophagy and stabilizes elongated polyglutamine [181].

Since the precise combination of cellular effects is different for each polyglutamine disease, the indirect approaches would be specific for one of the nine polyglutamine diseases, like Leuprorelin. It was a very promising candidate for SBMA treatment that even made it to the clinical trials. Leuprorelin is an LHRH agonist and inhibits the testosterone induced accumulation of the androgen receptor in the nucleus. It efficiently treated SBMA in the mouse model [182] but short term studies showed no significant effect in humans [183]. This finding was revised after a longer trial time, in which a decrease in disease progression could be observed [184]. In order to investigate the pharmacological potential of candidates that show their effect so slowly it would be necessary to have good, quantifiable biomarkers for the investigated disease. It would be an improvement of clinical trials for polyglutamine diseases if the oligomer load in blood or spinal fluid could be measured as an objective indicator of disease progression [118].

The latest approach was to test the possible therapeutic effects of gene silencing [185, 186] with antisense oligonucleotides, siRNA or shRNA [118, 187-190]. One drawback of this approach is the selective targeting of the affected allele. There are some approaches to do so but most studies just target both alleles [191-193]. Another problem is the application of nucleic acid therapeutics to the brain. In animal experiments, the adenoviral vectors were stereotaxically injected into the mice's striatum, which is no favorable treatment for human patients [118, 194].

1.9. THERAPEUTIC PEPTIDES

Peptides are suitable as polyglutamine binding partners as well. Such a peptide was found by Nagai et al [195]: QBP1 inhibited the polyglutamine aggregation *in vitro* and also reduced the cytotoxicity of polyglutamine proteins and prevented the formation of oligomers [195-197]. It suppressed neurodegeneration in *Drosophila* [198]. But the uptake from the periphery to the mouse brain proofed to be problematic and no therapeutic effect could be seen in the mouse model [118, 199]. Another polyglutamine binding peptoide is the HQP09 which binds to huntingtin and ataxin-3 and inhibits their aggregation [200]. This peptoide failed in the mouse model as well, possibly because it could not pass the blood brain barrier.

A peptide drug needs the ability to pass from the periphery to the brain and it has to be metabolically stable. L-peptides are readily degraded by the body's metabolic system. In contrast to D-peptides which are not as easily recognized by proteases [201]. This makes D-peptides promising drug candidates.

1.10.1.1. Bacteriophages

Filamentous bacteriophages (commonly known as phages) belong to the viruses [202]. They include some *Inoviridae* as M13 phages, f1 or fd [203-205]. Filamentous bacteriophages can infect gram-negative bacteria that have got an f-pilus, like *Escherichia coli*. These phages can replicate in bacteria without lysing them [206]. The most commonly used phages in phage display are M13 phages [207]. M13 phages are 6.5 nm wide and contain ss-DNA that is coated by a protein envelope [208, 209]. Their genome consists of 11 genes that code for the capsid proteins, DNA replicating proteins and the assembly protein [206].

1.10.1.2. The Method

Phage display is a high throughput screening method to find ligands for defined target molecules [207]. Peptide libraries can be displayed on bacteriophage's surface by including randomized cDNA into the phage genome, a fusion protein of the capsid protein and the peptide is formed in the phage envelope this way [206, 210, 211]. In most cases the peptides are attached to the capsid proteins pIII or pVIII. Libraries with 10^9-10^{10} different peptides can be screened for specific target binders *in vitro* via bio panning [206, 212].

The phage display selection can be divided into two main parts: the selection and the amplification [213]. During the selection an input of phages is incubated with the immobilized target, unbound phages are washed away and the output received this way should contain several target binders. This output is amplified in bacteria and is used as an input for the next round. After several selection rounds the target binders should be enriched [213]. In **Figure 1** the phage display procedure is depicted schematically.

Targets can be presented in different ways: immobilized on a surface, immobilized on magnetic beads or on the surface of cultured cells, even *in vivo* selections are possible [214, 215].
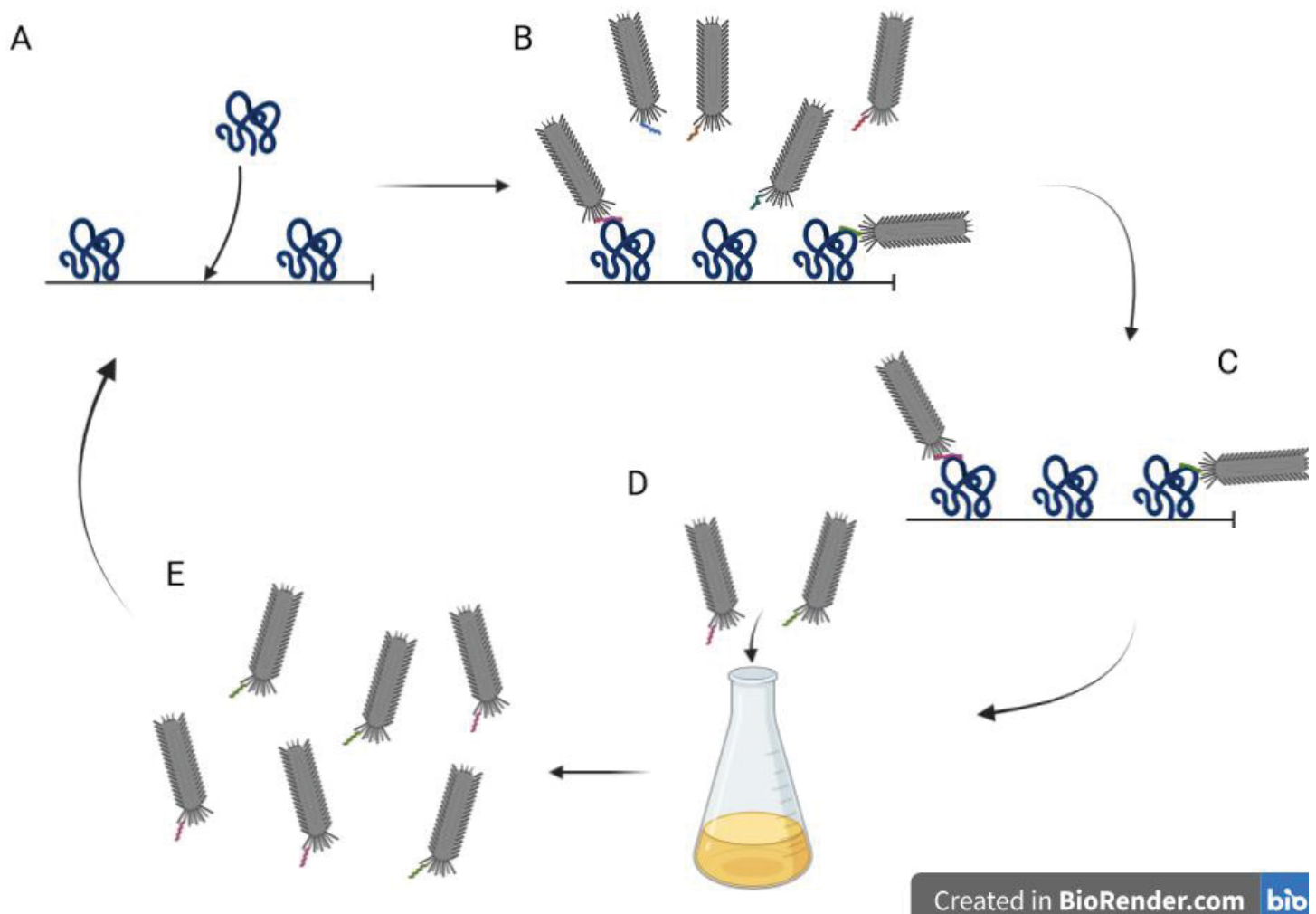
FIGURE 1: Phage display selection procedure

General procedure of a phage display selection. **A** Immobilization of a target protein on the surface. **B** The phage library with M13 phages displaying different randomized peptides on their surface is incubated with the immobilized target. Some of the peptides bind to the target. **C** Unbound phages are washed off. **D** Bound phages were eluted and get amplified with a bacterial culture. **E** Amplified phages are purified and used as input in the next selection round. This figure was created with BioRender (biorender.com).

1.10.1.3. Mirror image phage display

Peptide therapeutics can be degraded by physiological enzymes in the patients [201]. Given that D-peptides are significantly more stable compared to L-peptides, it would be advantageous to select D-peptide ligands for the targets. To this end a phage display selection can be carried out with a D-enantiomeric target. It follows that the "mirror image" of the selected peptide will bind to the native L-enantiomeric target [201, 216, 217]. It was already shown that this is a successful approach for neurodegenerative diseases. The selected D-enantiomeric peptide compound RD2 could improve the cognition and learning ability in a mouse model for Alzheimer's disease after intraperitoneal and even oral administration. So it is possible to find D- peptide compounds that pass the blood brain barrier after periphery administration [110].

2. AIM OF THE STUDY

Polyglutamine diseases are severe, fatal neurodegenerative diseases with no effective treatment available. All nine of these heritable trinucleotide repeat diseases share the same pathogenic mechanism; an elongated polyglutamine tract leading to misfolding and aggregation. A cytotoxic component is formed in this process, leading to neurodegeneration.

This common mechanism gives rise to the idea that one active substance that would inhibit the polyglutamine protein aggregation process might work as an effective treatment in all nine diseases. This compound should impede the sequestration of polyglutamine containing proteins to oligomers and aggregates by stabilizing its native conformation.

It was the aim of this study to find a drug candidate which meets these expectations. To this end a mirror image phage display selection was performed to find specific binders of polyglutamine sequences. The resulting D-peptide compounds were tested with respect to their ability to bind polyglutamine proteins and inhibit their aggregation. Furthermore, it was tested whether the peptide compound's effect was transferrable to other polyglutamine constructs they were not selected on.

3. MATERIALS AND METHODS

3.1. PEPTIDES AND PROTEINS USED IN THIS STUDY

An N-terminal biotin tag was fused to the polyglutamine proteins used as selection targets via a ttds-linker.

TABLE 1: Polyglutamine proteins used in this study

Name	Sequence	Synthesized by
D-K2Q23K2	kkqqqqqqqqqqqqqqqqqqqqqqqkk	JPT*
L-K2Q23K2	KKQQQQQQQQQQQQQQQQQQQQQQQKK	Peptides & elephants°
K2Q46K2	KKQQQQQQQQQQQQQQQQQQQQQQQ QQQQQQQQQQQQQQQQQQQQQQQKK	Peptides & elephants°

* JPT Peptide Technologies GmbH, Berlin, Germany
° peptides & elephants GmbH, Henningsdorf, Germany

The peptide compounds used in this study were synthesized with an amidated C-term.

TABLE 2: Peptides used in this study

Name	Sequence	Synthesized by
QF1D-1[+]	idvwdwwpdmtwqkql	Caslo"
QF1D-2[+]	fswewwphypatdsse	Caslo"
QF1D-3[+]	iewweypewGqwasft	Caslo"
QF1D-4[+]	sfqwwpqfpwqpeysi	Caslo"
QF1D-5[+]	vmewqpwqfnweawdt	Caslo"
QF1D-6[+]	stelafdhwdwewwsv	Caslo"
QF1D-7[+]	ewwpwfqeekwihwey	Caslo"
QF1D-8[+]	feywpmwGgieeGye	Caslo"
QF1D-9[+]	wdmewedwqywwyeek	Caslo"
QF1D-10[+]	mewpypwwsmdmdfpm	Caslo"
QF1D-13	spGtyitkawpeemnw	Caslo"
QF1D-14	mpyeirwtpnhvGdmn	Caslo"
QF1D-15	eheherwGyswhdmqt	Caslo"
QF1D-16	sqhnvffsqpwdrwht	Caslo"
QF1D-17	ikaysqqqnwldhphk	Caslo"
QF1D-18	shlqGhyrqvydpGfs	Caslo"
QF1D-19	hkshGvhpsqspymmi	Caslo"
QF1D-20	ehswvypysqyhwqrG	Caslo"
QF1D-21	dsvlppfilsttnqrs	Caslo"
QF1D-22	hvwkkndhhwepkywp	Caslo"
P8[&]	YDTPKHKDKTWPMM	Caslo"
QBP1[§]	SNWKWWPGIFD	Peptides & elephants°

° peptides & elephants GmbH, Henningsdorf, Germany
"CASLO ApS, Lyngby, Denmark
+ selected by Annika Krüger [218]
& selected by Karoline Santur
§ [195]

3.2. DISAGGREGATION OF POLYGLUTAMINE PROTEINS

It is known that polyglutamine proteins tend to aggregate spontaneously [69]. Therefore it is necessary to ensure that the used protein is in its monomeric state, whenever required. This was achieved by disaggregating the polyglutamine protein prior to usage. Polyglutamine proteins were disaggregated by incubating them overnight in 100% Trifluoroacetic acid (TFA), derived from a published disaggregation protocol [219]. ARQ46 was disaggregated by incubating it in 1:1 TFA/ Hexafluoroisopropanol (HFIP) for three days.

3.3. THIOFLAVIN T (THT)-ASSAYS

ThT-assays are suitable for monitoring the formation of amyloid aggregates. Binding to amyloid fibrils shifts the fluorophore's emission spectrum from 438 nm to 482 nm. Thus, the ThT-active aggregation can be monitored in terms of time and quantity by tracking the fluorescence intensity at 482 nm over time [220]. ThT-assays were performed as described before [221]. For peptides selected by Annika Krüger [218] the assay was performed in phosphate buffered saline (PBS) whereas for peptides selected on the disaggregated targets the assay was performed in Tris buffered saline (TBS). The lag-time was estimated as described elsewere [221].

3.4. SURFACE PLASMON RESONANCE (SPR)

The surface plasmon resonance technique utilizes the formation of surface plasmons when the electrical field energy of the photons of a plane-polarized light beam under total internal reflection conditions interacts with free electron constellations in a gold surface [222]. The surface plasmon resonance angle depends on the refractive index of the media and changes in a linear relationship when biomolecules bind to the surface [222, 223]. Consequently, this technique enables to measure molecular binding quantitatively. But it is necessary to immobilize one of the interaction partners in close proximity to the gold surface.

K2Q23K2 was immobilized on a CM5 chip (carboxymethylated dextran matrix, 100 nm wide) by Annika Krüger [218]. QF1D-1 and QF1D-2 were diluted in running buffer (PBS pH 7.4). The experiment was performed with a flow rate of 45 µl/min. The association time was 180 s, the dissociation time 900 s. Flow cell 1 (FC 1) served as reference which was activated with a 1:1 mixture of 0.05 M N-Hydroxysuccinimide (NHS) and 0.2 M ethyl(dimethylaminopropyl) carbodiimide (EDC) and quenched with 1 M ethanolamine without immobilizing anything [218].

For QF1D-13 and QF1D-14 the running buffer was TBS-T pH 7.5 with 0.05% Tween20. The experiment was performed with a flow rate of 45 µl/min as well. The association time was 110 s, the dissociation time 400 s.

The binding of QF2D-2 to polyglutamine proteins was investigated as was described elsewhere [221].

3.5. CD-Spectroscopy

Circular dichroism (CD) -spectroscopy uses plane-polarized light with opposite polarization. When this trespasses a protein sample, the two polarizations get absorbed differently. The ratio of absorbance determines the elipticity. Secondary protein structures show specific CD-spectra. Therefore, by measuring the elipticity of the respective wavelength range reveals the medium secondary structure of a protein sample [224].

The samples were dissolved in buffer (either sodium acetate buffer (NaAc) pH 6 or 10 mM Tris buffer pH 8). The CD-spectroscopy was performed with a CD spectrometer (J-1100, Jasco Deutschland GmbH, Pfungstadt, Germany) in a quartz crystal cuvette with 1 mm light path (Hellma analytics, Müllheim, Germany) with 5 accumulations. The samples were referenced with a measurement of the respective buffer.

3.6. MIRROR IMAGE PHAGE DISPLAY

The mirror image phage display was performed with D-biotin-K2Q23K2 as was described for D-biotin-ARQ23 [221]. In each selection round, 4 pmol of the target were immobilized in a well of the High capacity streptavidin coated Polystyrene plate with „SuperBlock" by Thermo scientific (Thermo Fisher scientific, Waltham, USA). The selection scheme is depicted in **Figure 2**.
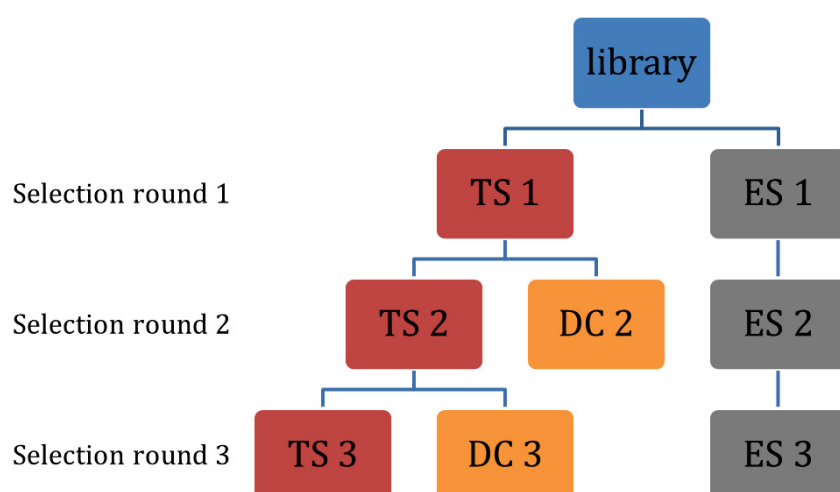
FIGURE 2: Selection scheme

In selection round 1, the Trico16 library served as input for the target selection (TS) on the D-biotin-ttds-K2Q23K2 and the empty selection (ES) on biotin-ttds. The eluted phages were amplified after each selection round and used as input in the next round. The direct control (DC) was performed with the TS input on biotin-ttds.

3.7. PRODUCTION OF SOLUBLE AGGREGATE FRAGMENTS

Soluble aggregate fragments of L-K2Q46K2 were produced as described for L-ARQ46 [221].

4. RESULTS

4.1. CHARACTERIZATION OF PEPTIDE COMPOUNDS SELECTED ON K2Q23K2

The aggregation of polyglutamine containing proteins causes several neurodegenerative diseases. Polyglutamine ligands stabilizing the native conformation would prevent or delay disease onset. To find such ligands, a mirror image phage display selection was performed by Annika Krüger on the D-biotin-K2Q23K2 [218]. Ten peptide compounds resulting from this selection were further characterized in ThT-aggregation assays and binding studies with the SPR technique.

Two peptides had an inhibiting effect on the ThT-active aggregation of K2Q46K2, QF1D-1 and QF1D-2 (**Figure 3**). At 24 h the fluorescence intensity of the sample containing QF1D-1 was 41% of the aggregation control's fluorescence intensity at this time point. QF1D-2 was even more effective, reducing the fluorescence intensity to 9% of that of the aggregation control.

In the aggregation control, aggregation started after a lag time of 2 h. QF1D-1 elongated the lag-time to 3 h and QF1D-2 elongated it by a factor five to 10 h.
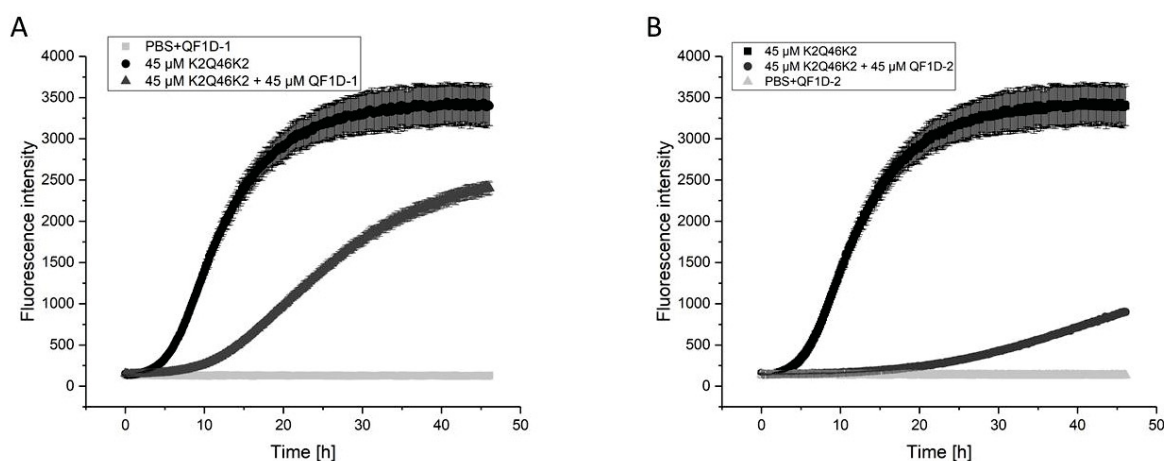
FIGURE 3: QF1D-1 and QF1D-2 inhibit ThT-active aggregation of L-K2Q46K2

ThT-assay with 45 μM K2Q46K2 in PBS pH 7.4 at 37°C with 300 rpm double orbital shaking. Fluorescence intensity was measured at λ_{ex} = 448 nm and λ_{em} = 482 nm every 8 minutes. **A** ThT-fluorescence intensity for 45 μM K2Q46K2 (black), equimolar K2Q46K2 and QF1D-1 (grey) and 45 μM QF1D-1 in PBS (light grey) **B** ThT-fluorescence intensity for 45 μM K2Q46K2 (black), equimolar K2Q46K2 and QF1D-2 (grey) and 45 μM QF1D-2 in PBS (light grey)

To test whether the effect observed in **Figure 3** is concentration dependent, the compounds were tested with K2Q46K2 being present in excess, in equimolar concentration and in sub stoichiometric ratio. Both compounds had a concentration dependent, inhibitory effect (**Figure 4**). When QF1D-1 was present in excess, it reduced the fluorescence intensity at 40 h to 32% of the aggregation control sample's fluorescence intensity. When QF1D-1 and K2Q46K2 were present in equimolar ratio, QF1D-1 still reduced the fluorescence intensity to 44% and even when only 22.5 μM QF1D-1 were mixed with 45 μM K2Q46K2, it still reduced the fluorescence intensity to 69%. The lag time was elongated in a concentration dependent manner as well, whereas K2Q46K2 alone had a lag time of 2.4 h, this was elongated to 4 h when 22.5 μM QF1D-1 were present, to 6.5 h when 45 μM QF1D-1 were there and even to 10 h for the sample containing 90 μM QF1D-1.

QF1D-2 reduced the fluorescence intensity even more then QF1D-1, by 70 % for the sample containing 22.5 μM QF1D-2, 90 % when QF1D-2 and K2Q46K2 were present in equimolar ratio and 93 % for the sample containing 90 μM QF1D-2. In this sample the lag time was elongated to 31.5 h, which equates to an increase by 1313 %.
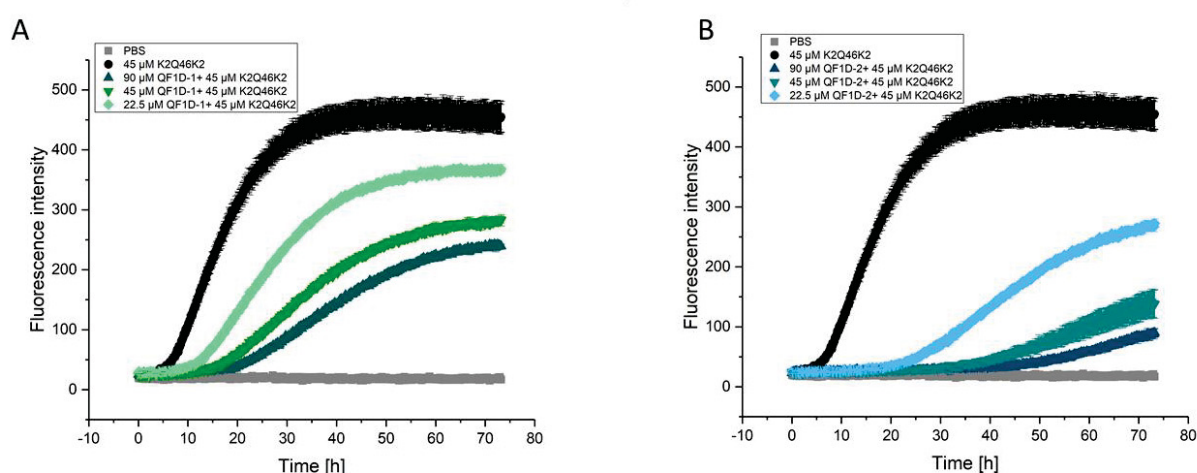

FIGURE 4: QF1D-1 and QF1D-2 inhibit ThT-active aggregation of L-K2Q46K2 in a concentration dependent manner

ThT-assay with 45 μM K2Q46K2 in PBS pH 7.4 at 37°C with 300 rpm double orbital shaking. Fluorescence intensity was measured at λ_{ex} = 448 nm and λ_{em} = 482 nm every 8 minutes. **A** ThT-Fluorescence intensity for 45 μM K2Q46K2 (black), 45 μM K2Q46K2 and 90 μM QF1D-1 (dark green), 45 μM K2Q46K2 and 45 μM QF1D-1 (green) and 45 μM K2Q46K2 and 22.5 μM QF1D-1 in PBS (light green) **B** ThT-Fluorescence intensity for 45 μM K2Q46K2 (black), 45 μM K2Q46K2 and 90 μM QF1D-2 (dark blue), 45 μM K2Q46K2 and 45 μM QF1D-2 (blue) and 45 μM K2Q46K2 and 22.5 μM QF1D-2 in PBS (light blue)

In patients treated with a compound, the main requirement is to inhibit seeded aggregation rather than *de novo* aggregation. To test the compounds ability under those conditions, 1% preformed aggregates were added to the samples. The aggregation was monitored with ThT (**Figure 5**). The addition of seeds eliminated the lag phase of the sample containing 50 μM K2Q46K2 only. QF1D-1 seemed to inhibit the ThT-active aggregation completely, whereas QF1D-2 had a strong inhibiting effect, reducing the fluorescence intensity to 66% of the aggregation control's fluorescence intensity at 40 h. In this sample a lag time of 12.5 h was measured.
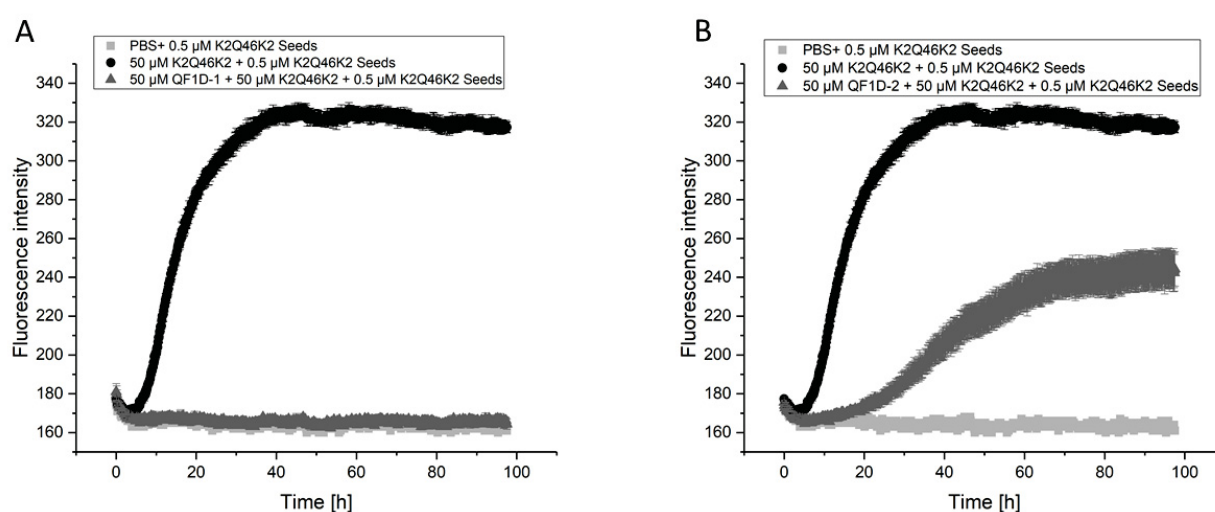
FIGURE 5: QF1D-1 and QF1D-2 inhibit ThT-active aggregation of L-K2Q46K2 in presence of seeds

ThT-assay with 50 μM K2Q46K2 and 1% preformed aggregates in PBS pH 7.4 at 37°C with 500 rpm double orbital shaking. Fluorescence intensity was measured at λ_{ex} = 450 nm and λ_{em} = 480 nm every 7 minutes. **A** ThT-Fluorescence intensity for 50 μM K2Q46K2 with 1% preformed aggregates (black), equimolar K2Q46K2 and QF1D-1 with 1% preformed aggregates (grey) and 0.5 μM preformed K2Q46K2 aggregates in PBS (light grey) **B** ThT-Fluorescence intensity for 50 μM K2Q46K2 with 1% preformed aggregates (black), equimolar K2Q46K2 and QF1D-1 with 1% preformed aggregates (grey) and 0.5 μM preformed K2Q46K2 aggregates in PBS (light grey)

The binding of QF1D-1 and QF1D-2 to the L-enantiomeric general polyglutamine construct K2Q23K2 was investigated using the SPR technique. Both compounds bound to K2Q23K2, although it was not possible to determine a K_D via the affinity fit due to the fact that no saturation was reached (**Figure 6**).

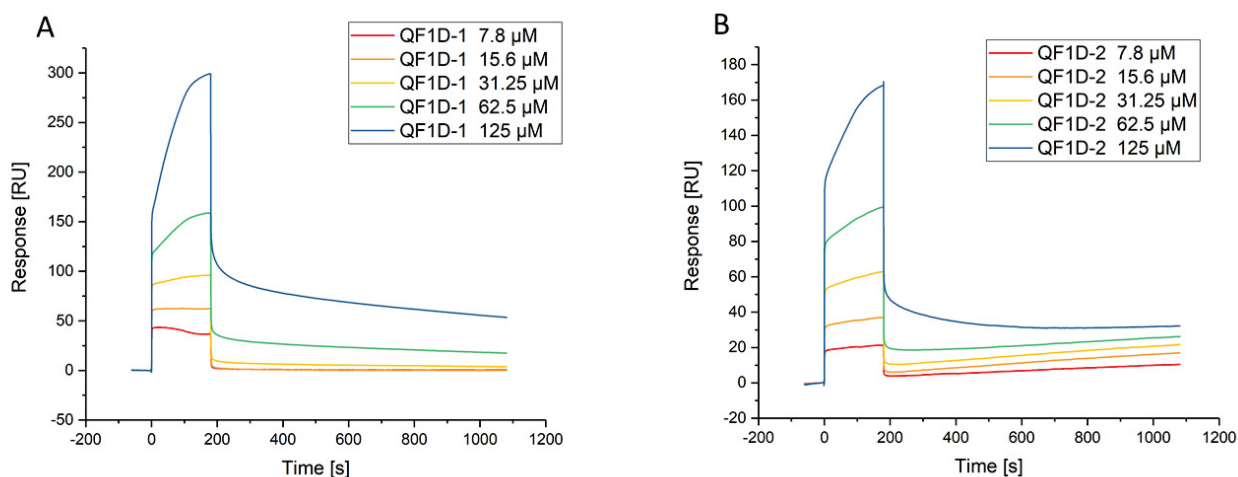**FIGURE 6: QF1D-1 and QF1D-2 bind to L-K2Q23K2**

L-K2Q23K2 was immobilized on a CM5 Chip via amino coupling by Annika Krüger [218]. Using PBS pH 7.4 as running buffer the binding of QF1D-1 and QF1D-2 to K2Q23K2 was investigated with the SPR technique. **A** Binding of QF1D-1 to K2Q23K2 with 125 µM being the highest concentration. **B** Binding of QF1D-2 to K2Q23K2 with 125 µM being the highest concentration.

It was noticed that the compound's effect decreased when the compound stock solution was stored over a longer time period and the concentration of the same sample varied. A size exclusion chromatography was performed to see whether the peptides would elute as expected. The peptide elution had more than one distinct peak, hinting the peptide sample was aggregated.

The peptides were selected on D-K2Q23K2 that was not thought to aggregate at low concentrations due to the lower number of glutamines [52]. Because of that assumption and the promising size exclusion chromatography results at that time, the target was not disaggregated prior to the selection by Annika Krüger [218].

A CD measurement of L-K2Q23K2 dissolved in buffer without disaggregation showed that the sample's secondary structure was beta-sheet (**Figure 7**). So the compounds have likely been selected on polyglutamine in beta-sheet conformation.
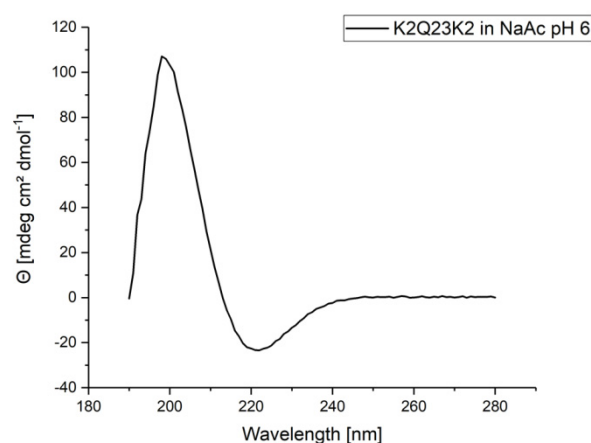

FIGURE 7: CD-spectrum of L-K2Q23K2 dissolved in buffer without prior disaggregation

CD-spectrum of lyophilized L-enantiomeric K2Q23K2 directly dissolved in NaAc buffer pH 6.

QF1D-1 and QF1D-2 were disaggregated with 100% TFA prior to another ThT-assay with monomeric L-K2Q46K2 (**Figure 8**). In this experiment QF1D-1 accelerated the aggregation of K2Q46K2. QF1D-2 still had an inhibiting effect but it was less effective than before, reducing the fluorescence intensity only to 82% of that of the aggregation control at 20 h, compared to the 9% that were observed before. The lag time was elongated by 142%, compared to 400% for the not disaggregated compound.
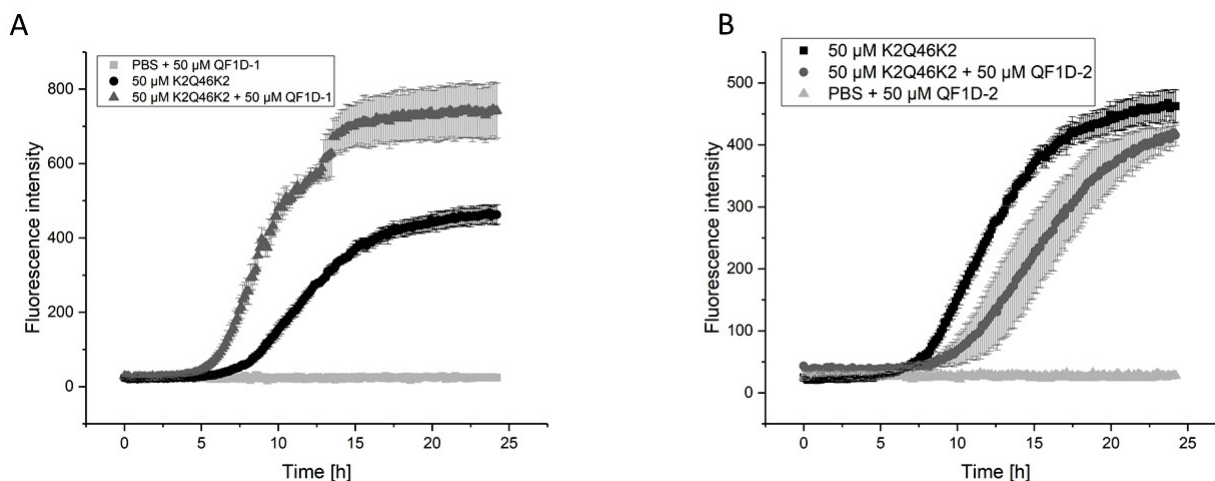
FIGURE 8: Disaggregated QF1D-1 and QF1D-2 modulate the ThT-active aggregation of K2Q46K2

ThT-assay with 50 µM K2Q46K2 in PBS pH 7.4 at 37°C with 300 rpm double orbital shaking. QF1D-1 and QF1D-2 were disaggregated prior to the measurement. Fluorescence intensity was measured at λ_{ex} = 448 nm and λ_{em} = 482 nm every 8 minutes. **A** ThT-Fluorescence intensity for 50 µM K2Q46K2 (black), equimolar K2Q46K2 and disaggregated QF1D-1 (grey) and 50 µM disaggregated QF1D-1 in PBS (light grey) **B** ThT-Fluorescence intensity for 50 µM K2Q46K2 (black), equimolar K2Q46K2 and disaggregated QF1D-2 (grey) and 50 µM disaggregated QF1D-2 in PBS (light grey)

The disaggregation step reduced QF1D-2's effectiveness or even eliminated that of QF1D-1. In a therapeutic context it is also difficult to administer self-aggregating compounds.

4.2. SELECTION AND CHARACTERIZATION OF PEPTIDE COMPOUNDS SELECTED ON D-K2Q23K2

In order to find new compounds that would bind to the monomeric polyglutamine target and stabilize its native conformation, two new mirror image phage display selections were performed with disaggregated targets. D-Biotin-K2Q23K2 served as selection target again, but this time it was disaggregated prior to the selection to ensure a monomeric, not misfolded target. A control sample of the disaggregated target was stored under the same conditions as the target samples. A CD measurement was performed to ensure that the target was still in its native conformation (**Figure 9**). The CD spectrum showed the structure that would be expected for a D-enantiomeric disaggregated polyglutamine protein, so the selection rounds were not performed on a beta-sheet structure.
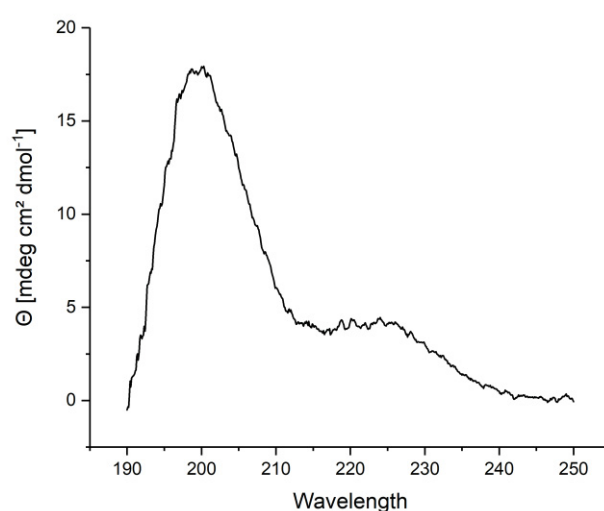
FIGURE 9: CD-spectrum of D-Biotin-K2Q23K2 disaggregated and redissolved in buffer

D-Biotin K2Q23K2 was disaggregated with 100% TFA. TFA was evaporated with N_2 gas treatment and the D-Biotin K2Q23K2 was redissolved in 10 mM Tris buffer pH 8 to a concentration of 50 µM. CD spectrum was recorded with this sample.

The selected sequences were analyzed via next generation sequencing (NGS) and target sequence analysis tool (TSAT) [225]. The clustering tool Hammock [226] was used to find similar motives among the sequences. The sequences were analyzed with respect to the ratio between the sequence's frequency in the target selection compared to its frequency in the empty selection. Whenever the sequence's frequency in the empty selection was zero, half of the most seldom sequence's value in the empty selection was

used for calculation. This ratio was called empty score. Furthermore, the sequence's frequency in the target selection was compared to its frequency in the library, referred to as enrichment factor. If the sequence's frequency in the library was zero, calculation was performed as described for the empty score. Considering the empty score, enrichment factor, cluster size (**Figure 10**) and ratio between target selection and direct control, ten sequences were chosen for further investigation (**Table 3**) in a ThT-assay with soluble aggregate fragments (**Figure 11**).
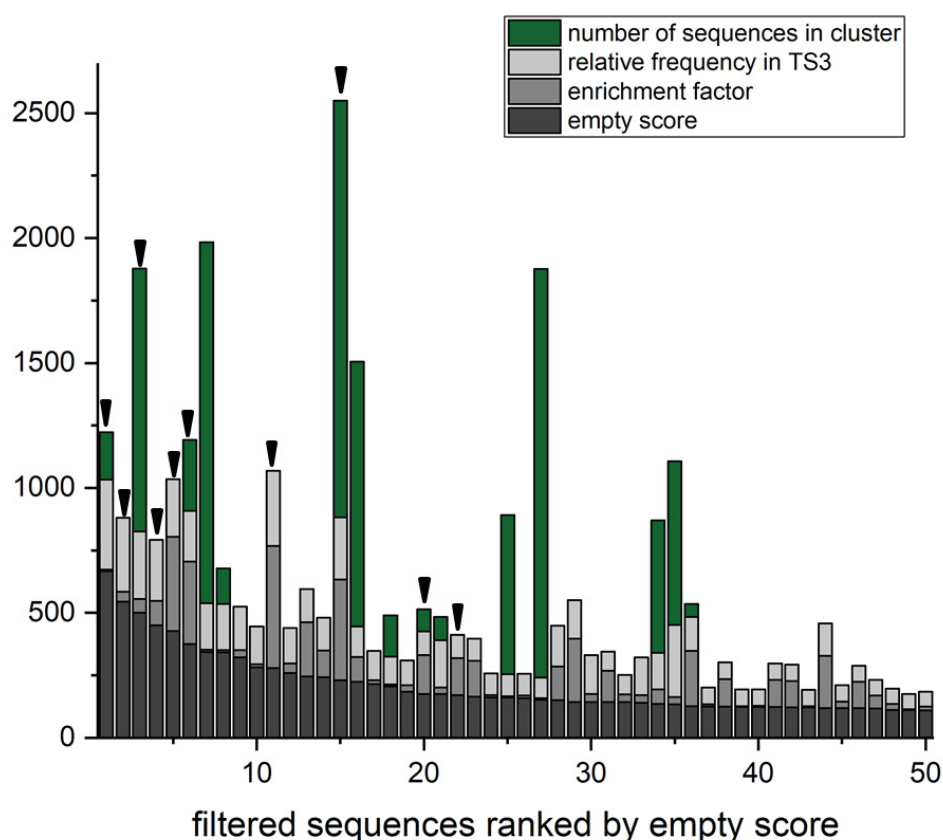
FIGURE 10: Sequences selected on D-Biotin K2Q23K2 ranked by their empty score

Peptides selected on D-Biotin K2Q23K2 were sequenced via NGS and analyzed with TSAT. The 50 sequences with the highest empty scores are depicted also considering the enrichment factor, relative frequency in target selection 3 (TS3) and the number of sequences in a cluster identified with the clustering tool Hammock [226]. Sequences marked with black arrows were further investigated in subsequent experiments.

TABLE 3: Sequences selected on D-Biotin K2Q23K2

Compound	Sequence	Frequence in original library	Number of sequences in cluster	Enrichment factor	TS3/DC3
QF1D-13	spGtyitkawpeemnw	59	189	6	2,1
QF1D-14	mpyeirwtpnhvGdmn	7		40	1,9
QF1D-15	eheherwGyswhdmqt	5	1052	55	1,1
QF1D-16	sqhnvffsqpwdrwht	2		99	2,3
QF1D-17	ikaysqqqnwldhphk	0		376	1,1
QF1D-18	shlqGhyrqvydpGfs	0	284	330	3,9
QF1D-19	hkshGvhpsqspymmi	0		489	2,1
QF1D-20	ehswvypysqyhwqrG	0	1668	403,8	1,3
QF1D-21	dsvlppfilsttnqrs	0	89	155	1,3
QF1D-22	hvwkkndhhwepkywp	0		149	1,8

Selected peptide compounds were pre-incubated with soluble aggregate fragments of L-K2Q46K2. In parallel to the peptide compounds, the soluble aggregate fragments were also incubated with QBP1, an L-enantiomeric peptide compound that is published to inhibit polyglutamine aggregation [195] and with P8, a peptide selected on SOD1 by Karoline Santur that should not bind to polyglutamine. The results for QBP1 were not reproducible between experiments. After 23 h, monomeric L-K2Q46K2 was added and the ThT-active aggregation was tracked (**Figure 11**). QF1D-13 and QF1D-14 had an inhibiting effect. With QF1D-13 and QF1D-14, aggregation onset was delayed compared to K2Q46K2 alone and the fluorescence intensity of the steady state was 78% of the sample incubated with P8 for QF1D-13 at 35 h and 83% for QF1D-14.
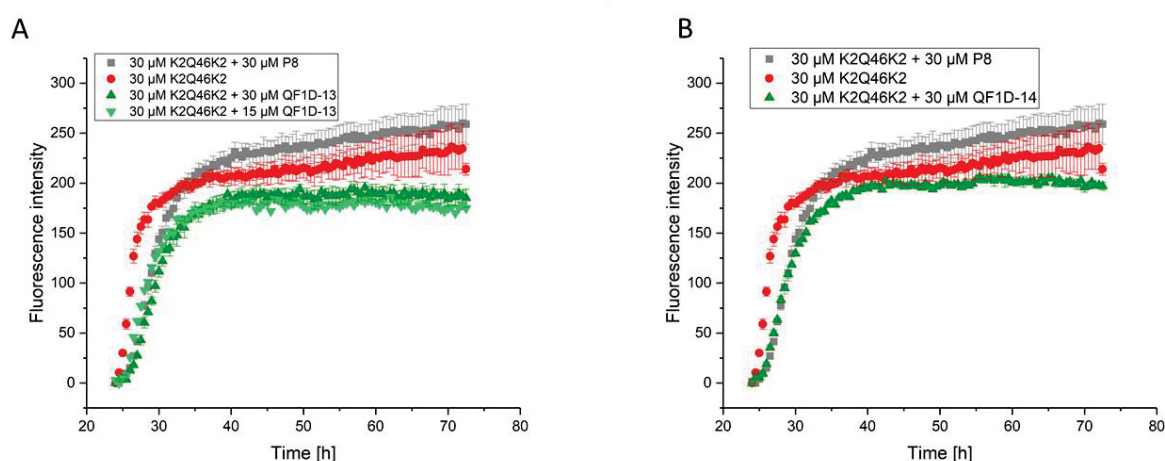
FIGURE 11: QF1D-13 and QF1D-14 decelerate the ThT-active aggregation of K2Q46K2 in presence of soluble aggregate fragments

Aggregated K2Q46K2 was sonicated and centrifuged at 100 000 g for 1 h at 4 °C to remove insoluble aggregates from the solution. The supernatant was incubated with the compounds for 23 h. ThT-assay with 30 μM K2Q46K2 and the preincubated sample in TBS pH 7.5 at 37°C with 300 rpm double orbital shaking. Fluorescence intensity was measured at λex = 410 nm and λem = 482 nm every 30 minutes. **A** ThT-Fluorescence intensity for 30 μM K2Q46K2 with soluble aggregate fragments (red), equimolar K2Q46K2 and P8 with soluble aggregate fragments (grey), equimolar K2Q46K2 and QF1D-13 with soluble aggregate fragments (dark green) and 2:1 K2Q46K2:QF1D-13 with soluble aggregate fragments (light green) **B** ThT-Fluorescence intensity for 30 μM K2Q46K2 with soluble aggregate fragments (red), equimolar K2Q46K2 and P8 with soluble aggregate fragments (grey) and equimolar K2Q46K2 and QF1D-14 with soluble aggregate fragments (dark green)

Another aggregation assay starting with monomeric L-K2Q46K2 showed that QF1D-13 and QF1D-14 inhibit the aggregation even in sub stoichiometric concentrations (**Figure 12**). The deviation for QF1D-13 was very high because there was no aggregation observable in some wells. Medially, QF1D-13 did reduce the fluorescence intensity to 17% percent of the steady state measured for the sample containing P8 at 15 h when the compound was present in equimolar concentration and to 53% when K2Q46K2 was present in excess. QF1D-14's effect was not as high, but it still reduced the fluorescence intensity to 37% of the fluorescence intensity with P8 at 15 h in equimolar ratio and to 75% when K2Q46K2 was present in excess. QBP1 had a stronger inhibiting effect than QF1D-13. When K2Q46K2 was present in excess, QF1D-14 elongated the lag time to 9.5 h, whereas QBP1 did not elongate the lag time at all under these conditions.
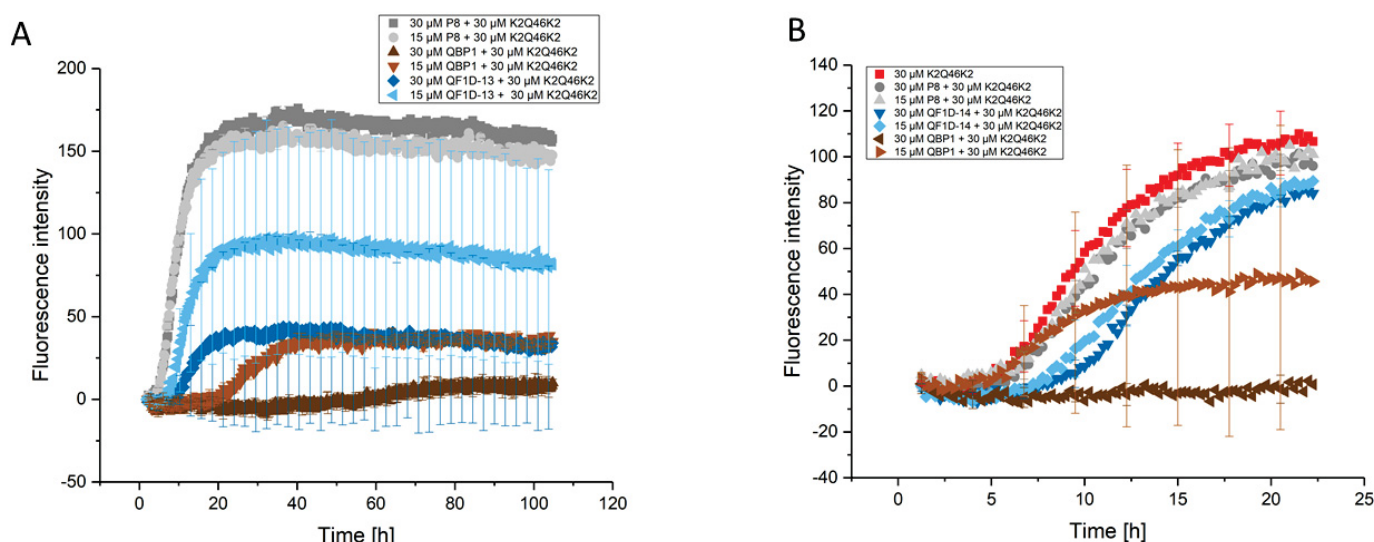
FIGURE 12: sub stoichiometric concentrations of QF1D-13 and QF1D-14 inhibit the aggregation of K2Q46K2

ThT-assay with 30 μM K2Q46K2 in TBS pH 7.5 at 37°C with 300 rpm double orbital shaking. Fluorescence intensity was measured at λex = 450 nm and λem = 480 nm every 15 minutes. **A** ThT-fluorescence intensity for 30 μM K2Q46K2 and P8 (grey), 30 μM K2Q46K2 and 30 μM QF1D-13 (dark blue), 30 μM K2Q46K2 and 15 μM QF1D-13 (light blue), 30 μM K2Q46K2 and 30 μM QBP1 (brown) and 30 μM K2Q46K2 and 15 μM QBP1 (light brown) **B** ThT-fluorescence intensity for 30 μm K2Q46K2 and P8 (grey), 30 μm K2Q46K2 and 30 μm QF1D-14 (dark blue), 30 μm K2Q46K2 and 15 μm QF1D-14 (light blue), 30 μm K2Q46K2 and QBP1 (brown) 30 μM K2Q46K2 and 15 μM QBP1 (light brown)

QF1D-14 bound to K2Q23K2 (**Figure 13**). But there was no saturation reached so it was not possible to determine a K_D value. In SPR measurements QF1D-13 did neither show binding to K2Q23K2 nor K2Q46K2.
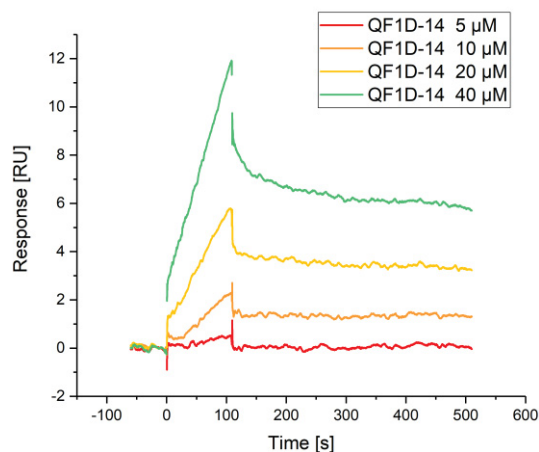
FIGURE 13: Sensorgram of QF1D-14 binding to L-K2Q23K2
L-K2Q23K2 was immobilized on a CM5 Chip with amino coupling. Using TBS-T pH 7.5 with 0.05% Tween20 as running buffer. The response was referenced with flow cell 1, which was activated and quenched without immobilizing anything. The binding of QF1D-14 to K2Q23K2 was investigated with the SPR technique.

4.3. PUBLISHED RESULTS:

INHIBITION OF POLYGLUTAMINE MISFOLDING WITH D-ENANTIOMERIC PEPTIDES IDENTIFIED BY MIRROR IMAGE PHAGE DISPLAY SELECTION BY PAULINE ELISABETH KOLKWITZ, JEANNINE MOHRLÜDER AND DIETER WILLBOLD [221]

Article

Inhibition of Polyglutamine Misfolding with D-Enantiomeric Peptides Identified by Mirror Image Phage Display Selection

Pauline Elisabeth Kolkwitz [1], Jeannine Mohrlüder [1] and Dieter Willbold [1,2,*]

[1] Institute of Biological Information Processing (IBI-7), Forschungszentrum Jülich, 52425 Jülich, Germany; p.kolkwitz@fz-juelich.de (P.E.K.); j.mohrlueder@fz-juelich.de (J.M.)
[2] Institut für Physikalische Biologie, Heinrich-Heine-Universität Düsseldorf, 40225 Düsseldorf, Germany
[*] Correspondence: d.willbold@fz-juelich.de

Abstract: Nine heritable diseases are known that are caused by unphysiologically elongated polyglutamine tracts in human proteins leading to misfolding, aggregation and neurodegeneration. Current therapeutic strategies include efforts to inhibit the expression of the respective gene coding for the polyglutamine-containing proteins. There are, however, concerns that this may interfere with the physiological function of the respective protein. We aim to stabilize the protein's native conformation by D-enantiomeric peptide ligands to prevent misfolding and aggregation, shift the equilibrium between aggregates and monomers towards monomers and dissolve already existing aggregates into non-toxic and functional monomers. Here, we performed a mirror image phage display selection on the polyglutamine containing a fragment of the androgen receptor. An elongated polyglutamine tract in the androgen receptor causes spinal and bulbar muscular atrophy (SBMA). The selected D-enantiomeric peptides were tested for their ability to inhibit polyglutamine-induced androgen receptor aggregation. We identified D-enantiomeric peptide QF2D-2 (sqsqwstpqGkwshwprrr) as the most promising candidate. It binds to an androgen receptor fragment with 46 consecutive glutamine residues and decelerates its aggregation, even in seeded experiments. Therefore, QF2D-2 may be a promising drug candidate for SBMA treatment or even for all nine heritable polyglutamine diseases, since its aggregation-inhibiting property was shown also for a more general polyglutamine target.

Keywords: polyglutamine diseases; protein misfolding diseases; phage display; all-D-peptide therapeutics; protein aggregation

1. Introduction

The folding and aggregation of proteins are usually considered to be competing mechanisms [1]. Aggregating proteins are often intrinsically disordered proteins (IDP) [2]. During the aggregation process, monomers of the aggregating protein form small, soluble oligomers which can accumulate into larger aggregates [3]. The most common aggregate structure is the cross-beta amyloid fibril, which has been described at atomic resolution for several examples [4–7].

Aggregates formed by misfolded proteins can lead to cytotoxic effects [8]. Several neurodegenerative diseases are caused by misfolded proteins, such as Alzheimer's disease (AD), Parkinson's disease (PD), prion encephalopathies, amyotrophic lateral sclerosis (ALS) or the heritable polyglutamine diseases, belonging to the triplet repeat diseases [9–11]. Several proteins contain sections with a number of consecutive glutamines, referred to as "polyglutamine proteins" or "polyQ proteins" [12,13]. Polyglutamine proteins form amyloids in a nucleated growth mechanism, with the critical nucleus's size depending on the length of the polyQ chain [14–16]. As observed for other amyloid proteins, the fibrils formed by polyglutamine proteins are able to seed, even between different polyQ lengths [17,18].

47

Today, nine heritable polyglutamine misfolding diseases are known, namely Huntington's chorea, spinal and bulbar muscular atrophy (SBMA) or Kennedy's disease, spinocerebellar muscular atrophy 1 (SCA1), SCA2, SCA3 or Machado-Joseph disease, SCA6, SCA7, SCA12, SCA17 and dentatorubral-pallidoluysian atrophy (DRPLA) or Haw River syndrome [19–29]. Still, no effective therapies are known [19]. Analogous to other protein misfolding diseases, the oligomers are thought to be the main toxic species in polyglutamine misfolding diseases [30–32].

Given that the misfolding and aggregation of proteins with an elongated polyglutamine tract is the cause of polyglutamine diseases, inhibiting the aggregation process by stabilizing the native conformation of the polyglutamine protein with a therapeutic agent that binds to natively folded polyglutamine-tracts may be a promising therapeutic approach. Peptides as monomer-stabilizing agents may be suitable as polyglutamine binding partners [33], since they offer a much more effective and specific binding to polyglutamine tracts than small molecules. In one example, a polyglutamine-binding peptide was able to suppress neurodegeneration in *Drosophila* [34]. Due to the degradation of peptides by metabolic processes [35], it is advantageous to deliver peptides that exclusively consist of amino acid residues in D-enantiomeric conformation (D-peptides). These all-D-peptides exhibit less immunogenity, if at all, and an elevated proteolytic stability compared to their L-enantiomeric counterparts [35,36].

A mirror image phage display selection can be carried out using a D-enantiomeric target. It follows that the D-enantiomeric "mirror image" of the selected peptide ligand can be synthesized and binds to the native L-enantiomeric target [35,37,38]. It was already shown that this is a successful approach for neurodegenerative diseases. As an example for Alzheimer's disease even by oral administration. It is an example for D-enantiomeric peptides that pass the blood–brain barrier after peripheral administration [39].

In the present study, we aimed to identify a D-enantiomeric peptide ligand of polyglutamine proteins that inhibits their aggregation. To this end, a phage display selection was performed with the mirror image of an androgen receptor fragment containing Q23-polyglutamine. A subset of the phage display selected peptides have been synthesized as D-enantiomeric peptides and were subsequently tested on the fragment of the L-enantiomeric construct of the androgen receptor with an elongated polyglutamine tract or a universal polyglutamine stretch, with respect to their ability to bind and inhibit their aggregation.

2. Materials and Methods

2.1. Polyglutamine Proteins and Compounds

The synthetic mirror image of the androgen receptor ARQ23$^{51–96}$ was obtained from JPT (JPT Peptide Technologies GmbH, Berlin, Germany) with an N-terminal biotin, connected to the peptide via Trioxatridecan-succinamic acid (ttds)-linker.

The selected all-D-peptide compounds were obtained from Caslo (CASLO ApS, Lyngby, Denmark), whereas L-ARQ46$^{51–96}$ and the universal polyglutamine peptide L-K2Q46K2 were obtained from peptides & elephants GmbH (Henningsdorf, Germany). All peptides used in this study are summarized in Table 1.

Table 1. Synthetic peptides used.

Name	Sequence	Synthesized by
D-ARQ23	GaslllllqqqqqqqqqqqqqqqqqqqqqqqqetsprqqqqqqGedGs	JPT
L-ARQ46	GASLLLLQQQQQQQQQQQQQQQQQQQQQQQQQQQQ QQQQQQQQQQQQQQQQQQQETSPRQQQQQQGEDGS	Peptides & elephants
L-K2Q46K2	KKQQQQQQQQQQQQQQQQQQQQQQQQQQ QQQQQQQQQQQQQQQQQQQQQQQQQKK	Peptides & elephants
QF2D-1	Gnprmteqhqsypphmrrr	Caslo
QF2D-2	sqsqwstpqGkwshwprrr	Caslo
QF2D-3	hnipqklGvwpwpeerrrr	Caslo
QF2D-4	rsfdenswqqflGpGerrr	Caslo
QF2D-5	Gyptypyntqsisswlrrr	Caslo
QF2D-6	sstlmaypnysmqGnerrr	Caslo
QF2D-7	hhwntawdpfhsvrrr	Caslo
QF2D-8	hqrdpswvlyGesrivrrr	Caslo
QF2D-9	eyeqhvkwpwinnqqhrrr	Caslo
QBP1	SNWKWWPGIFD	Peptides & elephants
P8	YDTPKHKDKTWPMM	Caslo

2.2. Disaggregation of Polyglutamine Proteins

Following the disaggregation protocol that Chen et al. published [40], the polyglutamine proteins were incubated for three days in 1:1 TFA/Hexafluoroisopropanol (HFIP) or overnight in 100% trifluoroacetic acid (TFA). Afterwards the solvent was evaporated with N_2 gas treatment and the polyglutamine protein redissolved in the experiment buffer.

2.3. Mirror Image Phage Display

The mirror image phage display was performed with D-Biotin-ttds-ARQ23 as target that was disaggregated in 100% TFA. The solvent was evaporated by N_2 gas treatment. The target was redissolved in Tris-buffered saline (TBS) pH 7.5. Furthermore, D-Biotin-ttds-ARQ23 was immobilized on a high capacity streptavidin coated polystyrene plate with "SuperBlock" by Thermo scientific (Thermo Fisher scientific, Waltham, MA, USA) for 30 min. TBS pH 7.5 with 0.1% Tween20 served as the selection and immobilization buffer. A total of 4 pmol of the target was immobilized on the surface for each selection round. In parallel, Biotin-ttds was immobilized in another well and served as negative control in the empty selection that was performed in parallel to the target selection. The immobilization was followed by blocking with BSA or milk powder (10 mg/mL) and quenching with biotin for 30 min. Alternating blocking agents were used to avoid selection of BSA or milk powder binders, starting with BSA in the first round. In each selection round 6×10^{11} Phages were used as input, starting with the Trico 16 library from Creative Biolabs (Lot: CBLX021820; Creative Biolabs Inc., Shirley, NY, USA). The phages were incubated with the target for 30 min. During the three selection rounds, the number of washing steps was increased from six in selection round 1 to 12 washing steps in the third selection round with TBS pH 7.5 with 0.1% Tween20 and 2 mg/mL BSA as washing buffer. The phages were eluted with 100 µL 0.2 M Glycin-HCl (pH 2.2) that was incubated in the well for 10 min at room temperature (RT). Consecutively the solution containing the eluted phages was removed from the plate and mixed with 25 µL 1 M tris-HCl pH 9.1. Of this neutralized phage containing solution (output), 110 µL were added to a 20 mL *Escherichia coli* K12 ER2738 culture that were grown in lysogeny broth (LB)-medium with 20 µL Tetracyclin to an OD_{600} of 0.1. 5 µL of the output were mixed with 95 µL LB medium and a dilution series from 10^{-2} to 10^{-8} was prepared with LB medium. 100 µL *E. coli* K12 E2738 were added to each well and the resulting 200 µL were plated with 800 µL of top agar (10 g Bacto-Trypton, 5 g yeast extract, 5 g NaCl, 1 g MgCl, 7 g agarose, 1 l H_2O) on 35×10 mm plates (Sarstedt, Nümbrecht, Germany) with IPTG-xGal agar (1 µL/mL stock solution containing 1.25 g IPTG, 1 g X-gal and 25 mL DMSO). The plaques were counted after an overnight incubation at 37 °C.

After 4 h incubation, the 20 mL *E. coli* ER2738 culture was centrifuged for 20 min at 2700 *g*, 4 °C. The supernatant was mixed with 7 mL PEG8000- 2.5 M NaCl to precipitate the phages and incubated overnight on ice. After a second incubation at 2700 *g*, 4 °C for 60 min, the phage containing pellet was redissolved in 1 mL TBS that were centrifuged for 5 min at 10,600 *g*. The supernatant was mixed with 200 µL PEG-NaCl and incubated on ice for 1 h to precipitate the phages. The precipitation was centrifuged for 45 min at 2600 *g*, the pellet was resuspended in 100 µL TBS (input). The input's phage concentration was determined by spectrophotometry [41] in TBS using a 1:10 dilution. This procedure was repeated for all selection rounds. In selection round two and three, the respective input was also added to a well prepared in a similar fashion to the empty selection well and served as a direct control.

The single-stranded phage DNA was prepared for analysis by next generation sequencing (NGS) as described previously [42].

The data evaluation was performed with the software Target Sequencing Analysis Tool (TSAT) and Hammock [43], as described previously [42].

2.4. SPR Measurements

Binding studies were performed with surface plasmon resonance (SPR) in a Biacore T200 device (Biacore, GE Healthcare, Uppsala, Sweden). The L-ARQ46 was immobilized on a CM5 Chip via amine coupling (1400 RU). The selected D-enantiomeric peptide compound QF2D-2 was dissolved in the running buffer (TBS pH 7.5 with 0.05% Tween) and served as the analyte in multi-cycle experiments, with the highest peptide concentration being 20 µM. Experiments were performed at 25 °C with a flow rate of 45 µL/min. After a contact time of 110 s and a dissociation time of 400 s, the surface was regenerated with low pH (Glycin-HCl, pH 2.2) for 30 s with a flow rate of 30 µL/min. The data were evaluated via affinity fit of the steady state using the biacore evaluation software.

Additionally, K2Q46K2 was immobilized on a polycarboxylate-chip with 200 nm matrix (530 RU). The selected D-enantiomeric peptide compound QF2D-2 was dissolved in running buffer (TBS pH 7.5 with 0.05% Tween) and served as analyte in multi-cycle experiments. Experiments were performed at 25 °C with a flow rate of 20 µL/min. After a contact time of 140 s and a dissociation time of 400 s. The data were evaluated via affinity fit of the steady state using the biacore evaluation software.

2.5. Thioflavin T Assays

Thioflavin T (ThT) assays were performed to monitor the time-dependent formation of amyloidogenic aggregates. The assays were performed at 37 °C in TBS pH 7.5 (15 µM ThT) with 300 rpm double orbital shaking. All buffers were sterile filtrated beforehand. Polyglutamine proteins were disaggregated as described before. The peptides were pre-diluted in TBS pH 7.5. The disaggregated polyglutamine protein in buffer was mixed with 15 µM ThT and the pre-diluted peptides in a 96-well half-area flat-bottom microplate (Corning, New York, NY, USA). During the experiment all wells contained 100 µL ThT solution. Sealing the plate with foil (Thermo Fisher Scientific, Waltham, MA, USA) helped to prevent evaporation. The progression of fluorescence intensity was tracked by a microplate reader (BMG Labtech, Ortenberg, Germany).

The lag-time was estimated as follows: the average variation of the curve was determined with the last ten values of the steady state. Since the signal usually dropped at the beginning of the measurement, those values were not considered as starting point. As soon as the steady signal at the beginning exceeded the average variation, the lag-time was considered to be over.

For seeded experiments, the slope of the curve was considered instead of the lag-time because seeding eliminated the lag-time. The slope was determined by plotting the first values and fitting with a linear fit. The considered period (2 to 3.5 h) was similar for the curves compared with.

2.6. Production of Soluble Aggregate Fragments

The disaggregated ARQ46 was diluted to 300 µM and incubated at 37 °C, 400 rpm. After 24 h large, white aggregates were visible in the tube. The sample was sonicated (Sonopuls, Bandelin electronic GmbH & Co. KG, Berlin, Germany) four times for 15 s with an amplitude of 60%. Between the sonification steps the sample was cooled on ice. Post sonification the sample was turbid. It was centrifuged at 100,000 g for 1 h at 4 °C to remove insoluble aggregates from the solution. The clear supernatant was used for seeding with soluble aggregate fragments.

2.7. CD Spectroscopy

After disaggregation, polyglutamine proteins were dissolved in TBS pH 7.5 and measured in a quartz crystal cuvette with 1 mm light path (Hellma Analytics, Müllheim, Germany) in a CD spectrometer (J-1100, Jasco Deutschland GmbH, Pfungstadt, Germany) with 4 acquisitions. The High tension voltage (HT) was monitored throughout the experiment. Data for which the HT exceeded 600 V were excluded. Buffer measurements served as references. Analogous, samples containing 50 µM ARQ46 and 50 µM QF2D-1 or QF2D-2 were measured and referenced with the measurement of 50 µM QF2D-1 or QF2D-2 alone. Subsequently, the ARQ46 alone and with QF2D-1 or QF2D-2 were aggregated at 37 °C and 400 rpm for 7 days. The CD spectra of the samples were monitored after 24 h, 48 h and 168 h of aggregation.

3. Results

3.1. Aggregation and Disaggregation of Polyglutamine Proteins

In this study we followed a novel approach to identify therapeutics for protein misfolding diseases by stabilizing the protein's native conformation with all-D-enantiomeric peptides as ligands. To this end it is essential to find binding partners of the monomeric target proteins.

It is well known that polyglutamine proteins aggregate spontaneously when the number of glutamines exceeds a certain threshold [16]. This was observed for the tested constructs L-K2Q46K2 and L-ARQ46. Because of their spontaneous aggregation behavior, it was necessary to ensure that experiments were performed with monomeric polyglutamine proteins, whenever requested. The published disaggregation protocol [40] was adapted for the investigated polyglutamine proteins. Circular dichroism (CD) experiments with the disaggregated samples showed a mixture of random coil and alpha-helical structure (Figure 1A, grey curve). This is consistent with published CD-experiments [18]. After incubation at 37 °C, the CD measurement showed 100% beta-sheet structure (Figure 1A, black curve). It follows that the disaggregation protocol is successful and the protein was in its native conformation and capable of spontaneous misfolding after the disaggregation procedure.

This is supported by the Thioflavin T (ThT) aggregation assays, which showed that ARQ46 and K2Q46K2 (practically identical behavior, data not shown) spontaneously formed amyloid fibrils after few hours lag time, when incubated in TBS pH 7.5 at 37 °C (Figure 1B). The length of the lag time was dependent on the polyglutamine peptide's concentration. It was observed that there was a longer and more reproducible lag-time in aggregation assays when ARQ46 was disaggregated in 1:1 TFA/HFIP. Lower concentrations of the ARQ46 then K2Q46K2 were required for similar aggregation results considering the lag time, which was eliminated by adding 5% seeds monomer equivalent.
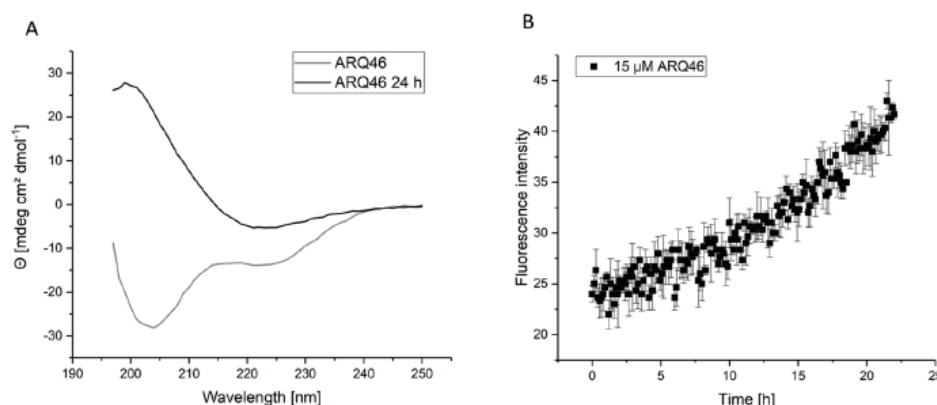
51

Figure 1. Disaggregation of ARQ46; Examination of ARQ46 post disaggregation. (**A**) CD-measurement of freshly disaggregated (100% TFA) ARQ46 (grey) in TBS pH 7.5 or the same sample incubated at 37 °C with 400 rpm shaking for 24 h (black). (**B**) ThT-Measurement of 15 μM ARQ46, disaggregated with 1:1 TFA/HFIP, in TBS pH 7.5 measured at 37 °C.

3.2. Mirror Image Phage Display Selection

3.2.1. Target Preparation

A mirror image phage display selection was performed to identify peptide ligands of polyglutamine proteins. To this end, a D-enantiomeric fragment of the androgen receptor comprised of amino acid residues 51 to 96 with a polyglutamine tract of 23 glutamines (D-ARQ23) was presented as target during the three selection rounds. An N-terminal biotin tag was connected via a ttds-linker to the D-ARQ23. Following the disaggregation protocol, with 100% TFA, the D-ARQ23 was disaggregated prior to the selection in order to assure its monomeric conformation. The disaggregation's success was verified via CD spectroscopy. The CD sample was stored analogous to the target samples and measured after the selection's completion to ensure the target stayed disaggregated for the selections time period. The resulting CD spectrum was opposite to the curve typical for disaggregated polyglutamine proteins (Figure 2), exactly as expected for a D-enantiomeric peptide.
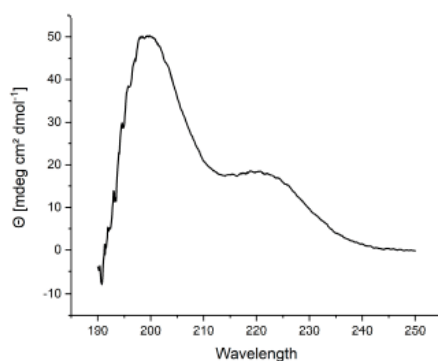
Figure 2. CD-spectrum of D-ARQ23 disaggregated with 100% TFA; Prior to the phage display selection D-ARQ23 was disaggregated with TFA to ensure selection on monomeric target. CD-spectrum was recorded in 10 mM Tris pH 8.

3.2.2. Selection and Evaluation

The selected phages from the phage library presenting 16mer peptides on their surface were analyzed via Next Generation Sequencing (NGS). The sequencing data were evaluated via TSAT, evaluation software developed by our work group [42] and the clustering tool

Hammock [43]. There was no general sequence alignment of all selected sequences possible. The sequences were ranked by their empty score, which is the ratio between the frequency of the respective sequence in the target selection and the empty selection. To ensure comparability, the frequency was normalized to parts per million, because NGS runs might have different read numbers.

In case the sequence is not present in the empty selection at all, half of the minimal empty value was used to calculate the empty score. The 50 sequences with the highest empty scores were compared regarding other parameters (Figure 3). One of those parameters is the enrichment factor, which is the ratio between the frequency in target selection round 3 and the frequency in the original library. If the sequence's frequency in the library was zero, the half-minimal value was used, as described for the empty score. The ratio of target selection and direct control was also taken into account. It gives good hints concerning the phage's target specificity, since the same input is presented to target or control well. If a sequence is more frequent in the target selection than the direct control it is highly probable that this sequence is a specific target binder. The last considered parameter was the formation of clusters, respectively sequences that are similar to each other. The Hammock tool was used to search the sequences for clusters. A cluster including many similar sequences can be used as a hint for target specific sequence enrichment. The selected sequences were also compared with those selected on a universal polyglutamine target, D-K2Q23K2. There were similarities in the preferred amino acid residues and also some sequences identical in both selections, another hint that this set-up is suitable to select specific polyglutamine binders.
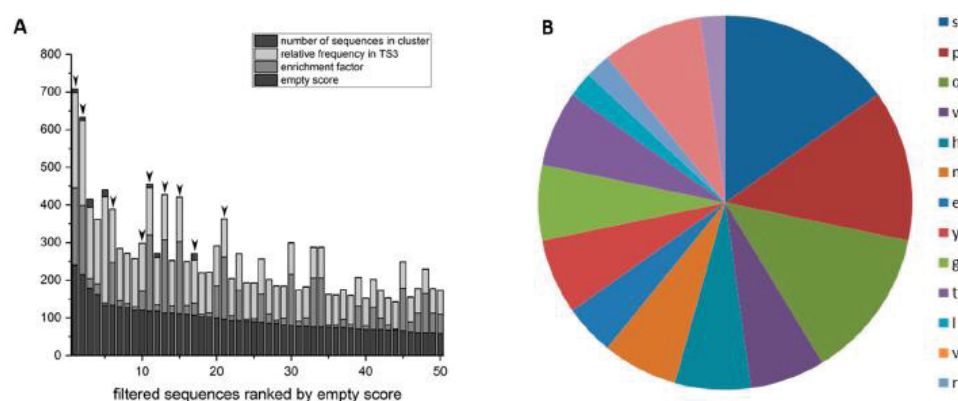
Figure 3. Sequences selected on D-ARQ23 ranked by empty score. (**A**) The sequences found by NGS sequencing were ranked by their empty score (deep dark grey). The sequences with the 50 highest empty scores are depicted. The enrichment factor (grey), relative frequency in target selection 3 (TS3; light grey) as well as the number of sequences with similar motives in the respective clusters (dark grey) are visualized within the bar chart. Sequences that were further investigated are marked with black arrows. (**B**) Amino acid residue type abundance in QF2D-1, QF2D-2 and QF2D-6.

Considering the described parameters, nine D-enantiomeric peptide sequences were chosen for further experimental investigations for their ability to inhibit the aggregation of polyglutamine proteins, marked with arrows in Figure 3. The peptides resulting from the marked sequences were named consecutively QF2D-1, QF2D-2 QF2D-3, QF2D-4, QF2D-5, QF2D-6, QF2D-7, QF2D-8 and QF2D-9. The sequences of the peptide and the considered parameters are shown in Table 2.

Table 2. D-peptides selected on ARQ23 that were further investigated with three additional, C-terminal arginine residues.

Peptide Name	Sequence	Empty Score	Enrichment Factor	Frequency in Library	Cluster Size	TS3/DC
QF2D-1	Gnprmteqhqsypphmrrr	240	205	1.2	9	2.7
QF2D-2	sqsqwstpqGkwshwprrr	215	184	1.2	8	9
QF2D-3	hnipqklGvwpwpeerrrr	134	114	1.2	1	6.1
QF2D-4	rsfdenswqqflGpGerrr	120	51	2.4	1	1.7
QF2D-5	Gyptypyntqsisswlrrr	118	202	0	10	5
QF2D-6	sstlmaypnysmqGnerrr	113	194	0	1	10.3
QF2D-7	hhwntawdpfhsvrrr	112	191	0	1	2
QF2D-8	hqrdpswvlyGesrivrrr	108	31	3.7	18	1.4
QF2D-9	eyeqhvkwpwinnqqhrrr	100	85	1.2	1	55.4

Overall, QF2D-1 had the highest empty score and enrichment factor. It was rare in the library and the leading sequence in a cluster with 8 other, similar sequences. It had a TS3/DC3 ratio bigger than 1, meaning it was more frequent in the target selection than in the direct control. The same was true for QF2D-2 that had the second highest empty score and a high enrichment factor. Similar to QF2D-1, it was rare in the library and found to be the leading sequence in a cluster. Compared to the other sequences it had the third highest ratio between Target selection and direct control.

The sequences with the third to fifth highest empty scores were excluded from further investigation, because they were also frequent in the library, meaning their enrichment factor was not as high.

We found that QF2D-3 had the sixth highest empty score and a high enrichment factor, as well as a high TS3/DC3 value, which is why it was tested.

The sequences with the seventh to ninth highest empty scores had low enrichment factors and were not included in any clusters; therefore they were not further investigated.

Additionally, QF2D-4 had the tenth highest empty score and was rare in the library, similar to QF2D-5, which was very rare in the library. QF2D-5 with the 11th highest empty score and had the second highest enrichment factor. It was also leading sequence in a cluster and had a high TS3/DC3 ratio. QF2D-7 was chosen for further investigation for the same reason.

However, QF2D-6 was also picked because of its high enrichment factor and the second highest TS3/DC3 ratio.

Moreover, QF2D-8 was the leading sequence in the cluster including the 18 sequences, whereas QF2D-9 had the highest TS3/DC3 ratio.

All other sequences were excluded, because their empty scores were not considered high enough.

By comparing the amino acid residue composition of the nine investigated peptides with the 50 leading sequences in the empty selection, it becomes apparent that three amino acid residues serine, proline and glutamine increased their proportion. Whereas serine, proline and glutamine make up 23% of the amino acid residues in the peptides selected in the empty selection, 33% of the amino acid residues in the nine selected peptides were serine, proline or glutamine. This becomes even more striking when we only consider the three peptides that had an effect in the seeded assay: QF2D-1, QF2D-2 and QF2D-6. 40% of the residues in these peptides are serine, proline or glutamine (Figure 3B). Their abundance nearly doubled in these peptides compared with the average of the empty selection.

Polyglutamine tracts modulate protein–protein interactions, especially between intrinsically disordered proteins [12]. It is not surprising that a glutamine rich sequence would be a preferred interaction partner for the monomeric polyglutamine target. Proline can interfere with the aggregation of polyglutamine proteins [44]. A proline-rich peptide could be effective in inhibiting the aggregation of polyglutamine proteins. The enrichment of specific residues compared to the empty selection is another hint that there was target-specific

selection pressure that led to the enrichment of sequences with a high frequency of serine, proline and glutamine.

Three arginine residues were added C-terminally to the peptides that were further investigated to increase the peptide's solubility. Arginines can increase cell membranes permeability [45].

3.3. Impact on Polyglutamine Aggregation

In order to screen the selected all D-peptide compounds for their effect on polyglutamine aggregation, QF2D-1, QF2D-2, QF2D-3, QF2D-4, QF2D-5, QF2D-6, QF2D-7, QF2D-8 and QF2D-9 were tested via ThT-assay. The fluorescence intensity of ThT is proportional to amyloid content of the sample. In this first screening with equimolar ratios between peptides and ARQ46, all nine compounds had an inhibitory effect. All of them delayed ARQ46 aggregation and reduced the fluorescence intensity of the steady state (Figure 4). None of the compounds were ThT-active when no polyglutamine protein was present. For QF2D-9 this control was not evaluable, because the well dried during the experiment. Interestingly, all nine compounds reduced the fluorescence intensity of the steady state rather similarly to approx. 70% of the fluorescence intensity measured for ARQ46. There was higher variety among the compounds with respect to the lag-time elongation. The lag-time elongation varied between 76% (QF2D-8) and 207% (QF2D-7).
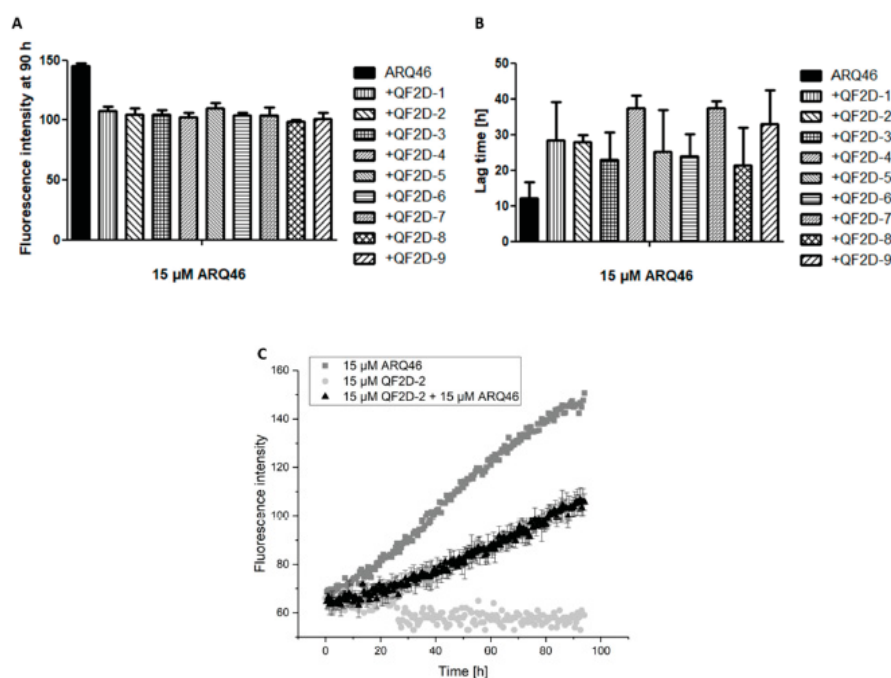
Figure 4. Compounds inhibit the aggregation of ARQ46; ThT assay with L-ARQ46 was performed at 37 °C in TBS pH 7.5. The progression of fluorescence intensity was measured every 30 min at λex = 410 nm and λem = 482 nm with 30 s agitation at 300 rpm before every measurement. (**A**) Fluorescence intensity measured at 90 h of the aggregation assay starting with 15 µM monomeric ARQ46 without peptide and with 15 µM QF2D-1, QF2D-2, QF2D-3, QF2D-4, QF2D-5, QF2D-6, QF2D-7, QF2D-8 or QF2D-9. (**B**) Lag time estimated from the aggregation assay of 15 µM monomeric ARQ46 without peptide and with 15 µM QF2D-1, QF2D-2, QF2D-3, QF2D-4, QF2D-5, QF2D-6, QF2D-7, QF2D-8 or QF2D-9. (**C**) Measurement example of the described ThT-assay with ARQ46 (dark grey) and QF2D-2 (black). QF2D-2 in TBS buffer alone served as a control (light grey). The mean fluorescence intensity is shown for each time point. The experiment was performed in three-fold determination.

Patients suffering from polyglutamine diseases present with aggregates in their neurons before symptom onset and therefore probably also before treatments start. Thus, a promising drug candidate should inhibit the aggregation in presence of pre-formed aggregates. Since small, soluble oligomers are suspected to be the main toxic species [46], the compounds were tested for their inhibitory effect in presence of soluble polyglutamine aggregate fragments (Figure 5). The effects of the compounds were compared with two controls. The first, P8, has been selected on SOD1 and should not bind to polyglutamine proteins. The second, QBP1, is claimed to inhibit the aggregation of polyglutamine proteins [33].
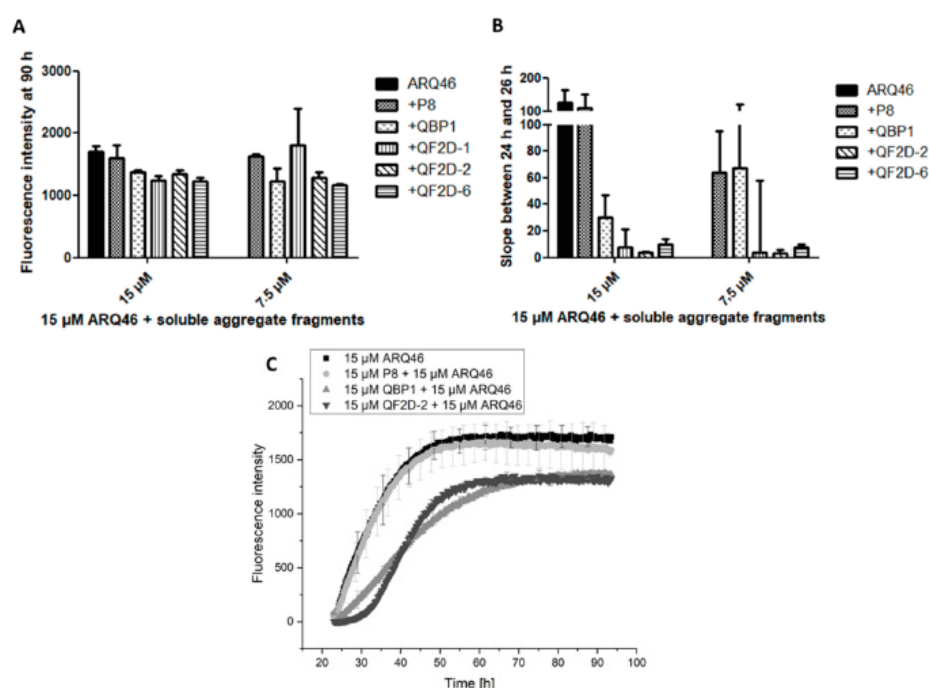

Figure 5. QF2D-1, QF2D-2 and QF2D-6 inhibit the aggregation of ARQ46 in presence of soluble aggregate fragment seeds; ARQ46 was aggregated, and the solution was subject to spinning at 100,000 g in an ultracentrifuge. The supernatant was preincubated with 15 μM and 7.5 μM of one of the selected compounds in TBS at 37 °C. After 23 h, 15 μM monomeric ARQ46 were added, and the fluorescence intensity was measured every 15 min at λex = 448 nm and λem = 482 nm with agitation at 300 rpm between measurements. P8 served as a control compound that was not selected on polyglutamine, whereas QBP1 is claimed to bind polyglutamine tracts and inhibit polyglutamine-driven aggregation. (**A**) Fluorescence intensity of P8, QBP1, QF2D-1, QF2D-2 and QF2D-6 in equimolar and sub stoichiometric ratio at 90 h. (**B**) The data points acquired between 24 h and 26 h- shortly after monomer addition- were fitted with a linear fit. The slope was compared. (**C**) Measurement example of the described ThT-assay with ARQ46 (black), P8 (light grey), QBP1 (grey) and QF2D-2 (dark grey). The mean fluorescence intensity is shown for each time point. The experiment was performed in two-fold determination.

In presence of soluble aggregates, there was no lag-phase observable for the sample containing only ARQ46 or ARQ46 and P8. To compare the aggregation onset, the slope of the curve between 24 h and 26 h, so shortly after monomer addition, was calculated with a linear fit of the curves (Figure 5B). This slope represents the formation rate of amyloid aggregates by the increase of ThT-fluorescence per hour. The curves measured for ARQ46 and P8 were the steepest. QF2D-1, QF2D-2 and QF2D-6 had an aggregation inhibiting effect

56

and decreased the slope, even when ARQ46 was present in excess. The effect of QF2D-1, QF2D-2 and QF2D-6 decreased the slope more effectively then QBP1, with QF2D-2 being the most and QF2D-6 being the least effective aggregation inhibiting compound. QF2D-2 reduced the slope by 96% compared with P8 and still by 86% compared to QBP1.

In the presence of soluble aggregate fragments, the effect of QBP1 was considerably smaller than that of the selected peptides. Since it is expected that a patient treated with a therapeutic agent for polyglutamine diseases already has aggregates formed in their neurons, the selected compounds might be more effective than QBP1 in this context.

During the aggregation process, the polyglutamine protein will change its secondary structure to a beta-sheet rich conformation. The selected compounds are expected to decelerate this transition by stabilizing the native conformation of the polyglutamine protein. The transition is monitored by CD spectroscopy. Freshly disaggregated, L-ARQ46 showed negative peaks at 222 nm and 205 nm, which is similar to the CD spectrum published by Chen et al. [18]. After 24 h incubation at 37 °C, the spectrum showed a positive peak at 200 nm range when no peptide was added to the sample. After 48 h incubation the spectrum showed that the sample was converted to beta-sheet [47,48] with a minimum at 220 nm and a maximum at 200 nm. (Figure 6A).

The sample containing QF2D-1 and ARQ46 (Figure 6B) did not show peaks in the positive or negative range after 24 h, probably because it was in the transition between the states since the CD spectrum is the median of the sample's secondary structure. After two days of incubation, the sample with QF2D-1 showed a maximum at 205 nm, similar to ARQ46 alone, which had a maximum at 201 nm. This could be due to slightly different beta-sheet structures. It seems as if QF2D-1 decelerated ARQ46's misfolding. The maximum at 205 nm is approx. 25% smaller than for ARQ46 alone, but after two days the transition seems to be complete as well.

This was not the case for the sample containing QF2D-2 and ARQ46 (Figure 6C,D). After 24 h incubation at 37 °C it still had a minimum at 205 nm although the minima's amplitude was reduced compared to the spectrum of the freshly disaggregated sample. The transition to beta-sheet structures did not seem to have progressed as in the other samples at this time point. After 48 h at 37 °C this sample had a positive peak at 205 nm as well, but it was 90% smaller than that of ARQ46 alone, making it plausible that the sample is still partly in random coil conformation. Seven days after the disaggregation, the sample with QF2D-2 was refolded to beta-sheet as well. As observed for QF2D-1 the maximum was smaller than that of ARQ46 alone. Consistent with the aggregation study results, QF2D-2 seems to delay the transition to beta-sheet structures.

Summarizing the results so far, QF2D-2 seems to be the most promising candidate. Thus, its effect on ARQ46 aggregation was also tested when soluble and insoluble aggregates served as seeds. Here, the inhibiting effect of QF2D-2 was even stronger than the one on solely soluble aggregate seeded aggregation (Figure 7). The stronger effect might be due to large, insoluble fibrils that make up the majority of the seeds and partly precipitate out of the solution and therefore have a lower seeding capability than soluble aggregates [49]. Smaller aggregates might also have larger surfaces that can interact with the monomers. Furthermore, smaller fibril fragments will also present more ends for elongation than fewer, longer fibrils.
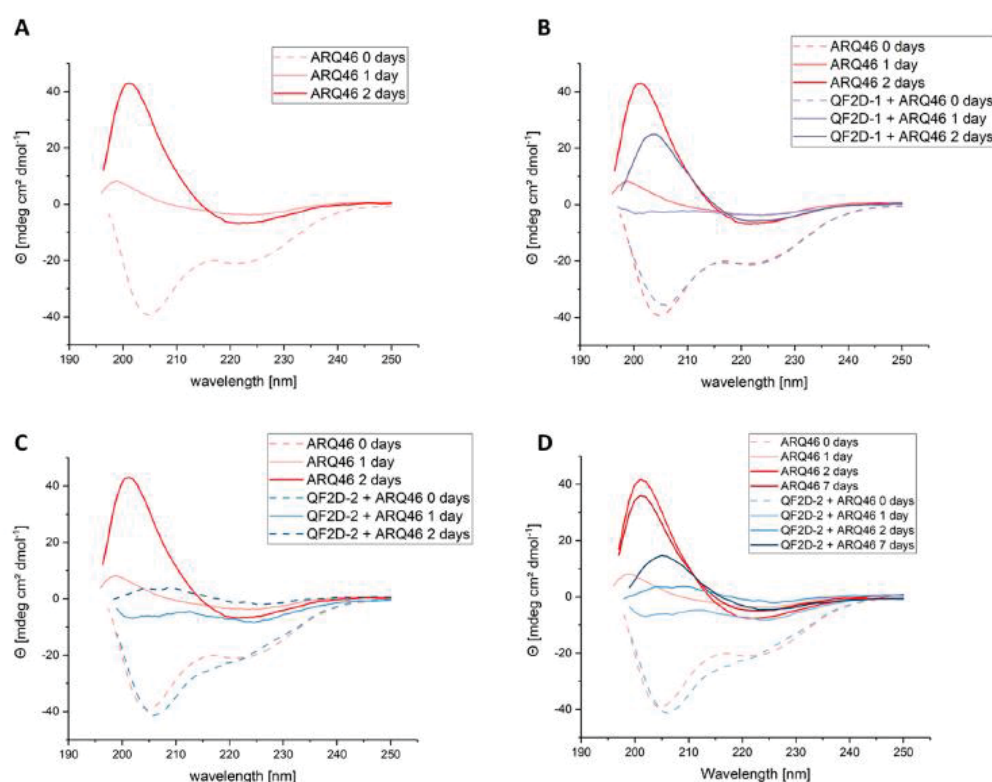
Figure 6. Investigation of structural change of ARQ46 in presence of QF2D-1 or QF2D-2 with CD spectroscopy; ARQ46 was disaggregated with 1:1 TFA/HFIP and diluted to 50 µM in TBS pH 7.5. 50 µM QF2D-1 or QF2D-2 were added to one sample. As a control and reference, 50 µM QF2D-1 or QF2D-2 alone were measured. (A) Spectra measured directly after disaggregation for 50 µM ARQ46 (rose, dashed)- referenced with buffer; 50 µM ARQ46 after 24 h incubation at 37 °C (rose, straight) and 50 µM ARQ46 after 48 h incubation at 37 °C (red, straight) (B) Spectra measured directly after disaggregation for 50 µM ARQ46 (rose, dashed)- referenced with buffer; equimolar ARQ46 and QF2D-1 (light purple, dashed)- referenced with QF2D-1 in TBS; 50 µM ARQ46 after 24 h incubation at 37 °C (rose, straight) and equimolar ARQ46 and QF2D-1 (light purple, straight)- referenced with QF2D-1 in TBS and 50 µM ARQ46 after 48 h incubation at 37 °C (red, straight) and equimolar ARQ46 and QF2D-1 (purple, straight)- referenced with QF2D-1 in TBS (C) Spectra measured directly after disaggregation for 50 µM ARQ46 (rose, dashed)- referenced with buffer and equimolar ARQ46 and QF2D-2 (light blue, dashed)- referenced with QF2D-2 in TBS; 50 µM ARQ46 after 24 h incubation at 37 °C (rose, straight) and equimolar ARQ46 and QF2D-2 (light blue, straight)- referenced with QF2D-2 in TBS and 50 µM ARQ46 after 48 h incubation at 37 °C (red, straight) and equimolar ARQ46 and QF2D-2 (light blue, straight)- referenced with QF2D-2 in TBS (D) Spectra measured directly after disaggregation for 50 µM ARQ46 (rose, dashed)- referenced with buffer; equimolar ARQ46 and QF2D-2 (light blue, dashed)- referenced with QF2D-2 in TBS; 50 µM ARQ46 after 24 h incubation at 37 °C (rose, straight) and equimolar ARQ46 and QF2D-2 (light blue, straight)- referenced with QF2D-2 in TBS; 50 µM ARQ46 after 48 h incubation at 37 °C (red) and equimolar ARQ46 and QF2D-2 (blue)- referenced with QF2D-2 in TBS; 50 µM ARQ46 after 168 h incubation at 37 °C (dark red) and equimolar ARQ46 and QF2D-2 (dark blue)- referenced with QF2D-2 in TBS.
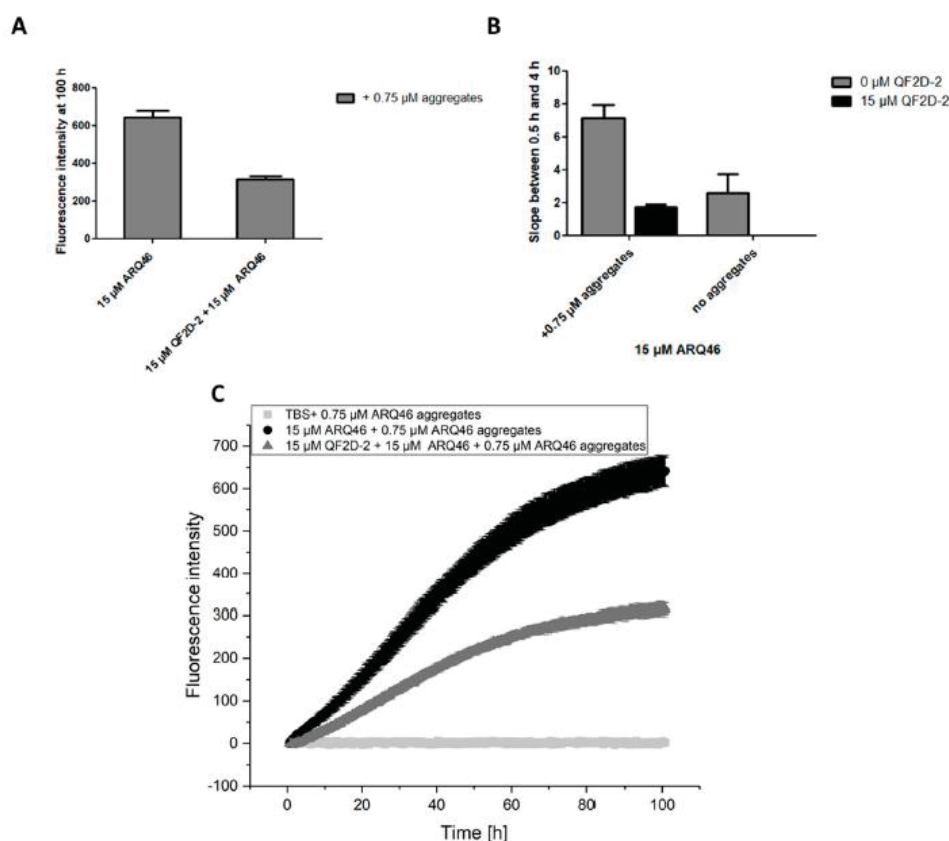
58

Figure 7. QF2D-2 inhibits the aggregation of ARQ46 in presence of soluble and insoluble seeds; ThT assay with L-ARQ46 was performed at 37 °C in TBS pH 7.5. Pre-formed ARQ46 aggregates were added in an amount of 5% monomer equivalent. The progression of fluorescence intensity was measured every 8 min at $\lambda ex = 448$ nm and $\lambda em = 482$ nm with agitation at 300 rpm between measurements. (**A**) Fluorescence intensity measured at 100 h of the aggregation assay starting with 15 μM monomeric ARQ46, 0.75 μM soluble and insoluble ARQ46 aggregates and 15 μM QF2D-2. (**B**) The data points acquired between 0.5 h and 4 h were fitted with a linear fit. The slope was compared with the one measured for ARQ46 aggregation without seeds. (**C**) Measurement of ThT-fluorescence intensity with 15 μM ARQ46 (black) and 15 μM QF2D-2 (dark grey). 15 μM QF2D-2 with 0.75 μM ARQ46 aggregates served as control. The mean fluorescence intensity is shown for each time point. The experiment was performed in three-fold determination.

The aggregation experiment with monomeric ARQ46 was repeated with control compounds P8, which had a slight inhibiting effect on the aggregation when present in equimolar concentration, but the aggregation was similar to that of ARQ46 alone when P8 was present in a sub stoichiometric relation. When the aggregation experiment began with monomeric ARQ46, QBP1 drastically inhibited the aggregation, differing from the results of the seeded assay (Figure 5). QF2D-2 had an inhibiting effect, even when ARQ46 was in excess but in contrast to the seeded assay with soluble aggregate fragments the effect was not as strong as QBP1's effect. QF2D-2 lowered the fluorescence intensity of the steady state and elongated the lag time compared to ARQ46 alone and with P8 (data not shown).

As described before, QF2D-2 inhibits aggregation when the polyglutamine protein is present in excess. This was verified in another aggregation experiment, showing that

QF2D-2 had an inhibiting effect in a 1:3 ratio (QF2D-1:ARQ46). The effect was concentration dependend (Figure 8).
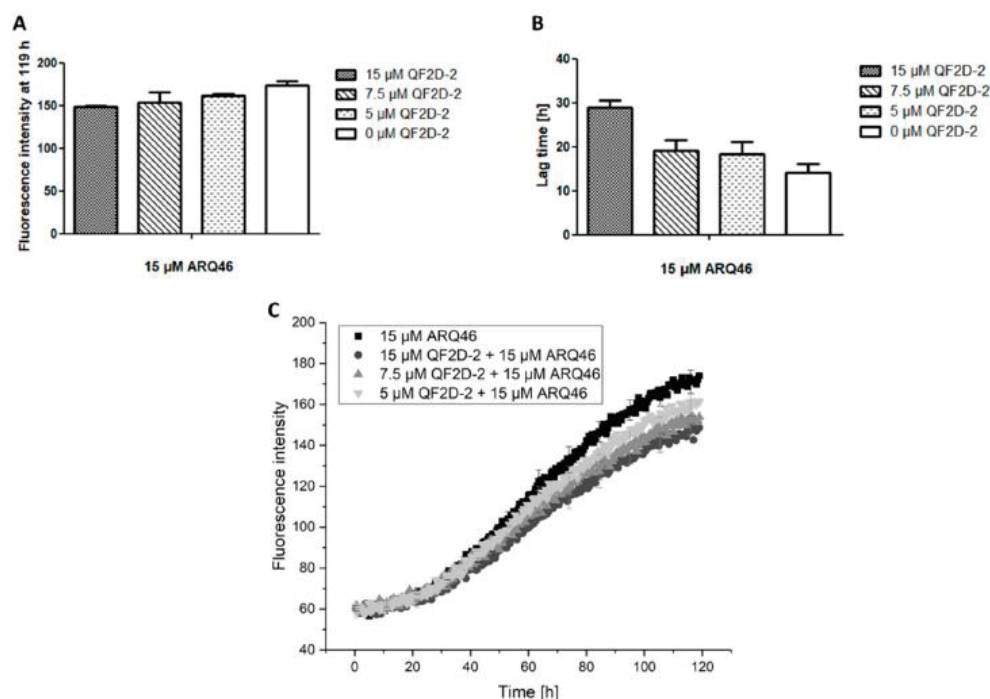

Figure 8. Effect of different QF2D-2 concentrations on the aggregation of ARQ46; ThT assay with L-ARQ46 was performed at 37 °C in TBS pH 7.5. The progression of fluorescence intensity was measured every 30 min at λex = 410 nm and λem = 482 nm with 30 sec agitation at 300 rpm before every measurement. (**A**) Fluorescence intensity measured at 119 h of the aggregation assay starting with 15 μM monomeric ARQ46 and 15 μM QF2D-2, 7.5 μM QF2D-2 or 5 μM QF2D-2. (**B**) Lag time estimated from the aggregation assay of 15 μM monomeric ARQ46 and 15 μM QF2D-2, 7.5 μM QF2D-2 or 5 μM QF2D-2. (**C**) Measurement example of the described ThT-assay with 15 μM ARQ46 (black), 15 μM QF2D-2 (dark grey), 7.5 μM (grey) and 5 μM QF2D-2 (light grey). The mean fluorescence intensity is shown for each time point. The experiment was performed in three-fold determination.

3.4. Binding to Polyglutamine Proteins

The binding properties of QF2D-2 to L-polyglutamine proteins were investigated by SPR. The QF2D-2 showed detectable binding to L-ARQ46. It bound with a K_D of 11 μM when L-ARQ46 was immobilized on the chip (data not shown).

This study aimed to identify ligands for polyglutamine-containing proteins. In order to investigate whether QF2D-2's effect is constrained to the androgen receptor fragment used in the study, further SPR experiments were performed to investigate QF2D-2's binding to more general polyglutamine constructs (L-K2Q23K2 and K2Q46K2). The glutamine flanking lysines were introduced to increase solubility in aqueous buffers [40].

Indeed, QF2D-2 bound to the general polyglutamine construct K2Q46K2 and inhibited its aggregation. It lowered the fluorescence intensity of the steady state and elongated the lag time compared to the effect of P8 (Figure 9). Thus, it may be feasible to transfer the compound's inhibitory effect on aggregation to other polyglutamine containing proteins.
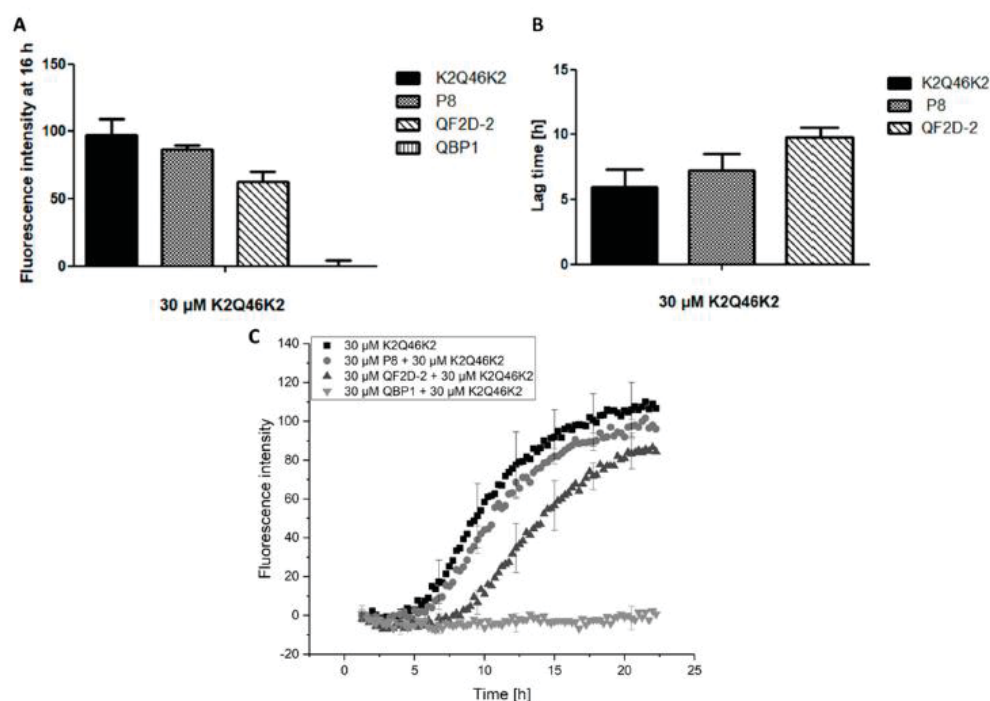
Figure 9. QF2D-2 inhibits the aggregation of K2Q46K2; ThT assay with L-K2Q46K2 was performed at 37 °C in TBS pH 7.5. The progression of fluorescence intensity was measured every 15 min at $\lambda ex = 450$ nm and $\lambda em = 480$ nm with 300 s agitation at 300 rpm before every measurement. (**A**) Fluorescence intensity measured at 16 h of the aggregation assay starting with 30 µM monomeric K2Q46K2 and 30 µM QF2D-2, P8 or QBP1. (**B**) Lag times estimated from the aggregation assay of 30 µM monomeric K2Q46K2 and 30 µM QF2D-2 or P8. (**C**) Measurement example of described ThT-assay with K2Q46K2 (black) and QF2D-2 (dark grey) as well as P8 (grey) or QBP1 (light grey). The experiment was performed in three-fold determination.

4. Discussion

The development of suitable therapeutics for SBMA is urgent, since no causative therapy is known. Instead of inhibiting or reducing the expression of the respective gene coding for the polyglutamine containing proteins [50–52], we aim to stabilize the protein's native conformation by D-enantiomeric peptide ligands to prevent misfolding and aggregation, shift the equilibrium between aggregates and monomers towards monomers and dissolve the already existing aggregates into non-toxic and functional monomers. To this end a mirror image phage display selection was performed on a fragment of the androgen receptor, in which an elongated polyglutamine tract causes SBMA.

As is known, QBP1 is an L-enantiomeric peptide, which was selected on polyglutamine that had a therapeutic effect in *Drosophila* [34], but did not yield beneficial neurological effects in a respective mouse model [53–55].

L-enantiomeric peptide compounds metabolize rather quickly. Thus, we develop D-enantiomeric peptide ligands of polyglutamine proteins, a principle that was already shown to be effective in other neurodegenerative diseases [39]. D-enantiomeric peptides are, metabolically, considerably more stable [35], thus regular administration can lead to higher concentrations in the tissue.

5. Conclusions

An unphysiologically elongated polyglutamine tract causes protein misfolding and aggregation, leading to neurodegeneration. We performed a mirror image phage display selection on an all D-enantiomeric polyglutamine target to identify all D-enantiomeric peptide ligands for L-enantiomeric polyglutamine proteins. During the subsequent characterization of the all D-enantiomeric peptide compounds, we identified QF2D-2 to be the most promising among the nine compounds tested. Furthermore, QF2D-2 delayed the ThT-active aggregation of ARQ46, even under seeding conditions. CD spectroscopy measurements showed that QF2D-2 stabilizes ARQ46 in its native conformation and delays the transition to beta-sheet rich structures. Additionally, QF2D-2 not only bound to ARQ46 and inhibited its ThT-active aggregation, but also the more general target K2Q46K2, suggesting that it may be used and further developed as a more general compound, targeting and stabilizing polyglutamine containing proteins.

References

1. Pastore, A.; Temussi, P.A. The two faces of Janus: Functional interactions and protein aggregation. *Curr. Opin. Struct. Biol.* **2012**, *22*, 30–37. [CrossRef]
2. Lapidus, L.J. Understanding protein aggregation from the view of monomer dynamics. *Mol. BioSyst.* **2013**, *9*, 29–35. [CrossRef]
3. Adegbuyiro, A.; Sedighi, F.; Pilkington, A.W.t.; Groover, S.; Legleiter, J. Proteins Containing Expanded Polyglutamine Tracts and Neurodegenerative Disease. *Biochemistry* **2017**, *56*, 1199–1217. [CrossRef] [PubMed]
4. Gremer, L.; Schölzel, D.; Schenk, C.; Reinartz, E.; Labahn, J.; Ravelli, R.B.; Tusche, M.; Lopez-Iglesias, C.; Hoyer, W.; Heise, H.; et al. Fibril structure of amyloid-β (1–42) by cryo–electron microscopy. *Science* **2017**, *358*, 116–119. [CrossRef] [PubMed]
5. Roder, C.; Vettore, N.; Mangels, L.N.; Gremer, L.; Ravelli, R.B.G.; Willbold, D.; Hoyer, W.; Buell, A.K.; Schroder, G.F. Atomic structure of PI3-kinase SH3 amyloid fibrils by cryo-electron microscopy. *Nat. Commun.* **2019**, *10*, 3754. [CrossRef] [PubMed]
6. Rothlein, C.; Miettinen, M.S.; Borwankar, T.; Burger, J.; Mielke, T.; Kumke, M.U.; Ignatova, Z. Architecture of polyglutamine-containing fibrils from time-resolved fluorescence decay. *J. Biol. Chem.* **2014**, *289*, 26817–26828. [CrossRef]
7. Willbold, D.; Strodel, B.; Schroder, G.F.; Hoyer, W.; Heise, H. Amyloid-type Protein Aggregation and Prion-like Properties of Amyloids. *Chem. Rev.* **2021**, *121*, 8285–8307. [CrossRef]
8. Hartl, F.U. Protein Misfolding Diseases. *Annu. Rev. Biochem.* **2017**, *86*, 21–26. [CrossRef]
9. Spillantini, M.G.; Bird, T.D.; Ghetti, B. Frontotemporal dementia and Parkinsonism linked to chromosome 17: A new group of tauopathies. *Brain Pathol.* **1998**, *8*, 387–402. [CrossRef]
10. Hardy, J.; Selkoe, D.J. The amyloid hypothesis of Alzheimer's disease: Progress and problems on the road to therapeutics. *Science* **2002**, *297*, 353–356. [CrossRef]
11. Nordlund, A.; Oliveberg, M. SOD1-associated ALS: A promising system for elucidating the origin of protein-misfolding disease. *HFSP J.* **2008**, *2*, 354–364. [CrossRef]
12. Schaefer, M.H.; Wanker, E.E.; Andrade-Navarro, M.A. Evolution and function of CAG/polyglutamine repeats in protein-protein interaction networks. *Nucleic Acids Res.* **2012**, *40*, 4273–4287. [CrossRef]
13. Butland, S.L.; Devon, R.S.; Huang, Y.; Mead, C.L.; Meynert, A.M.; Neal, S.J.; Lee, S.S.; Wilkinson, A.; Yang, G.S.; Yuen, M.M.; et al. CAG-encoded polyglutamine length polymorphism in the human genome. *BMC Genom.* **2007**, *8*, 126. [CrossRef]
14. Chen, S.; Ferrone, F.A.; Wetzel, R. Huntington's disease age-of-onset linked to polyglutamine aggregation nucleation. *Proc. Natl. Acad. Sci. USA* **2002**, *99*, 11884–11889. [CrossRef]
15. Kar, K.; Jayaraman, M.; Sahoo, B.; Kodali, R.; Wetzel, R. Critical nucleus size for disease-related polyglutamine aggregation is repeat-length dependent. *Nat. Struct. Mol. Biol.* **2011**, *18*, 328–336. [CrossRef]

16. Landrum, E.; Wetzel, R. Biophysical underpinnings of the repeat length dependence of polyglutamine amyloid formation. *J. Biol. Chem.* **2014**, *289*, 10254–10260. [CrossRef] [PubMed]

17. Trevino, R.S.; Lauckner, J.E.; Sourigues, Y.; Pearce, M.M.; Bousset, L.; Melki, R.; Kopito, R.R. Fibrillar structure and charge determine the interaction of polyglutamine protein aggregates with the cell surface. *J. Biol. Chem.* **2012**, *287*, 29722–29728. [CrossRef]

18. Chen, S.; Berthelier, V.; Yang, W.; Wetzel, R. Polyglutamine aggregation behavior in vitro supports a recruitment mechanism of cytotoxicity. *J. Mol. Biol.* **2001**, *311*, 173–182. [CrossRef]

19. Takeuchi, T.; Nagai, Y. Protein Misfolding and Aggregation as a Therapeutic Target for Polyglutamine Diseases. *Brain Sci.* **2017**, *7*, 128. [CrossRef] [PubMed]

20. MacDonald, M.; Ambrose, C.; Duyao, M.; Myers, R.; Lin, C.; Srinidhi, L.; Barnes, G.; Taylor, S.; James, M.; Groot, N. The Huntington's Disease Collaborative Research Group. A novel gene containing a trinucleotide repeat that is expanded and unstable on Huntington's disease chromosomes. *Cell* **1993**, *72*, 971–983. [CrossRef]

21. La Spada, A.R.; Wilson, E.M.; Lubahn, D.B.; Harding, A.; Fischbeck, K.H. Androgen receptor gene mutations in X-linked spinal and bulbar muscular atrophy. *Nature* **1991**, *352*, 77–79. [CrossRef]

22. Orr, H.T.; Chung, M.-y.; Banfi, S.; Kwiatkowski, T.J.; Servadio, A.; Beaudet, A.L.; McCall, A.E.; Duvick, L.A.; Ranum, L.P.; Zoghbi, H.Y. Expansion of an unstable trinucleotide CAG repeat in spinocerebellar ataxia type 1. *Nat. Genet.* **1993**, *4*, 221–226. [CrossRef] [PubMed]

23. Pulst, S.M.; Santos, N.; Wang, D.; Yang, H.; Huynh, D.; Velazquez, L.; Figueroa, K.P. Spinocerebellar ataxia type 2: PolyQ repeat variation in the CACNA1A calcium channel modifies age of onset. *Brain* **2005**, *128*, 2297–2303. [CrossRef] [PubMed]

24. Kawaguchi, Y.; Okamoto, T.; Taniwaki, M.; Aizawa, M.; Inoue, M.; Katayama, S.; Kawakami, H.; Nakamura, S.; Nishimura, M.; Akiguchi, I. CAG expansions in a novel gene for Machado-Joseph disease at chromosome 14q32. 1. *Nat. Genet.* **1994**, *8*, 221–228. [CrossRef] [PubMed]

25. Zhuchenko, O.; Bailey, J.; Bonnen, P.; Ashizawa, T.; Stockton, D.W.; Amos, C.; Dobyns, W.B.; Subramony, S.; Zoghbi, H.Y.; Lee, C.C. Autosomal dominant cerebellar ataxia (SCA6) associated with small polyglutamine expansions in the α 1A-voltage-dependent calcium channel. *Nat. Genet.* **1997**, *15*, 62–69. [CrossRef]

26. Benton, C.; De Silva, R.; Rutledge, S.; Bohlega, S.; Ashizawa, T.; Zoghbi, H. Molecular and clinical studies in SCA-7 define a broad clinical spectrum and the infantile phenotype. *Neurology* **1998**, *51*, 1081–1086. [CrossRef]

27. David, G.; Abbas, N.; Stevanin, G.; Dürr, A.; Yvert, G.; Cancel, G.; Weber, C.; Imbert, G.; Saudou, F.; Antoniou, E. Cloning of the SCA7 gene reveals a highly unstable CAG repeat expansion. *Nat. Genet.* **1997**, *17*, 65–70. [CrossRef] [PubMed]

28. Nakamura, K.; Jeong, S.-Y.; Uchihara, T.; Anno, M.; Nagashima, K.; Nagashima, T.; Ikeda, S.-i.; Tsuji, S.; Kanazawa, I. SCA17, a novel autosomal dominant cerebellar ataxia caused by an expanded polyglutamine in TATA-binding protein. *Hum. Mol. Genet.* **2001**, *10*, 1441–1448. [CrossRef]

29. Ueno, S.-I.; Kondoh, K.; Komure, Y.; Komure, O.; Kuno, S.; Kawai, J.; Hazama, F.; Sano, A. Somatic mosaicism of CAG repeat in dentatorubral-pallidoluysian atrophy (DRPLA). *Hum. Mol. Genet.* **1995**, *4*, 663–666. [CrossRef]

30. Gutekunst, C.-A.; Li, S.-H.; Yi, H.; Mulroy, J.S.; Kuemmerle, S.; Jones, R.; Rye, D.; Ferrante, R.J.; Hersch, S.M.; Li, X.-J. Nuclear and neuropil aggregates in Huntington's disease: Relationship to neuropathology. *J. Neurosci.* **1999**, *19*, 2522–2534. [CrossRef]

31. Kuemmerle, S.; Gutekunst, C.A.; Klein, A.M.; Li, X.J.; Li, S.H.; Beal, M.F.; Hersch, S.M.; Ferrante, R.J. Huntingtin aggregates may not predict neuronal death in Huntington's disease. *Ann. Neurol.* **1999**, *46*, 842–849. [CrossRef]

32. Huynh, D.P.; Figueroa, K.; Hoang, N.; Pulst, S.-M. Nuclear localization or inclusion body formation of ataxin-2 are not necessary for SCA2 pathogenesis in mouse or human. *Nat. Genet.* **2000**, *26*, 44. [CrossRef]

33. Nagai, Y.; Tucker, T.; Ren, H.; Kenan, D.J.; Henderson, B.S.; Keene, J.D.; Strittmatter, W.J.; Burke, J.R. Inhibition of polyglutamine protein aggregation and cell death by novel peptides identified by phage display screening. *J. Biol. Chem.* **2000**, *275*, 10437–10442. [CrossRef] [PubMed]

34. Nagai, Y.; Fujikake, N.; Ohno, K.; Higashiyama, H.; Popiel, H.A.; Rahadian, J.; Yamaguchi, M.; Strittmatter, W.J.; Burke, J.R.; Toda, T. Prevention of polyglutamine oligomerization and neurodegeneration by the peptide inhibitor QBP1 in *Drosophila*. *Hum. Mol. Genet.* **2003**, *12*, 1253–1259. [CrossRef] [PubMed]

35. Schumacher, T.N.; Mayr, L.M.; Minor, D.L.; Milhollen, M.A.; Burgess, M.W.; Kim, P.S. Identification of D-peptide ligands through mirror-image phage display. *Science* **1996**, *271*, 1854–1857. [CrossRef] [PubMed]

36. Elfgen, A.; Santiago-Schübel, B.; Gremer, L.; Kutzsche, J.; Willbold, D. Surprisingly high stability of the Aβ oligomer eliminating all-d-enantiomeric peptide D3 in media simulating the route of orally administered drugs. *Eur. J. Pharm. Sci.* **2017**, *107*, 203–207. [CrossRef] [PubMed]

37. Wiesehan, K.; Willbold, D. Mirror-image phage display: Aiming at the mirror. *ChemBioChem* **2003**, *4*, 811–815. [CrossRef]

38. Funke, S.A.; Willbold, D. Mirror image phage display—A method to generate D-peptide ligands for use in diagnostic or therapeutical applications. *Mol. BioSyst.* **2009**, *5*, 783–786. [CrossRef]

39. Van Groen, T.; Schemmert, S.; Brener, O.; Gremer, L.; Ziehm, T.; Tusche, M.; Nagel-Steger, L.; Kadish, I.; Schartmann, E.; Elfgen, A.; et al. The Abeta oligomer eliminating D-enantiomeric peptide RD2 improves cognition without changing plaque pathology. *Sci. Rep.* **2017**, *7*, 16275. [CrossRef]

40. Chen, S.; Wetzel, R. Solubilization and disaggregation of polyglutamine peptides. *Protein Sci.* **2001**, *10*, 887–891. [CrossRef]

63

41. Casadevall, A.; Day, L.A. DNA packing in the filamentous viruses fd, Xf, Pfl and Pf3. *Nucleic Acids Res.* **1982**, *10*, 2467–2481. [CrossRef] [PubMed]

42. Santur, K.; Reinartz, E.; Lien, Y.; Tusche, M.; Altendorf, T.; Sevenich, M.; Tamguney, G.; Mohrluder, J.; Willbold, D. Ligand-Induced Stabilization of the Native Human Superoxide Dismutase 1. *ACS Chem. Neurosci.* **2021**, *12*, 2520–2528. [CrossRef]

43. Krejci, A.; Hupp, T.R.; Lexa, M.; Vojtesek, B.; Muller, P. Hammock: A hidden Markov model-based peptide clustering algorithm to identify protein-interaction consensus motifs in large datasets. *Bioinformatics* **2016**, *32*, 9–16. [CrossRef]

44. Bhattacharyya, A.; Thakur, A.K.; Chellgren, V.M.; Thiagarajan, G.; Williams, A.D.; Chellgren, B.W.; Creamer, T.P.; Wetzel, R. Oligoproline effects on polyglutamine conformation and aggregation. *J. Mol. Biol.* **2006**, *355*, 524–535. [CrossRef] [PubMed]

45. Futaki, S.; Goto, S.; Sugiura, Y. Membrane permeability commonly shared among arginine-rich peptides. *J. Mol. Recognit.* **2003**, *16*, 260–264. [CrossRef]

46. Kim, Y.E.; Hosp, F.; Frottin, F.; Ge, H.; Mann, M.; Hayer-Hartl, M.; Hartl, F.U. Soluble Oligomers of PolyQ-Expanded Huntingtin Target a Multiplicity of Key Cellular Factors. *Mol. Cell* **2016**, *63*, 951–964. [CrossRef]

47. Terzi, E.; Hoelzemann, G.; Seelig, J. Reversible Random Coil-. beta.-Sheet Transition of the Alzheimer. beta.-Amyloid Fragment. *Biochemistry* **1994**, *33*, 1345–1350. [CrossRef]

48. Kar, K.; Hoop, C.L.; Drombosky, K.W.; Baker, M.A.; Kodali, R.; Arduini, I.; van der Wel, P.C.; Horne, W.S.; Wetzel, R. beta-hairpin-mediated nucleation of polyglutamine amyloid formation. *J. Mol. Biol.* **2013**, *425*, 1183–1197. [CrossRef]

49. Lam, H.T.; Graber, M.C.; Gentry, K.A.; Bieschke, J. Stabilization of alpha-Synuclein Fibril Clusters Prevents Fragmentation and Reduces Seeding Activity and Toxicity. *Biochemistry* **2016**, *55*, 675–685. [CrossRef] [PubMed]

50. Lim, W.F.; Forouhan, M.; Roberts, T.C.; Dabney, J.; Ellerington, R.; Speciale, A.A.; Manzano, R.; Lieto, M.; Sangha, G.; Banerjee, S.; et al. Gene therapy with AR isoform 2 rescues spinal and bulbar muscular atrophy phenotype by modulating AR transcriptional activity. *Sci. Adv.* **2021**, *7*, eabi6896. [CrossRef]

51. Lieberman, A.P.; Yu, Z.; Murray, S.; Peralta, R.; Low, A.; Guo, S.; Yu, X.X.; Cortes, C.J.; Bennett, C.F.; Monia, B.P. Peripheral androgen receptor gene suppression rescues disease in mouse models of spinal and bulbar muscular atrophy. *Cell Rep.* **2014**, *7*, 774–784. [CrossRef]

52. Sahashi, K.; Katsuno, M.; Hung, G.; Adachi, H.; Kondo, N.; Nakatsuji, H.; Tohnai, G.; Iida, M.; Bennett, C.F.; Sobue, G. Silencing neuronal mutant androgen receptor in a mouse model of spinal and bulbar muscular atrophy. *Hum. Mol. Genet.* **2015**, *24*, 5985–5994. [CrossRef] [PubMed]

53. Popiel, H.A.; Nagai, Y.; Fujikake, N.; Toda, T. Delivery of the aggregate inhibitor peptide QBP1 into the mouse brain using PTDs and its therapeutic effect on polyglutamine disease mice. *Neurosci. Lett.* **2009**, *449*, 87–92. [CrossRef] [PubMed]

54. Popiel, H.A.; Takeuchi, T.; Fujita, H.; Yamamoto, K.; Ito, C.; Yamane, H.; Muramatsu, S.; Toda, T.; Wada, K.; Nagai, Y. Hsp40 gene therapy exerts therapeutic effects on polyglutamine disease mice via a non-cell autonomous mechanism. *PLoS ONE* **2012**, *7*, e51069. [CrossRef] [PubMed]

55. Popiel, H.A.; Takeuchi, T.; Burke, J.R.; Strittmatter, W.J.; Toda, T.; Wada, K.; Nagai, Y. Inhibition of protein misfolding/aggregation using polyglutamine binding peptide QBP1 as a therapy for the polyglutamine diseases. *Neurotherapeutics* **2013**, *10*, 440–446. [CrossRef] [PubMed]

4.4. SUPPLEMENTARY RESULTS FOR QF2D-2

QF2D-2 is an all-D peptide compound that was selected on the fragment of the androgen receptor. It has an aggregation inhibiting effect on polyglutamine proteins and delays the structural transition of ARQ46 from random coil to beta-sheet [221].

The binding of QF2D-2 to L-ARQ46 and L-K2Q46K2 was investigated with the SPR technique. QF2D-2 bound to ARQ46 (**Figure 14 A,B**) and K2Q46K2 (**Figure 14 C,D**) with K_D values in the low micromolar range.
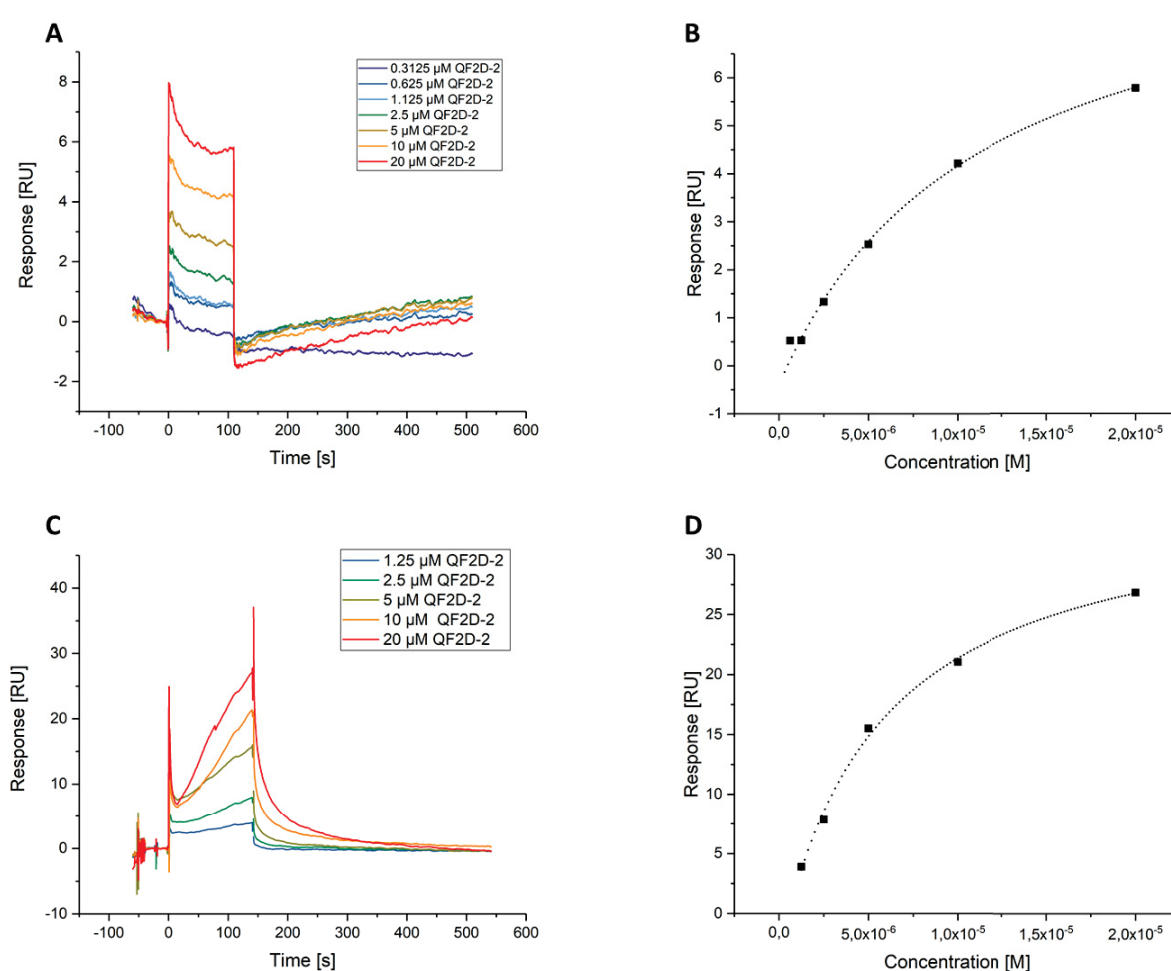
FIGURE 14: Binding of QF2D-2 to polyglutamine proteins measured with SPR

ARQ46 or K2Q46K2 were immobilized via amine coupling. QF2D-2 served as analyte, the running buffer was TBS with 0.05% Tween20. The response was referenced with Flow cell 1, which was activated and quenched without immobilizing anything. **A** Sensorgram of QF2D-2 binding to ARQ46. **B** Response of QF2D-2 binding to ARQ46 at the end of the dissociation time plotted against concentration. The K_D of 11.2 µM was determined with the affinity fit. **C** Sensorgram of QF2D-2 binding to K2Q46K2. **D** Response of QF2D-2 binding to K2Q46K2 at the end of the dissociation time plotted against concentration. The K_D of 5 µM was determined by affinity fit.

In addition, it was tested whether QF2D-2 could interrupt ARQ46 aggregation and disassemble the formed aggregates. To do so, the compound was added 22 h after experiment start so after lag time termination. Compound addition slightly shifted the curve to the right but there was no hint on disassembly (**Figure 15**).
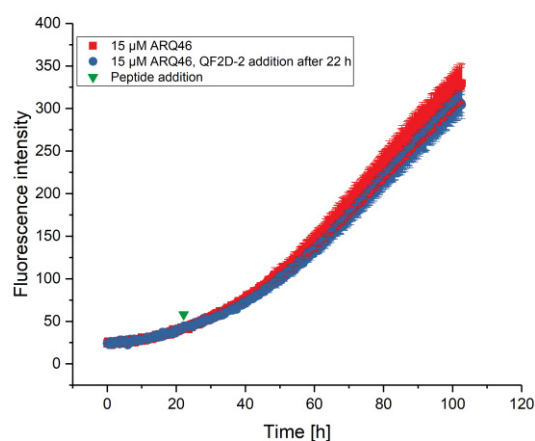
FIGURE 15: ThT-active aggregation of ARQ46 with QF2D-2 added after aggregation onset

ThT-assay with 15 µM ARQ46 in TBS pH 7.5 at 37°C with 300 rpm double orbital shaking. Fluorescence intensity was measured at λex = 410 nm and λem = 482 nm every 30 minutes. ThT-fluorescence intensity for 15 µM ARQ46 (red) and 15 µM ARQ46 with 15 µM QF2D-2 (blue) added after 22 h.

5. DISCUSSION

Polyglutamine diseases are fatal, heritable diseases for which no causative therapy is known to this day. An elongated polyglutamine tract causes the protein to misfold into a cytotoxic conformation that leads to cell death and neurodegeneration. It would be beneficial to prevent misfolding by stabilizing the native, monomeric conformation. This aim is targeted with different strategies. One approach is the development of intrabodies that target mutant huntingtin (mHTT) and inhibit its aggregation [227]. However, intrabodies are very specific and therefore only target one polyglutamine disease like HD, whereas the compounds selected on K2Q23K2 are general polyglutamine binders that could be effective in all polyglutamine misfolding diseases. Furthermore, it is not trivial to administer intrabodies to the brain [228]. This is not as problematic for smaller compounds like peptides. QBP1 is a polyglutamine binding peptide compound that had positive effects in animal models. It reduced neurodegeneration in *Drosophila* and weight loss in mice [198, 199]. Nevertheless, QBP1 is an L-enantiomeric peptide, which are known to be metabolized rather fast. A more protease resistant option are peptoids [229]. The peptoid HQP09 inhibited the aggregation of polyglutamine proteins but the substance had no effect in animal models when it was injected subcutaneously [200]. Presumably, it did not reach the brain. Another way to generate peptides that are metabolically more stable is to find D-enantiomeric peptide ligands of the target protein [230]. In contrast to HQP09, peripheral administration of D-enantiomeric peptide compounds for the treatment of neurodegenerative diseases can be effective [110]. But it still has to be elucidated whether the peptides selected and characterized in this study feature this ability as well.

A designed L-enantiomeric peptide comprised of arginine and glutamine residues was able to reach the brain and showed a positive effect in mice, though the compound tends to self-aggregate [231]. The data regarding QF1D-1 and QF1D-2 illustrate that self-aggregating compounds can differ in their effects, depending on the aggregation state.

Apart from peptide compounds, the native conformation can also be stabilized by chemical chaperones, which thereby inhibit or delay aggregation [232]. A chemical chaperone that inhibits polyglutamine aggregation effectively in animal studies is arginine [233]. It is currently tested in japanese patients suffering from polyglutamine diseases [228].

Instead of stabilizing the native conformation and thereby inhibit aggregation, phenotype improvement may be achieved by reducing the expression of mutant polyglutamine proteins, e.g. with antisense oligonucleotides (ASO). This approach was already tested in patients [228, 234]. But administration is not trivial, especially if the target is located in deeper brain regions [189]. The ASO was administered intrathecally but the necessary permanent administration is not optimal for the treated patients compared with D-peptide compounds that possibly may be administered orally [110].

In order to find D-enantiomeric peptide ligands for polyglutamine proteins, mirror image phage display selections were performed. This method is suitable to find target specific, D-enantiomeric peptide ligands [216, 217].

The selected drug candidates were tested in ThT-assays with respect to their ability to inhibit ThT-active aggregation. ThT is a fluorophore whose emission spectrum shifts to 482 nm when it binds to amyloid fibrils [220]. It follows that the formation of amyloid fibrils can be monitored by measuring the fluorescence at 482 nm. The signal intensity correlates with the amount of formed ThT-active aggregates [220], which enables quantification of the peptide compound's inhibiting effect on the formation of amyloid fibrils.

When QF1D-1 and QF1D-2 were measured with the SPR technique, it was not possible to observe saturation. This could be due to the self-aggregating properties of the compounds. Presumably, the compounds bind to already bound compounds increasing the response with increasing concentration and no saturation can be reached.

Treatment of neurodegenerative diseases usually starts after symptoms occur. At this time point there will already be misfolded proteins and aggregates in the cells. An effective compound must inhibit the aggregation under seeding conditions. Whereas inhibition of *de novo* aggregation only requires stabilizing the monomers in their native conformation, under seeding conditions it is required to prevent monomer recruitment and optimally dissolve preformed aggregates into their monomeric components. QF1D-1 and QF1D-2 did inhibit the aggregation when seeds were present.

Further CD-measurements revealed that K2Q23K2, although it easily dissolved in aqueous buffer, was folded into a beta-sheet structure. This could have been provoked by the lyophilization. Since Annika Krüger assumed the Q23-construct would not aggregate at low concentrations and therefore did not disaggregate the target prior to selection, she most likely selected on beta-sheet structures. This could explain why the selected peptide compounds show self-aggregating tendencies. Binders of amyloid, beta-sheet structures most likely will aggregate with themselves into such or similar structures.

Disaggregated QF1D-1 lost its inhibiting effect and that of QF1D-2 was attenuated. The previous experiments showed that the compounds themselves do not form ThT-active aggregates. Probably the pre-formed compound aggregates initiated the polyglutamine proteins to form non-ThT-active aggregates as well. But when both reagents are monomeric from the start, compounds could aggregate with the polyglutamine proteins into ThT-active fibrils, which would explain why the disaggregated QF1D-1 accelerated the aggregation.

Self-aggregating compounds are not suitable as therapeutics, since their concentration and efficacy depend on the aggregation state. This would contradict a reliable and reproducible administration. Due to that a new selection was performed.

To ensure the new selection was performed on a monomeric target that was not folded into beta-sheet structures, the D-biotin K2Q23K2 was disaggregated prior to the selection. In parallel to the target samples, some of the D-biotin K2Q23K2 samples were kept as controls. The controls were stored like the selection targets. A CD-measurement was performed with the target control samples. The spectrum was the mirror image of the typical spectrum for disaggregated polyglutamine proteins [45], as would be expected for a D-enantiomeric protein. It follows that the selection was performed on monomeric target that was not misfolded into beta-sheet.

The evaluation via NGS enables a good overview of the sequence's distribution in target selection and empty selection. In the empty selection the ttds-linker was immobilized with biotin. This enabled to reference the target selection for linker ligands, so only target binders would obtain a high empty score. The evaluation revealed that sequences became enriched in the target selection, some being leading sequence in clusters. Some sequences were selected on D-K2Q23K2 and D-ARQ23, indicating that in both cases there was specific selection pressure favoring polyglutamine binders.

Since oligomers are thought to be the toxic species [62, 104], the effectiveness was tested in presence of soluble aggregate fragments. QF1D-13 and QF1D-14 had an inhibiting effect compared to the control peptide compound P8, which was selected on SOD1 and should therefore not bind to polyglutamine. So both peptide compounds, QF1D-13 and QF1D-14, feature the most essential ability of a promising drug candidate- the ability to inhibit seeded aggregation.

Although SPR measurements indicated binding of QF1D-14 to K2Q23K2, no saturation was reached. With increasing compound concentration, unspecific interactions become more weighted in the overall signal, which can prevent saturation effects.

QF2D-2 showed strong matrix binding in the SPR measurements. But the binding to L-ARQ46 was faster. Referencing with FC1, on which nothing was immobilized, caused a drop of the referenced curve after the first rise due to a shifted rise of the reference signal. This resulted in an unusually shaped binding curve that prevented a kinetic fit.

An optimal drug candidate would not only inhibit aggregation, but also disassemble already formed aggregates. To test whether QF2D-2 was able to do so, it was added to L-ARQ46 after aggregation onset. Later addition of the compound after lag-time termination, shifted the ThT-curve marginally to the right. Disassembly of aggregates with the compound would result in clear reduction of the ThT-signal. Presumably, QF2D-2 impeded the monomer recruitment, which marginally decreased the slope. This would be consistent with the observation that QF2D-2 decelerates seeded aggregation, presumably through hampering secondary nucleation and monomer recruitment.

6. SUMMARY AND OUTLOOK

In this study mirror image phage display selections were performed to identify D-enantiomeric peptide ligands for polyglutamine proteins. A general D-enantiomeric polyglutamine protein with flanking lysines and a D-enantiomeric fragment of the androgen receptor served as targets. Both selections were successful and several D-enantiomeric peptide compounds were characterized with respect to their ability to inhibit the amyloidogenic aggregation of polyglutamine proteins and their binding properties.

QF2D-2 was the D-peptide compound with the most promising characteristics. QF2D-2 was selected on the fragment of the androgen receptor. It decelerated the aggregation of the same fragment with an elongated polyglutamine tract, even in presence of seeds and bound to it with a K_D in the low micromolar range. QF2D-2 also bound to the general polyglutamine construct and decelerated its aggregation. CD-spectroscopic measurements showed that the presence of QF2D-2 delayed the transition of ARQ46 from its disaggregated state to beta-sheet rich structures.

An elongated polyglutamine tract causes the androgen receptor to misfold and aggregate which causes SBMA. This is a common mechanism in nine heritable polyglutamine diseases. To this day, no causative therapy is available for these fatal diseases, so it is an urgent need to find effective therapeutics.

Since QF2D-2 showed effectiveness in the experiments with the general polyglutamine protein, it might be a drug candidate for all nine polyglutamine misfolding diseases. After further optimization with respect to binding affinity, aggregation inhibition properties, and blood brain barrier permeability, QF2D-2 has the potential to be tested in animal models and even clinical trials if the neurological phenotype in the animal models would be improved. An optimized QF2D-2 could be an effective treatment for the nine heritable polyglutamine misfolding diseases.

REFERENCES

1. Orr, H.T. and H.Y. Zoghbi, *Trinucleotide repeat disorders.* Annu Rev Neurosci, 2007. **30**: p. 575-621.10.1146/annurev.neuro.29.051605.113042
2. Schaefer, M.H., E.E. Wanker, and M.A. Andrade-Navarro, *Evolution and function of CAG/polyglutamine repeats in protein-protein interaction networks.* Nucleic Acids Res, 2012. **40**(10): p. 4273-87.10.1093/nar/gks011
3. Hayden, D.D.O.M.a.M.R., *Neurodegeneration: Role of repeats in protein clearance.* Nature, 2017. **545.7652**: p. 33-34.10.1101/116178
4. Creighton, T.E., *Proteins: structures and molecular properties.* 1993: Macmillan
5. Butland, S.L., R.S. Devon, Y. Huang, C.L. Mead, A.M. Meynert, S.J. Neal, S.S. Lee, A. Wilkinson, G.S. Yang, M.M. Yuen, M.R. Hayden, R.A. Holt, B.R. Leavitt, and B.F. Ouellette, *CAG-encoded polyglutamine length polymorphism in the human genome.* BMC Genomics, 2007. **8**: p. 126.10.1186/1471-2164-8-126
6. Pelassa, I., D. Cora, F. Cesano, F.J. Monje, P.G. Montarolo, and F. Fiumara, *Association of polyalanine and polyglutamine coiled coils mediates expansion disease-related protein aggregation and dysfunction.* Human molecular genetics, 2014. **23**(13): p. 3402-3420
7. Totzeck, F., M.A. Andrade-Navarro, and P. Mier, *The Protein Structure Context of PolyQ Regions.* PLoS One, 2017. **12**(1): p. e0170801.10.1371/journal.pone.0170801
8. Fiumara, F., L. Fioriti, E.R. Kandel, and W.A. Hendrickson, *Essential role of coiled coils for aggregation and activity of Q/N-rich prions and PolyQ proteins.* Cell, 2010. **143**(7): p. 1121-35.10.1016/j.cell.2010.11.042
9. Karlin, S. and C. Burge, *Trinucleotide repeats and long homopeptides in genes and proteins associated with nervous system disease and development.* Proceedings of the National Academy of Sciences, 1996. **93**(4): p. 1560-1565
10. Alba, M.M. and R. Guigó, *Comparative analysis of amino acid repeats in rodents and humans.* Genome research, 2004. **14**(4): p. 549-554
11. Harrison, P.M., *Exhaustive assignment of compositional bias reveals universally prevalent biased regions: analysis of functional associations in human and Drosophila.* BMC Bioinformatics, 2006. **7**: p. 441.10.1186/1471-2105-7-441
12. Rui, Y.N., Z. Xu, B. Patel, Z. Chen, D. Chen, A. Tito, G. David, Y. Sun, E.F. Stimming, H.J. Bellen, A.M. Cuervo, and S. Zhang, *Huntingtin functions as a scaffold for selective macroautophagy.* Nat Cell Biol, 2015. **17**(3): p. 262-75.10.1038/ncb3101
13. Ashkenazi, A., C.F. Bento, T. Ricketts, M. Vicinanza, F. Siddiqi, M. Pavel, F. Squitieri, M.C. Hardenberg, S. Imarisio, F.M. Menzies, and D.C. Rubinsztein, *Polyglutamine tracts regulate beclin 1-dependent autophagy.* Nature, 2017. **545**(7652): p. 108-111.10.1038/nature22078
14. Crick, S.L., M. Jayaraman, C. Frieden, R. Wetzel, and R.V. Pappu, *Fluorescence correlation spectroscopy shows that monomeric polyglutamine molecules form collapsed structures in aqueous solutions.* Proceedings of the National Academy of Sciences, 2006. **103**(45): p. 16764-16769
15. Gerbich, T.M. and A.S. Gladfelter, *Moving beyond disease to function: Physiological roles for polyglutamine-rich sequences in cell decisions.* Curr Opin Cell Biol, 2021. **69**: p. 120-126.10.1016/j.ceb.2021.01.003
16. Dobson, C.M., *Protein folding and misfolding.* Nature, 2003. **426**(6968): p. 884-890
17. Gething, M.-J. and J. Sambrook, *Protein folding in the cell.* Nature, 1992. **355**(6355): p. 33-45
18. Balchin, D., M. Hayer-Hartl, and F.U. Hartl, *In vivo aspects of protein folding and quality control.* Science, 2016. **353**(6294): p. aac4354.10.1126/science.aac4354
19. Miyata, Y., T. Shibata, M. Aoshima, T. Tsubata, and E. Nishida, *The molecular chaperone TRiC/CCT binds to the Trp-Asp 40 (WD40) repeat protein WDR68 and promotes its folding, protein kinase DYRK1A binding, and nuclear accumulation.* J Biol Chem, 2014. **289**(48): p. 33320-32.10.1074/jbc.M114.586115

20. Brehme, M., C. Voisine, T. Rolland, S. Wachi, J.H. Soper, Y. Zhu, K. Orton, A. Villella, D. Garza, M. Vidal, H. Ge, and R.I. Morimoto, *A chaperome subnetwork safeguards proteostasis in aging and neurodegenerative disease.* Cell Rep, 2014. **9**(3): p. 1135-50.10.1016/j.celrep.2014.09.042

21. Richarme, G. and M. Kohiyama, *Specificity of the Escherichia coli chaperone DnaK (70-kDa heat shock protein) for hydrophobic amino acids.* Journal of Biological Chemistry, 1993. **268**(32): p. 24074-24077

22. Pelham, H.R., *Speculations on the functions of the major heat shock and glucose-regulated proteins.* Cell, 1986. **46**(7): p. 959-961

23. Prischi, F., C. Pastore, M. Carroni, C. Iannuzzi, S. Adinolfi, P. Temussi, and A. Pastore, *Of the vulnerability of orphan complex proteins: the case study of the E. coli IscU and IscS proteins.* Protein expression and purification, 2010. **73**(2): p. 161-166

24. Saric, A., A.K. Buell, G. Meisl, T.C.T. Michaels, C.M. Dobson, S. Linse, T.P.J. Knowles, and D. Frenkel, *Physical determinants of the self-replication of protein fibrils.* Nat Phys, 2016. **12**(9): p. 874-880.10.1038/nphys3828

25. Soto, C., *Protein misfolding and disease; protein refolding and therapy.* FEBS letters, 2001. **498**(2-3): p. 204-207

26. Pastore, A. and P.A. Temussi, *The two faces of Janus: functional interactions and protein aggregation.* Curr Opin Struct Biol, 2012. **22**(1): p. 30-7.10.1016/j.sbi.2011.11.007

27. Lapidus, L.J., *Understanding protein aggregation from the view of monomer dynamics.* Mol Biosyst, 2013. **9**(1): p. 29-35.10.1039/c2mb25334h

28. Murphy, R.M., *Peptide aggregation in neurodegenerative disease.* Annu Rev Biomed Eng, 2002. **4**: p. 155-74.10.1146/annurev.bioeng.4.092801.094202

29. Iuchi, S., G. Hoffner, P. Verbeke, P. Djian, and H. Green, *Oligomeric and polymeric aggregates formed by proteins containing expanded polyglutamine.* Proceedings of the National Academy of Sciences, 2003. **100**(5): p. 2409-2414

30. Michaels, T.C.T., C.A. Weber, and L. Mahadevan, *Optimal control strategies for inhibition of protein aggregation.* Proc Natl Acad Sci U S A, 2019. **116**(29): p. 14593-14598.10.1073/pnas.1904090116

31. Adegbuyiro, A., F. Sedighi, A.W.t. Pilkington, S. Groover, and J. Legleiter, *Proteins Containing Expanded Polyglutamine Tracts and Neurodegenerative Disease.* Biochemistry, 2017. **56**(9): p. 1199-1217.10.1021/acs.biochem.6b00936

32. Knowles, T.P., C.A. Waudby, G.L. Devlin, S.I. Cohen, A. Aguzzi, M. Vendruscolo, E.M. Terentjev, M.E. Welland, and C.M. Dobson, *An analytical solution to the kinetics of breakable filament assembly.* Science, 2009. **326**(5959): p. 1533-1537

33. Rambaran, R.N. and L.C. Serpell, *Amyloid fibrils: abnormal protein assembly.* Prion, 2008. **2**(3): p. 112-7.10.4161/pri.2.3.7488

34. Eanes, E. and G.G. Glenner, *X-ray diffraction studies on amyloid filaments.* Journal of Histochemistry & Cytochemistry, 1968. **16**(11): p. 673-677

35. Frost, B. and M.I. Diamond, *Prion-like mechanisms in neurodegenerative diseases.* Nat Rev Neurosci, 2010. **11**(3): p. 155-9.10.1038/nrn2786

36. Seeley, W.W., R.K. Crawford, J. Zhou, B.L. Miller, and M.D. Greicius, *Neurodegenerative diseases target large-scale human brain networks.* Neuron, 2009. **62**(1): p. 42-52.10.1016/j.neuron.2009.03.024

37. Meisl, G., X. Yang, C.M. Dobson, S. Linse, and T.P. Knowles, *A general reaction network unifies the aggregation behaviour of the A β42 peptide and its variants.* arXiv preprint arXiv:1604.00828, 2016

38. Meisl, G., X. Yang, B. Frohm, T.P. Knowles, and S. Linse, *Quantitative analysis of intrinsic and extrinsic factors in the aggregation mechanism of Alzheimer-associated Abeta-peptide.* Sci Rep, 2016. **6**: p. 18728.10.1038/srep18728

39. Cui, X., Q. Liang, Y. Liang, M. Lu, Y. Ding, and B. Lu, *TR-FRET assays of Huntingtin protein fragments reveal temperature and polyQ length-dependent conformational changes.* Sci Rep, 2014. **4**: p. 5601.10.1038/srep05601

40. Nekooki-Machida, Y., M. Kurosawa, N. Nukina, K. Ito, T. Oda, and M. Tanaka, *Distinct conformations of in vitro and in vivo amyloids of huntingtin-exon1 show different cytotoxicity.* Proceedings of the National Academy of Sciences, 2009. **106**(24): p. 9679-9684

41. Matsumoto, G., S. Kim, and R.I. Morimoto, *Huntingtin and mutant SOD1 form aggregate structures with distinct molecular properties in human cells.* J Biol Chem, 2006. **281**(7): p. 4477-85.10.1074/jbc.M509201200

42. Vitalis, A., X. Wang, and R.V. Pappu, *Quantitative characterization of intrinsic disorder in polyglutamine: insights from analysis based on polymer theories.* Biophys J, 2007. **93**(6): p. 1923-37.10.1529/biophysj.107.110080

43. Kim, M.W., Y. Chelliah, S.W. Kim, Z. Otwinowski, and I. Bezprozvanny, *Secondary structure of Huntingtin amino-terminal region.* Structure, 2009. **17**(9): p. 1205-12.10.1016/j.str.2009.08.002

44. Zhemkov, V.A., A.A. Kulminskaya, I.B. Bezprozvanny, and M. Kim, *The 2.2-Angstrom resolution crystal structure of the carboxy-terminal region of ataxin-3.* FEBS Open Bio, 2016. **6**(3): p. 168-78.10.1002/2211-5463.12029

45. Chen, S., V. Berthelier, W. Yang, and R. Wetzel, *Polyglutamine aggregation behavior in vitro supports a recruitment mechanism of cytotoxicity.* J Mol Biol, 2001. **311**(1): p. 173-82.10.1006/jmbi.2001.4850

46. Perutz, M.F., T. Johnson, M. Suzuki, and J.T. Finch, *Glutamine repeats as polar zippers: their possible role in inherited neurodegenerative diseases.* Proceedings of the National Academy of Sciences, 1994. **91**(12): p. 5355-5358

47. Digambaranath, J.L., T.V. Campbell, A. Chung, M.J. McPhail, K.E. Stevenson, M.A. Zohdy, and J.M. Finke, *An accurate model of polyglutamine.* Proteins, 2011. **79**(5): p. 1427-40.10.1002/prot.22970

48. Hoop, C.L., H.K. Lin, K. Kar, G. Magyarfalvi, J.M. Lamley, J.C. Boatz, A. Mandal, J.R. Lewandowski, R. Wetzel, and P.C. van der Wel, *Huntingtin exon 1 fibrils feature an interdigitated beta-hairpin-based polyglutamine core.* Proc Natl Acad Sci U S A, 2016. **113**(6): p. 1546-51.10.1073/pnas.1521933113

49. Legleiter, J., E. Mitchell, G.P. Lotz, E. Sapp, C. Ng, M. DiFiglia, L.M. Thompson, and P.J. Muchowski, *Mutant huntingtin fragments form oligomers in a polyglutamine length-dependent manner in vitro and in vivo.* J Biol Chem, 2010. **285**(19): p. 14777-90.10.1074/jbc.M109.093708

50. Walters, R.H. and R.M. Murphy, *Examining polyglutamine peptide length: a connection between collapsed conformations and increased aggregation.* J Mol Biol, 2009. **393**(4): p. 978-92.10.1016/j.jmb.2009.08.034

51. Thakur, A.K., M. Jayaraman, R. Mishra, M. Thakur, V.M. Chellgren, I.J. Byeon, D.H. Anjum, R. Kodali, T.P. Creamer, J.F. Conway, A.M. Gronenborn, and R. Wetzel, *Polyglutamine disruption of the huntingtin exon 1 N terminus triggers a complex aggregation mechanism.* Nat Struct Mol Biol, 2009. **16**(4): p. 380-9.10.1038/nsmb.1570

52. Kar, K., M. Jayaraman, B. Sahoo, R. Kodali, and R. Wetzel, *Critical nucleus size for disease-related polyglutamine aggregation is repeat-length dependent.* Nat Struct Mol Biol, 2011. **18**(3): p. 328-36.10.1038/nsmb.1992

53. Poirier, M.A., H. Li, J. Macosko, S. Cai, M. Amzel, and C.A. Ross, *Huntingtin spheroids and protofibrils as precursors in polyglutamine fibrilization.* J Biol Chem, 2002. **277**(43): p. 41032-7.10.1074/jbc.M205809200

54. Wacker, J.L., M.H. Zareie, H. Fong, M. Sarikaya, and P.J. Muchowski, *Hsp70 and Hsp40 attenuate formation of spherical and annular polyglutamine oligomers by partitioning monomer.* Nat Struct Mol Biol, 2004. **11**(12): p. 1215-22.10.1038/nsmb860

55. Jayaraman, M., R. Kodali, B. Sahoo, A.K. Thakur, A. Mayasundari, R. Mishra, C.B. Peterson, and R. Wetzel, *Slow amyloid nucleation via alpha-helix-rich oligomeric intermediates in short polyglutamine-containing huntingtin fragments.* J Mol Biol, 2012. **415**(5): p. 881-99.10.1016/j.jmb.2011.12.010

56. Jayaraman, M., R. Mishra, R. Kodali, A.K. Thakur, L.M. Koharudin, A.M. Gronenborn, and R. Wetzel, *Kinetically competing huntingtin aggregation pathways control amyloid polymorphism and properties.* Biochemistry, 2012. **51**(13): p. 2706-16.10.1021/bi3000929

57. Ruggeri, F.S., S. Vieweg, U. Cendrowska, G. Longo, A. Chiki, H.A. Lashuel, and G. Dietler, *Nanoscale studies link amyloid maturity with polyglutamine diseases onset.* Sci Rep, 2016. **6**: p. 31155.10.1038/srep31155

58. Behrends, C., C.A. Langer, R. Boteva, U.M. Bottcher, M.J. Stemp, G. Schaffar, B.V. Rao, A. Giese, H. Kretzschmar, K. Siegers, and F.U. Hartl, *Chaperonin TRiC promotes the assembly of polyQ expansion proteins into nontoxic oligomers.* Mol Cell, 2006. **23**(6): p. 887-97.10.1016/j.molcel.2006.08.017

59. Bernacki, J.P. and R.M. Murphy, *Length-dependent aggregation of uninterrupted polyalanine peptides.* Biochemistry, 2011. **50**(43): p. 9200-11.10.1021/bi201155g

60. Lee, C.C., R.H. Walters, and R.M. Murphy, *Reconsidering the mechanism of polyglutamine peptide aggregation.* Biochemistry, 2007. **46**(44): p. 12810-12820

61. Nucifora, F.C., M. Sasaki, M.F. Peters, H. Huang, J.K. Cooper, M. Yamada, H. Takahashi, S. Tsuji, J. Troncoso, and V.L. Dawson, *Interference by huntingtin and atrophin-1 with cbp-mediated transcription leading to cellular toxicity.* Science, 2001. **291**(5512): p. 2423-2428

62. Jochum, T., M.E. Ritz, C. Schuster, S.F. Funderburk, K. Jehle, K. Schmitz, F. Brinkmann, M. Hirtz, D. Moss, and A.C. Cato, *Toxic and non-toxic aggregates from the SBMA and normal forms of androgen receptor have distinct oligomeric structures.* Biochim Biophys Acta, 2012. **1822**(6): p. 1070-8.10.1016/j.bbadis.2012.02.006

63. Williamson, T.E., A. Vitalis, S.L. Crick, and R.V. Pappu, *Modulation of polyglutamine conformations and dimer formation by the N-terminus of huntingtin.* J Mol Biol, 2010. **396**(5): p. 1295-309.10.1016/j.jmb.2009.12.017

64. Sahoo, B., I. Arduini, K.W. Drombosky, R. Kodali, L.H. Sanders, J.T. Greenamyre, and R. Wetzel, *Folding Landscape of Mutant Huntingtin Exon1: Diffusible Multimers, Oligomers and Fibrils, and No Detectable Monomer.* PLoS One, 2016. **11**(6): p. e0155747.10.1371/journal.pone.0155747

65. Sahoo, B., D. Singer, R. Kodali, T. Zuchner, and R. Wetzel, *Aggregation behavior of chemically synthesized, full-length huntingtin exon1.* Biochemistry, 2014. **53**(24): p. 3897-907.10.1021/bi500300c

66. Vitalis, A. and R.V. Pappu, *Assessing the contribution of heterogeneous distributions of oligomers to aggregation mechanisms of polyglutamine peptides.* Biophys Chem, 2011. **159**(1): p. 14-23.10.1016/j.bpc.2011.04.006

67. Scherzinger, E., A. Sittler, K. Schweiger, V. Heiser, R. Lurz, R. Hasenbank, G.P. Bates, H. Lehrach, and E.E. Wanker, *Self-assembly of polyglutamine-containing huntingtin fragments into amyloid-like fibrils: implications for Huntington's disease pathology.* Proceedings of the National Academy of Sciences, 1999. **96**(8): p. 4604-4609

68. Scherzinger, E., R. Lurz, M. Turmaine, L. Mangiarini, B. Hollenbach, R. Hasenbank, G.P. Bates, S.W. Davies, H. Lehrach, and E.E. Wanker, *Huntingtin-encoded polyglutamine expansions form amyloid-like protein aggregates in vitro and in vivo.* Cell, 1997. **90**(3): p. 549-558

69. Chen, S., V. Berthelier, J.B. Hamilton, B. O'Nuallai, and R. Wetzel, *Amyloid-like features of polyglutamine aggregates and their assembly kinetics.* Biochemistry, 2002. **41**(23): p. 7391-7399

70. Chen, S., F.A. Ferrone, and R. Wetzel, *Huntington's disease age-of-onset linked to polyglutamine aggregation nucleation.* Proceedings of the National Academy of sciences, 2002. **99**(18): p. 11884-11889

71. Landrum, E. and R. Wetzel, *Biophysical underpinnings of the repeat length dependence of polyglutamine amyloid formation.* J Biol Chem, 2014. **289**(15): p. 10254-60.10.1074/jbc.C114.552943

72.   Trevino, R.S., J.E. Lauckner, Y. Sourigues, M.M. Pearce, L. Bousset, R. Melki, and R.R. Kopito, *Fibrillar structure and charge determine the interaction of polyglutamine protein aggregates with the cell surface.* J Biol Chem, 2012. **287**(35): p. 29722-8.10.1074/jbc.M112.372474

73.   Scarafone, N., C. Pain, A. Fratamico, G. Gaspard, N. Yilmaz, P. Filee, M. Galleni, A. Matagne, and M. Dumoulin, *Amyloid-like fibril formation by polyQ proteins: a critical balance between the polyQ length and the constraints imposed by the host protein.* PLoS One, 2012. **7**(3): p. e31253.10.1371/journal.pone.0031253

74.   Bhattacharyya, A., A.K. Thakur, V.M. Chellgren, G. Thiagarajan, A.D. Williams, B.W. Chellgren, T.P. Creamer, and R. Wetzel, *Oligoproline effects on polyglutamine conformation and aggregation.* J Mol Biol, 2006. **355**(3): p. 524-35.10.1016/j.jmb.2005.10.053

75.   Smaoui, M.R., C. Mazza-Anthony, and J. Waldispuhl, *Investigating Mutations to Reduce Huntingtin Aggregation by Increasing Htt-N-Terminal Stability and Weakening Interactions with PolyQ Domain.* Comput Math Methods Med, 2016. **2016**: p. 6247867.10.1155/2016/6247867

76.   Saunders, H.M. and S.P. Bottomley, *Multi-domain misfolding: understanding the aggregation pathway of polyglutamine proteins.* Protein Eng Des Sel, 2009. **22**(8): p. 447-51.10.1093/protein/gzp033

77.   Lakhani, V.V., F. Ding, and N.V. Dokholyan, *Polyglutamine induced misfolding of huntingtin exon1 is modulated by the flanking sequences.* PLoS Comput Biol, 2010. **6**(4): p. e1000772.10.1371/journal.pcbi.1000772

78.   Ossato, G., M.A. Digman, C. Aiken, T. Lukacsovich, J.L. Marsh, and E. Gratton, *A two-step path to inclusion formation of huntingtin peptides revealed by number and brightness analysis.* Biophys J, 2010. **98**(12): p. 3078-85.10.1016/j.bpj.2010.02.058

79.   Li, L., H. Liu, P. Dong, D. Li, W.R. Legant, J.B. Grimm, L.D. Lavis, E. Betzig, R. Tjian, and Z. Liu, *Real-time imaging of Huntingtin aggregates diverting target search and gene transcription.* Elife, 2016. **5**.10.7554/eLife.17056

80.   Beam, M., M.C. Silva, and R.I. Morimoto, *Dynamic imaging by fluorescence correlation spectroscopy identifies diverse populations of polyglutamine oligomers formed in vivo.* J Biol Chem, 2012. **287**(31): p. 26136-45.10.1074/jbc.M112.362764

81.   Oppong, E., G. Stier, M. Gaal, R. Seeger, M. Stoeck, M.A. Delsuc, A.C.B. Cato, and B. Kieffer, *An Amyloidogenic Sequence at the N-Terminus of the Androgen Receptor Impacts Polyglutamine Aggregation.* Biomolecules, 2017. **7**(2).10.3390/biom7020044

82.   Petrakis, S., M.H. Schaefer, E.E. Wanker, and M.A. Andrade-Navarro, *Aggregation of polyQ-extended proteins is promoted by interaction with their natural coiled-coil partners.* Bioessays, 2013. **35**(6): p. 503-7.10.1002/bies.201300001

83.   de Chiara, C. and A. Pastore, *Kaleidoscopic protein-protein interactions in the life and death of ataxin-1: new strategies against protein aggregation.* Trends Neurosci, 2014. **37**(4): p. 211-8.10.1016/j.tins.2014.02.003

84.   Hartl, F.U., *Protein Misfolding Diseases.* Annu Rev Biochem, 2017. **86**: p. 21-26.10.1146/annurev-biochem-061516-044518

85.   Spillantini, M.G., T.D. Bird, and B. Ghetti, *Frontotemporal dementia and Parkinsonism linked to chromosome 17: a new group of tauopathies.* Brain pathology, 1998. **8**(2): p. 387-402

86.   Hardy, J. and D.J. Selkoe, *The amyloid hypothesis of Alzheimer's disease: progress and problems on the road to therapeutics.* science, 2002. **297**(5580): p. 353-356

87.   Nordlund, A. and M. Oliveberg, *SOD1-associated ALS: a promising system for elucidating the origin of protein-misfolding disease.* HFSP J, 2008. **2**(6): p. 354-64.10.2976/1.2995726

88.   Douglas, P.M. and A. Dillin, *Protein homeostasis and aging in neurodegeneration.* J Cell Biol, 2010. **190**(5): p. 719-29.10.1083/jcb.201005144

89.   La Spada, A.R., E.M. Wilson, D.B. Lubahn, A. Harding, and K.H. Fischbeck, *Androgen receptor gene mutations in X-linked spinal and bulbar muscular atrophy.* Nature, 1991. **352**(6330): p. 77-79

90. van Ham, T.J., K.L. Thijssen, R. Breitling, R.M. Hofstra, R.H. Plasterk, and E.A. Nollen, *C. elegans model identifies genetic modifiers of alpha-synuclein inclusion formation during aging.* PLoS Genet, 2008. **4**(3): p. e1000027.10.1371/journal.pgen.1000027

91. Kitada, T., S. Asakawa, N. Hattori, H. Matsumine, Y. Yamamura, S. Minoshima, M. Yokochi, Y. Mizuno, and N. Shimizu, *Mutations in the parkin gene cause autosomal recessive juvenile parkinsonism.* nature, 1998. **392**(6676): p. 605-608

92. Bentahir, M., O. Nyabi, J. Verhamme, A. Tolia, K. Horre, J. Wiltfang, H. Esselmann, and B. De Strooper, *Presenilin clinical mutations can affect gamma-secretase activity by different mechanisms.* J Neurochem, 2006. **96**(3): p. 732-42.10.1111/j.1471-4159.2005.03578.x

93. West, A.B., D.J. Moore, S. Biskup, A. Bugayenko, W.W. Smith, C.A. Ross, V.L. Dawson, and T.M. Dawson, *Parkinson's disease-associated mutations in leucine-rich repeat kinase 2 augment kinase activity.* Proceedings of the National Academy of Sciences, 2005. **102**(46): p. 16842-16847

94. Temussi, P.A., L. Masino, and A. Pastore, *From Alzheimer to Huntington: why is a structural understanding so difficult?* The EMBO journal, 2003. **22**(3): p. 355-361

95. El-Daher, M.T., E. Hangen, J. Bruyere, G. Poizat, I. Al-Ramahi, R. Pardo, N. Bourg, S. Souquere, C. Mayet, G. Pierron, S. Leveque-Fort, J. Botas, S. Humbert, and F. Saudou, *Huntingtin proteolysis releases non-polyQ fragments that cause toxicity through dynamin 1 dysregulation.* EMBO J, 2015. **34**(17): p. 2255-71.10.15252/embj.201490808

96. Moussa, C.E.-H., C. Wersinger, Y. Tomita, and A. Sidhu, *Differential cytotoxicity of human wild type and mutant α-synuclein in human neuroblastoma SH-SY5Y cells in the presence of dopamine.* Biochemistry, 2004. **43**(18): p. 5539-5550

97. Selkoe, D.J., *Alzheimer's disease results from the cerebral accumulation and cytotoxicity of amyloid\beta-protein.* Journal of Alzheimer's Disease, 2001. **3**(1): p. 75-82

98. Wang, M.S., S. Boddapati, S. Emadi, and M.R. Sierks, *Curcumin reduces α-synuclein induced cytotoxicity in Parkinson's disease cell model.* BMC neuroscience, 2010. **11**(1): p. 57

99. Bhatia, N.K., A. Srivastava, N. Katyal, N. Jain, M.A.I. Khan, B. Kundu, and S. Deep, *Curcumin binds to the pre-fibrillar aggregates of Cu/Zn superoxide dismutase (SOD1) and alters its amyloidogenic pathway resulting in reduced cytotoxicity.* Biochimica et Biophysica Acta (BBA)-Proteins and Proteomics, 2015. **1854**(5): p. 426-436

100. Fath, T., J. Eidenmüller, and R. Brandt, *Tau-mediated cytotoxicity in a pseudohyperphosphorylation model of Alzheimer's disease.* Journal of Neuroscience, 2002. **22**(22): p. 9733-9741

101. LaFevre-Bernt, M.A. and L.M. Ellerby, *Kennedy's disease. Phosphorylation of the polyglutamine-expanded form of androgen receptor regulates its cleavage by caspase-3 and enhances cell death.* J Biol Chem, 2003. **278**(37): p. 34918-24.10.1074/jbc.M302841200

102. Prusiner, S.B. and K.K. Hsiao, *Human prion diseases.* Annals of Neurology: Official Journal of the American Neurological Association and the Child Neurology Society, 1994. **35**(4): p. 385-395

103. Saudou, F., S. Finkbeiner, D. Devys, and M.E. Greenberg, *Huntingtin acts in the nucleus to induce apoptosis but death does not correlate with the formation of intranuclear inclusions.* Cell, 1998. **95**(1): p. 55-66

104. Campioni, S., B. Mannini, M. Zampagni, A. Pensalfini, C. Parrini, E. Evangelisti, A. Relini, M. Stefani, C.M. Dobson, C. Cecchi, and F. Chiti, *A causative link between the structure of aberrant protein oligomers and their toxicity.* Nat Chem Biol, 2010. **6**(2): p. 140-7.10.1038/nchembio.283

105. Reixach, N., S. Deechongkit, X. Jiang, J.W. Kelly, and J.N. Buxbaum, *Tissue damage in the amyloidoses: Transthyretin monomers and nonnative oligomers are the major cytotoxic species in tissue culture.* Proceedings of the National Academy of Sciences, 2004. **101**(9): p. 2817-2822

106. Kumar, R., S. Das, G.M. Mohite, S.K. Rout, S. Halder, N.N. Jha, S. Ray, S. Mehra, V. Agarwal, and S.K. Maji, *Cytotoxic Oligomers and Fibrils Trapped in a Gel-like State of alpha-Synuclein Assemblies.* Angew Chem Int Ed Engl, 2018. **57**(19): p. 5262-5266.10.1002/anie.201711854

107. Malisauskas, M., J. Ostman, A. Darinskas, V. Zamotin, E. Liutkevicius, E. Lundgren, and L.A. Morozova-Roche, *Does the cytotoxic effect of transient amyloid oligomers from common equine lysozyme in vitro imply innate amyloid toxicity?* J Biol Chem, 2005. **280**(8): p. 6269-75.10.1074/jbc.M407273200

108. Chiti, F. and C.M. Dobson, *Protein misfolding, functional amyloid, and human disease.* Annu Rev Biochem, 2006. **75**: p. 333-66.10.1146/annurev.biochem.75.101304.123901

109. Kim, Y.E., F. Hosp, F. Frottin, H. Ge, M. Mann, M. Hayer-Hartl, and F.U. Hartl, *Soluble Oligomers of PolyQ-Expanded Huntingtin Target a Multiplicity of Key Cellular Factors.* Mol Cell, 2016. **63**(6): p. 951-64.10.1016/j.molcel.2016.07.022

110. van Groen, T., S. Schemmert, O. Brener, L. Gremer, T. Ziehm, M. Tusche, L. Nagel-Steger, I. Kadish, E. Schartmann, A. Elfgen, D. Jurgens, A. Willuweit, J. Kutzsche, and D. Willbold, *The Abeta oligomer eliminating D-enantiomeric peptide RD2 improves cognition without changing plaque pathology.* Sci Rep, 2017. **7**(1): p. 16275.10.1038/s41598-017-16565-1

111. Olzscha, H., S.M. Schermann, A.C. Woerner, S. Pinkert, M.H. Hecht, G.G. Tartaglia, M. Vendruscolo, M. Hayer-Hartl, F.U. Hartl, and R.M. Vabulas, *Amyloid-like aggregates sequester numerous metastable proteins with essential cellular functions.* Cell, 2011. **144**(1): p. 67-78.10.1016/j.cell.2010.11.050

112. Freibaum, B.D., Y. Lu, R. Lopez-Gonzalez, N.C. Kim, S. Almeida, K.H. Lee, N. Badders, M. Valentine, B.L. Miller, P.C. Wong, L. Petrucelli, H.J. Kim, F.B. Gao, and J.P. Taylor, *GGGGCC repeat expansion in C9orf72 compromises nucleocytoplasmic transport.* Nature, 2015. **525**(7567): p. 129-33.10.1038/nature14974

113. Woerner, A.C., F. Frottin, D. Hornburg, L.R. Feng, F. Meissner, M. Patra, J. Tatzelt, M. Mann, K.F. Winklhofer, and F.U. Hartl, *Cytoplasmic protein aggregates interfere with nucleocytoplasmic transport of protein and RNA.* Science, 2016. **351**(6269): p. 173-176

114. Choe, Y.J., S.H. Park, T. Hassemer, R. Korner, L. Vincenz-Donnelly, M. Hayer-Hartl, and F.U. Hartl, *Failure of RQC machinery causes protein aggregation and proteotoxic stress.* Nature, 2016. **531**(7593): p. 191-5.10.1038/nature16973

115. Park, S.H., Y. Kukushkin, R. Gupta, T. Chen, A. Konagai, M.S. Hipp, M. Hayer-Hartl, and F.U. Hartl, *PolyQ proteins interfere with nuclear degradation of cytosolic proteins by sequestering the Sis1p chaperone.* Cell, 2013. **154**(1): p. 134-45.10.1016/j.cell.2013.06.003

116. Mannini, B., R. Cascella, M. Zampagni, M. van Waarde-Verhagen, S. Meehan, C. Roodveldt, S. Campioni, M. Boninsegna, A. Penco, A. Relini, H.H. Kampinga, C.M. Dobson, M.R. Wilson, C. Cecchi, and F. Chiti, *Molecular mechanisms used by chaperones to reduce the toxicity of aberrant protein oligomers.* Proceedings of the National Academy of Sciences, 2012. **109**(31): p. 12479-12484.10.1073/pnas.1117799109

117. Budworth, H. and C.T. McMurray, *A brief history of triplet repeat diseases*, in *Trinucleotide Repeat Protocols*. 2013, Springer. p. 3-17.

118. Takeuchi, T. and Y. Nagai, *Protein Misfolding and Aggregation as a Therapeutic Target for Polyglutamine Diseases.* Brain Sci, 2017. **7**(10).10.3390/brainsci7100128

119. Doyu, M., G. Sobue, E. Mukai, T. Kachi, T. Yasuda, T. Mitsuma, and A. Takahashi, *Severity of X-linked recessive bulbospinal neuronopathy correlates with size of the tandem CAG repeat in androgen receptor gene.* Annals of neurology, 1992. **32**(5): p. 707-710

120. Duyao, M.P., A.B. Auerbach, A. Ryan, F. Persichetti, G.T. Barnes, S.M. McNeil, P. Ge, J.-P. Vonsattel, J.F. Gusella, and A.L. Joyner, *Inactivation of the mouse Huntington's disease gene homolog Hdh.* Science, 1995. **269**(5222): p. 407-410

121. Jodice, C., P. Malaspina, F. Persichetti, A. Novelletto, M. Spadaro, P. Giunti, C. Morocutti, L. Terrenato, A.E. Harding, and M. Frontali, *Effect of trinucleotide repeat length and parental sex on phenotypic variation in spinocerebellar ataxia I.* American journal of human genetics, 1994. **54**(6): p. 959

122. Ren, P.H., J.E. Lauckner, I. Kachirskaia, J.E. Heuser, R. Melki, and R.R. Kopito, *Cytoplasmic penetration and persistent infection of mammalian cells by polyglutamine aggregates.* Nat Cell Biol, 2009. **11**(2): p. 219-25.10.1038/ncb1830

123. MacDonald, M., C. Ambrose, M. Duyao, R. Myers, C. Lin, L. Srinidhi, G. Barnes, S. Taylor, M. James, and N. Groot, *The Huntington's Disease Collaborative Research Group (1993) A novel gene containing a trinucleotide repeat that is expanded and unstable on Huntington's disease chromosomes.* Cell. **72**(6): p. 971-983

124. Orr, H.T., M.-y. Chung, S. Banfi, T.J. Kwiatkowski, A. Servadio, A.L. Beaudet, A.E. McCall, L.A. Duvick, L.P. Ranum, and H.Y. Zoghbi, *Expansion of an unstable trinucleotide CAG repeat in spinocerebellar ataxia type 1.* Nature genetics, 1993. **4**(3): p. 221-226

125. Pulst, S.M., N. Santos, D. Wang, H. Yang, D. Huynh, L. Velazquez, and K.P. Figueroa, *Spinocerebellar ataxia type 2: polyQ repeat variation in the CACNA1A calcium channel modifies age of onset.* Brain, 2005. **128**(Pt 10): p. 2297-303.10.1093/brain/awh586

126. Kawaguchi, Y., T. Okamoto, M. Taniwaki, M. Aizawa, M. Inoue, S. Katayama, H. Kawakami, S. Nakamura, M. Nishimura, and I. Akiguchi, *CAG expansions in a novel gene for Machado-Joseph disease at chromosome 14q32. 1.* Nature genetics, 1994. **8**(3): p. 221-228

127. Zhuchenko, O., J. Bailey, P. Bonnen, T. Ashizawa, D.W. Stockton, C. Amos, W.B. Dobyns, S. Subramony, H.Y. Zoghbi, and C.C. Lee, *Autosomal dominant cerebellar ataxia (SCA6) associated with small polyglutamine expansions in the α 1A-voltage-dependent calcium channel.* Nature genetics, 1997. **15**(1): p. 62-69

128. Benton, C., R. De Silva, S. Rutledge, S. Bohlega, T. Ashizawa, and H. Zoghbi, *Molecular and clinical studies in SCA-7 define a broad clinical spectrum and the infantile phenotype.* Neurology, 1998. **51**(4): p. 1081-1086

129. David, G., N. Abbas, G. Stevanin, A. Dürr, G. Yvert, G. Cancel, C. Weber, G. Imbert, F. Saudou, and E. Antoniou, *Cloning of the SCA7 gene reveals a highly unstable CAG repeat expansion.* Nature genetics, 1997. **17**(1): p. 65-70

130. Nakamura, K., S.-Y. Jeong, T. Uchihara, M. Anno, K. Nagashima, T. Nagashima, S.-i. Ikeda, S. Tsuji, and I. Kanazawa, *SCA17, a novel autosomal dominant cerebellar ataxia caused by an expanded polyglutamine in TATA-binding protein.* Human molecular genetics, 2001. **10**(14): p. 1441-1448

131. Ueno, S.-i., K. Kondoh, Y. Komure, O. Komure, S. Kuno, J. Kawai, F. Hazama, and A. Sano, *Somatic mosaicism of CAG repeat in dentatorubral-pallidoluysian atrophy (DRPLA).* Human molecular genetics, 1995. **4**(4): p. 663-666

132. Wexler, N.S., A.B. Young, R.E. Tanzi, H. Travers, S. Starosta-Rubinstein, J.B. Penney, S.R. Snodgrass, I. Shoulson, F. Gomez, and M.A.R. Arroyo, *Homozygotes for Huntington's disease.* Nature, 1987. **326**(6109): p. 194-197

133. Myers, R., J. Leavitt, L. Farrer, J. Jagadeesh, H. McFarlane, C. Mastromauro, R. Mark, and J. Gusella, *Homozygote for Huntington disease.* American journal of human genetics, 1989. **45**(4): p. 615

134. DiFiglia, M., E. Sapp, K.O. Chase, S.W. Davies, G.P. Bates, J. Vonsattel, and N. Aronin, *Aggregation of huntingtin in neuronal intranuclear inclusions and dystrophic neurites in brain.* Science, 1997. **277**(5334): p. 1990-1993

135. Ordway, J.M., S. Tallaksen-Greene, C.-A. Gutekunst, E.M. Bernstein, J.A. Cearley, H.W. Wiener, L.S. Dure IV, R. Lindsey, S.M. Hersch, and R.S. Jope, *Ectopically expressed CAG repeats cause intranuclear inclusions and a progressive late onset neurological phenotype in the mouse.* Cell, 1997. **91**(6): p. 753-763

136. Becher, M.W., J.A. Kotzuk, A.H. Sharp, S.W. Davies, G.P. Bates, D.L. Price, and C.A. Ross, *Intranuclear Neuronal Inclusions in Huntington's Disease and Dentatorubral and Pallidoluysian Atrophy: Correlation between the Density of Inclusions andIT15CAG Triplet Repeat Length.* Neurobiology of disease, 1998. **4**(6): p. 387-397

137. Paulson, H., M. Perez, Y. Trottier, J. Trojanowski, S. Subramony, S. Das, P. Vig, J.-L. Mandel, K. Fischbeck, and R. Pittman, *Intranuclear inclusions of expanded polyglutamine protein in spinocerebellar ataxia type 3.* Neuron, 1997. **19**(2): p. 333-344

138. Vonsattel, J.-P., R.H. Myers, T.J. Stevens, R.J. Ferrante, E.D. Bird, and E.P. Richardson, *Neuropathological classification of Huntington's disease.* Journal of Neuropathology & Experimental Neurology, 1985. **44**(6): p. 559-577

139. Dragatsis, I., M.S. Levine, and S. Zeitlin, *Inactivation of Hdh in the brain and testis results in progressive neurodegeneration and sterility in mice.* Nature genetics, 2000. **26**(3): p. 300-306

140. Arbizu, T., J. Santamaría, J. Gomez, A. Quílez, and J.P. Serra, *A family with adult spinal and bulbar muscular atrophy, X-linked inheritance and associated testicular failure.* Journal of the neurological sciences, 1983. **59**(3): p. 371-382

141. Kratter, I.H. and S. Finkbeiner, *PolyQ disease: too many Qs, too much function?* Neuron, 2010. **67**(6): p. 897-9.10.1016/j.neuron.2010.09.012

142. Yu, Z., N. Dadgar, M. Albertelli, A. Scheller, R.L. Albin, D.M. Robins, and A.P. Lieberman, *Abnormalities of germ cell maturation and sertoli cell cytoskeleton in androgen receptor 113 CAG knock-in mice reveal toxic effects of the mutant protein.* Am J Pathol, 2006. **168**(1): p. 195-204.10.2353/ajpath.2006.050619

143. Gutekunst, C.-A., S.-H. Li, H. Yi, J.S. Mulroy, S. Kuemmerle, R. Jones, D. Rye, R.J. Ferrante, S.M. Hersch, and X.-J. Li, *Nuclear and neuropil aggregates in Huntington's disease: relationship to neuropathology.* Journal of Neuroscience, 1999. **19**(7): p. 2522-2534

144. Kuemmerle, S., C.A. Gutekunst, A.M. Klein, X.J. Li, S.H. Li, M.F. Beal, S.M. Hersch, and R.J. Ferrante, *Huntingtin aggregates may not predict neuronal death in Huntington's disease.* Annals of neurology, 1999. **46**(6): p. 842-849

145. Huynh, D.P., K. Figueroa, N. Hoang, and S.-M. Pulst, *Nuclear localization or inclusion body formation of ataxin-2 are not necessary for SCA2 pathogenesis in mouse or human.* Nature genetics, 2000. **26**(1): p. 44

146. Arrasate, M., S. Mitra, E.S. Schweitzer, M.R. Segal, and S. Finkbeiner, *Inclusion body formation reduces levels of mutant huntingtin and the risk of neuronal death.* nature, 2004. **431**(7010): p. 805-810

147. Leitman, J., F. Ulrich Hartl, and G.Z. Lederkremer, *Soluble forms of polyQ-expanded huntingtin rather than large aggregates cause endoplasmic reticulum stress.* Nat Commun, 2013. **4**: p. 2753.10.1038/ncomms3753

148. Jiang, Y., S.R. Chadwick, and P. Lajoie, *Endoplasmic reticulum stress: the cause and solution to Huntington's disease?* Brain research, 2016. **1648**: p. 650-657

149. Ueda, M., S. Li, M. Itoh, M.-x. Wang, M. Hayakawa, S. Islam, K. Nakagawa, H. Chen, and T. Nakagawa, *Expanded polyglutamine embedded in the endoplasmic reticulum causes membrane distortion and coincides with Bax insertion.* Biochemical and biophysical research communications, 2016. **474**(2): p. 259-263

150. Berger, T.R., H.L. Montie, P. Jain, J. Legleiter, and D.E. Merry, *Identification of novel polyglutamine-expanded aggregation species in spinal and bulbar muscular atrophy.* Brain Res, 2015. **1628**(Pt B): p. 254-264.10.1016/j.brainres.2015.09.033

151. Chen-Plotkin, A.S., G. Sadri-Vakili, G.J. Yohrling, M.W. Braveman, C.L. Benn, K.E. Glajch, D.P. DiRocco, L.A. Farrell, D. Krainc, and S. Gines, *Decreased association of the transcription factor Sp1 with genes downregulated in Huntington's disease.* Neurobiology of disease, 2006. **22**(2): p. 233-241

152. Benn, C.L., T. Sun, G. Sadri-Vakili, K.N. McFarland, D.P. DiRocco, G.J. Yohrling, T.W. Clark, B. Bouzou, and J.H. Cha, *Huntingtin modulates transcription, occupies gene promoters in vivo, and binds directly to DNA in a polyglutamine-dependent manner.* J Neurosci, 2008. **28**(42): p. 10720-33.10.1523/JNEUROSCI.2126-08.2008

153. Illuzzi, J., S. Yerkes, H. Parekh-Olmedo, and E.B. Kmiec, *DNA breakage and induction of DNA damage response proteins precede the appearance of visible mutant huntingtin aggregates.* J Neurosci Res, 2009. **87**(3): p. 733-47.10.1002/jnr.21881

154. Bence, N.F., R.M. Sampat, and R.R. Kopito, *Impairment of the ubiquitin-proteasome system by protein aggregation.* Science, 2001. **292**(5521): p. 1552-1555

155. Gidalevitz, T., A. Ben-Zvi, K.H. Ho, H.R. Brignull, and R.I. Morimoto, *Progressive disruption of cellular protein folding in models of polyglutamine diseases.* Science, 2006. **311**(5766): p. 1471-1474

156. Harjes, P. and E.E. Wanker, *The hunt for huntingtin function: interaction partners tell many different stories.* Trends in Biochemical Sciences, 2003. **28**(8): p. 425-433.10.1016/s0968-0004(03)00168-3

157. Burke, K.A., K.J. Kauffman, C.S. Umbaugh, S.L. Frey, and J. Legleiter, *The interaction of polyglutamine peptides with lipid membranes is regulated by flanking sequences associated with huntingtin.* J Biol Chem, 2013. **288**(21): p. 14993-5005.10.1074/jbc.M112.446237

158. Gao, X., W.A.t. Campbell, M. Chaibva, P. Jain, A.E. Leslie, S.L. Frey, and J. Legleiter, *Cholesterol Modifies Huntingtin Binding to, Disruption of, and Aggregation on Lipid Membranes.* Biochemistry, 2016. **55**(1): p. 92-102.10.1021/acs.biochem.5b00900

159. Costa, V., M. Giacomello, R. Hudec, R. Lopreiato, G. Ermak, D. Lim, W. Malorni, K.J. Davies, E. Carafoli, and L. Scorrano, *Mitochondrial fission and cristae disruption increase the response of cell models of Huntington's disease to apoptotic stimuli.* EMBO Mol Med, 2010. **2**(12): p. 490-503.10.1002/emmm.201000102

160. Enard, W., S. Gehre, K. Hammerschmidt, S.M. Hölter, T. Blass, M. Somel, M.K. Brückner, C. Schreiweis, C. Winter, and R. Sohr, *A humanized version of Foxp2 affects cortico-basal ganglia circuits in mice.* Cell, 2009. **137**(5): p. 961-971

161. Slow, E.J., J. van Raamsdonk, D. Rogers, S.H. Coleman, R.K. Graham, Y. Deng, R. Oh, N. Bissada, S.M. Hossain, Y.Z. Yang, X.J. Li, E.M. Simpson, C.A. Gutekunst, B.R. Leavitt, and M.R. Hayden, *Selective striatal neuronal loss in a YAC128 mouse model of Huntington disease.* Hum Mol Genet, 2003. **12**(13): p. 1555-67.10.1093/hmg/ddg169

162. Haaga, J., C.N. Buckles, and J.D. Gunton, *Molecular Dynamics Study of Early Stage Kinetics of Polyglutamine Aggregation.* Biophysical Journal, 2017. **112**(3).10.1016/j.bpj.2016.11.2763

163. Heiser, V., E. Scherzinger, A. Boeddrich, E. Nordhoff, R. Lurz, N. Schugardt, H. Lehrach, and E.E. Wanker, *Inhibition of huntingtin fibrillogenesis by specific antibodies and small molecules: implications for Huntington's disease therapy.* Proceedings of the National Academy of Sciences, 2000. **97**(12): p. 6739-6744

164. Lecerf, J.-M., T.L. Shirley, Q. Zhu, A. Kazantsev, P. Amersdorfer, D.E. Housman, A. Messer, and J.S. Huston, *Human single-chain Fv intrabodies counteract in situ huntingtin aggregation in cellular models of Huntington's disease.* Proceedings of the National Academy of Sciences, 2001. **98**(8): p. 4764-4769

165. Khoshnan, A., J. Ko, and P.H. Patterson, *Effects of intracellular expression of anti-huntingtin antibodies of various specificities on mutant huntingtin aggregation and toxicity.* Proceedings of the National Academy of Sciences, 2002. **99**(2): p. 1002-1007

166. Colby, D.W., Y. Chu, J.P. Cassady, M. Duennwald, H. Zazulak, J.M. Webster, A. Messer, S. Lindquist, V.M. Ingram, and K.D. Wittrup, *Potent inhibition of huntingtin aggregation and cytotoxicity by a disulfide bond-free single-domain intracellular antibody.* Proceedings of the National Academy of Sciences, 2004. **101**(51): p. 17616-17621

167. Wolfgang, W.J., T.W. Miller, J.M. Webster, J.S. Huston, L.M. Thompson, J.L. Marsh, and A. Messer, *Suppression of Huntington's disease pathology in Drosophila by human single-chain Fv antibodies.* Proceedings of the National Academy of Sciences, 2005. **102**(32): p. 11563-11568

168. Wang, C.E., H. Zhou, J.R. McGuire, V. Cerullo, B. Lee, S.H. Li, and X.J. Li, *Suppression of neuropil aggregates and neurological symptoms by an intracellular antibody implicates the cytoplasmic toxicity of mutant huntingtin.* J Cell Biol, 2008. **181**(5): p. 803-16.10.1083/jcb.200710158

169. Hockly, E., J. Tse, A.L. Barker, D.L. Moolman, J.L. Beunard, A.P. Revington, K. Holt, S. Sunshine, H. Moffitt, K. Sathasivam, B. Woodman, E.E. Wanker, P.A. Lowden, and G.P. Bates, *Evaluation of the benzothiazole aggregation inhibitors riluzole and PGL-135 as therapeutics for Huntington's disease.* Neurobiol Dis, 2006. **21**(1): p. 228-36.10.1016/j.nbd.2005.07.007

170. Sanchez, I., C. Mahlke, and J. Yuan, *Pivotal role of oligomerization in expanded polyglutamine neurodegenerative disorders.* Nature, 2003. **421**(6921): p. 373-379

171. Bodner, R.A., T.F. Outeiro, S. Altmann, M.M. Maxwell, S.H. Cho, B.T. Hyman, P.J. McLean, A.B. Young, D.E. Housman, and A.G. Kazantsev, *Pharmacological promotion of inclusion formation: a therapeutic approach for Huntington's and Parkinson's diseases.* Proceedings of the National Academy of Sciences, 2006. **103**(11): p. 4246-4251

172. Ehrnhoefer, D.E., M. Duennwald, P. Markovic, J.L. Wacker, S. Engemann, M. Roark, J. Legleiter, J.L. Marsh, L.M. Thompson, S. Lindquist, P.J. Muchowski, and E.E. Wanker, *Green tea (-)-epigallocatechin-gallate modulates early events in huntingtin misfolding and reduces toxicity in Huntington's disease models.* Hum Mol Genet, 2006. **15**(18): p. 2743-51.10.1093/hmg/ddl210

173. Bonanomi, M., A. Natalello, C. Visentin, V. Pastori, A. Penco, G. Cornelli, G. Colombo, M.G. Malabarba, S.M. Doglia, and A. Relini, *Epigallocatechin-3-gallate and tetracycline differently affect ataxin-3 fibrillogenesis and reduce toxicity in spinocerebellar ataxia type 3 model.* Human molecular genetics, 2014. **23**(24): p. 6542-6552

174. Visentin, C., F. Pellistri, A. Natalello, J. Vertemara, M. Bonanomi, E. Gatta, A. Penco, A. Relini, L. De Gioia, C. Airoldi, M.E. Regonesi, and P. Tortora, *Epigallocatechin-3-gallate and related phenol compounds redirect the amyloidogenic aggregation pathway of ataxin-3 towards non-toxic aggregates and prevent toxicity in neural cells and Caenorhabditis elegans animal model.* Hum Mol Genet, 2017. **26**(17): p. 3271-3284.10.1093/hmg/ddx211

175. Wong, H.K., P.O. Bauer, M. Kurosawa, A. Goswami, C. Washizu, Y. Machida, A. Tosaki, M. Yamada, T. Knopfel, T. Nakamura, and N. Nukina, *Blocking acid-sensing ion channel 1 alleviates Huntington's disease pathology via an ubiquitin-proteasome system-dependent mechanism.* Hum Mol Genet, 2008. **17**(20): p. 3223-35.10.1093/hmg/ddn218

176. Bauer, P.O., H.K. Wong, F. Oyama, A. Goswami, M. Okuno, Y. Kino, H. Miyazaki, and N. Nukina, *Inhibition of Rho kinases enhances the degradation of mutant huntingtin.* J Biol Chem, 2009. **284**(19): p. 13153-64.10.1074/jbc.M809229200

177. Saitoh, Y., N. Fujikake, Y. Okamoto, H.A. Popiel, Y. Hatanaka, M. Ueyama, M. Suzuki, S. Gaumer, M. Murata, and K. Wada, *p62 plays a protective role in the autophagic degradation of polyglutamine protein oligomers in polyglutamine disease model flies.* Journal of Biological Chemistry, 2015. **290**(3): p. 1442-1453

178. Sittler, A., R. Lurz, G. Lueder, J. Priller, M.K. Hayer-Hartl, F.U. Hartl, H. Lehrach, and E.E. Wanker, *Geldanamycin activates a heat shock response and inhibits huntingtin aggregation in a cell culture model of Huntington's disease.* Human molecular genetics, 2001. **10**(12): p. 1307-1315

179. Hay, D.G., K. Sathasivam, S. Tobaben, B. Stahl, M. Marber, R. Mestril, A. Mahal, D.L. Smith, B. Woodman, and G.P. Bates, *Progressive decrease in chaperone protein levels in a mouse model of Huntington's disease and induction of stress proteins as a therapeutic approach.* Hum Mol Genet, 2004. **13**(13): p. 1389-405.10.1093/hmg/ddh144

180. Kumar, R., *Role of androgen receptor polyQ chain elongation in Kennedy's disease and use of natural osmolytes as potential therapeutic targets.* IUBMB life, 2012. **64**(11): p. 879-884

181. Tanaka, M., Y. Machida, S. Niu, T. Ikeda, N.R. Jana, H. Doi, M. Kurosawa, M. Nekooki, and N. Nukina, *Trehalose alleviates polyglutamine-mediated pathology in a mouse model of Huntington disease.* Nat Med, 2004. **10**(2): p. 148-54.10.1038/nm985

182. Katsuno, M., H. Adachi, M. Doyu, M. Minamiyama, C. Sang, Y. Kobayashi, A. Inukai, and G. Sobue, *Leuprorelin rescues polyglutamine-dependent phenotypes in a transgenic mouse model of spinal and bulbar muscular atrophy.* Nature medicine, 2003. **9**(6): p. 768-773

183. Katsuno, M., H. Banno, K. Suzuki, Y. Takeuchi, M. Kawashima, I. Yabe, H. Sasaki, M. Aoki, M. Morita, I. Nakano, K. Kanai, S. Ito, K. Ishikawa, H. Mizusawa, T. Yamamoto, S. Tsuji, K. Hasegawa, T. Shimohata, M. Nishizawa, H. Miyajima, F. Kanda, Y. Watanabe, K. Nakashima, A. Tsujino, T. Yamashita, M. Uchino, Y. Fujimoto, F. Tanaka, and G. Sobue, *Efficacy and safety of leuprorelin in patients with spinal and bulbar muscular atrophy (JASMITT study): a multicentre, randomised, double-blind, placebo-controlled trial.* The Lancet Neurology, 2010. **9**(9): p. 875-884.10.1016/s1474-4422(10)70182-4

184. Hashizume, A., M. Katsuno, K. Suzuki, A. Hirakawa, Y. Hijikata, S. Yamada, T. Inagaki, H. Banno, and G. Sobue, *Long-term treatment with leuprorelin for spinal and bulbar muscular atrophy: natural history-controlled study.* Journal of Neurology, Neurosurgery & Psychiatry, 2017. **88**(12): p. 1026-1032.10.1136/jnnp-2017-316015

185. Keiser, M.S., H.B. Kordasiewicz, and J.L. McBride, *Gene suppression strategies for dominantly inherited neurodegenerative diseases: lessons from Huntington's disease and spinocerebellar ataxia.* Hum Mol Genet, 2016. **25**(R1): p. R53-64.10.1093/hmg/ddv442

186. Fiszer, A. and W.J. Krzyzosiak, *Oligonucleotide-based strategies to combat polyglutamine diseases.* Nucleic Acids Res, 2014. **42**(11): p. 6787-810.10.1093/nar/gku385

187. Scoles, D.R., P. Meera, M.D. Schneider, S. Paul, W. Dansithong, K.P. Figueroa, G. Hung, F. Rigo, C.F. Bennett, T.S. Otis, and S.M. Pulst, *Antisense oligonucleotide therapy for spinocerebellar ataxia type 2.* Nature, 2017. **544**(7650): p. 362-366.10.1038/nature22044

188. Sahashi, K., M. Katsuno, G. Hung, H. Adachi, N. Kondo, H. Nakatsuji, G. Tohnai, M. Iida, C.F. Bennett, and G. Sobue, *Silencing neuronal mutant androgen receptor in a mouse model of spinal and bulbar muscular atrophy.* Human molecular genetics, 2015. **24**(21): p. 5985-5994

189. Kordasiewicz, H.B., L.M. Stanek, E.V. Wancewicz, C. Mazur, M.M. McAlonis, K.A. Pytel, J.W. Artates, A. Weiss, S.H. Cheng, L.S. Shihabuddin, G. Hung, C.F. Bennett, and D.W. Cleveland, *Sustained therapeutic reversal of Huntington's disease by transient repression of huntingtin synthesis.* Neuron, 2012. **74**(6): p. 1031-44.10.1016/j.neuron.2012.05.009

190. Lieberman, A.P., Z. Yu, S. Murray, R. Peralta, A. Low, S. Guo, X.X. Yu, C.J. Cortes, C.F. Bennett, and B.P. Monia, *Peripheral androgen receptor gene suppression rescues disease in mouse models of spinal and bulbar muscular atrophy.* Cell reports, 2014. **7**(3): p. 774-784

191. Drouet, V., M. Ruiz, D. Zala, M. Feyeux, G. Auregan, K. Cambon, L. Troquier, J. Carpentier, S. Aubert, N. Merienne, F. Bourgois-Rocha, R. Hassig, M. Rey, N. Dufour, F. Saudou, A.L. Perrier, P. Hantraye, and N. Deglon, *Allele-specific silencing of mutant huntingtin in rodent brain and human stem cells.* PLoS One, 2014. **9**(6): p. e99341.10.1371/journal.pone.0099341

192. Nobrega, C., I. Nascimento-Ferreira, I. Onofre, D. Albuquerque, N. Deglon, and L.P. de Almeida, *RNA interference mitigates motor and neuropathological deficits in a cerebellar mouse model of Machado-Joseph disease.* PLoS One, 2014. **9**(8): p. e100086.10.1371/journal.pone.0100086

193. Rue, L., M. Banez-Coronel, J. Creus-Muncunill, A. Giralt, R. Alcala-Vida, G. Mentxaka, B. Kagerbauer, M.T. Zomeno-Abellan, Z. Aranda, V. Venturi, E. Perez-Navarro, X. Estivill, and E. Marti, *Targeting CAG repeat RNAs reduces Huntington's disease phenotype independently of huntingtin levels.* J Clin Invest, 2016. **126**(11): p. 4319-4330.10.1172/JCI83185

194. Popiel, H.A., T. Takeuchi, H. Fujita, K. Yamamoto, C. Ito, H. Yamane, S. Muramatsu, T. Toda, K. Wada, and Y. Nagai, *Hsp40 gene therapy exerts therapeutic effects on polyglutamine disease mice via a non-cell autonomous mechanism.* PLoS One, 2012. **7**(11): p. e51069.10.1371/journal.pone.0051069

195. Nagai, Y., T. Tucker, H. Ren, D.J. Kenan, B.S. Henderson, J.D. Keene, W.J. Strittmatter, and J.R. Burke, *Inhibition of polyglutamine protein aggregation and cell death by novel peptides identified by phage display screening.* Journal of Biological Chemistry, 2000. **275**(14): p. 10437-10442

196. Takahashi, Y., Y. Okamoto, H.A. Popiel, N. Fujikake, T. Toda, M. Kinjo, and Y. Nagai, *Detection of polyglutamine protein oligomers in cells by fluorescence correlation spectroscopy.* J Biol Chem, 2007. **282**(33): p. 24039-48.10.1074/jbc.M704789200

197. Nagai, Y., T. Inui, H.A. Popiel, N. Fujikake, K. Hasegawa, Y. Urade, Y. Goto, H. Naiki, and T. Toda, *A toxic monomeric conformer of the polyglutamine protein.* Nat Struct Mol Biol, 2007. **14**(4): p. 332-40.10.1038/nsmb1215

198. Nagai, Y., N. Fujikake, K. Ohno, H. Higashiyama, H.A. Popiel, J. Rahadian, M. Yamaguchi, W.J. Strittmatter, J.R. Burke, and T. Toda, *Prevention of polyglutamine oligomerization and neurodegeneration by the peptide inhibitor QBP1 in Drosophila.* Hum Mol Genet, 2003. **12**(11): p. 1253-9.10.1093/hmg/ddg144

199. Popiel, H.A., Y. Nagai, N. Fujikake, and T. Toda, *Delivery of the aggregate inhibitor peptide QBP1 into the mouse brain using PTDs and its therapeutic effect on polyglutamine disease mice.* Neurosci Lett, 2009. **449**(2): p. 87-92.10.1016/j.neulet.2008.06.015

200. Chen, X., J. Wu, Y. Luo, X. Liang, C. Supnet, M.W. Kim, G.P. Lotz, G. Yang, P.J. Muchowski, T. Kodadek, and I. Bezprozvanny, *Expanded polyglutamine-binding peptoid as a novel therapeutic agent for treatment of Huntington's disease.* Chem Biol, 2011. **18**(9): p. 1113-25.10.1016/j.chembiol.2011.06.010

201. Schumacher, T.N., L.M. Mayr, D.L. Minor, M.A. Milhollen, M.W. Burgess, and P.S. Kim, *Identification of D-peptide ligands through mirror-image phage display.* Science, 1996. **271**(5257): p. 1854-1857

202. Rakonjac, J., N.J. Bennett, J. Spagnuolo, D. Gagic, and M. Russel, *Filamentous bacteriophage: biology, phage display and nanotechnology applications.* Current issues in molecular biology, 2011. **13**(2): p. 51

203. Hoffmann-Berling, H., D.A. Marvin, and H. Dürwald, *Ein fädiger DNS-Phage (fd) und ein sphärischer RNS-Phage (fr), wirtsspezifisch für männliche Stämme von E. coli.* Zeitschrift für Naturforschung B, 1963. **18**(11): p. 876-883

204. Hofschneider, P.H., *Untersuchungen über „kleine "E. coli K 12 Bakteriophagen.* Zeitschrift für Naturforschung B, 1963. **18**(3): p. 203-210

205. Loeb, T., *Isolation of a bacteriophage specific for the F+ and Hfr mating types of Escherichia coli K-12.* Science, 1960. **131**(3404): p. 932-933

206. Hamzeh-Mivehroud, M., A.A. Alizadeh, M.B. Morris, W.B. Church, and S. Dastmalchi, *Phage display as a technology delivering on the promise of peptide drug discovery.* Drug Discov Today, 2013. **18**(23-24): p. 1144-57.10.1016/j.drudis.2013.09.001

207. Pande, J., M.M. Szewczyk, and A.K. Grover, *Phage display: concept, innovations, applications and future.* Biotechnology advances, 2010. **28**(6): p. 849-858

208. Bratkovic, T., *Progress in phage display: evolution of the technique and its application.* Cell Mol Life Sci, 2010. **67**(5): p. 749-67.10.1007/s00018-009-0192-2

209. Specthrie, L., E. Bullitt, K. Horiuchi, P. Model, M. Russel, and L. Makowski, *Construction of a microphage variant of filamentous bacteriophage.* Journal of molecular biology, 1992. **228**(3): p. 720-724

210. Smith, G.P. and V.A. Petrenko, *Phage display.* Chemical reviews, 1997. **97**(2): p. 391-410

211. Sidhu, S.S., *Phage display in pharmaceutical biotechnology.* Current opinion in biotechnology, 2000. **11**(6): p. 610-616

212. Eldridge, G.M. and G.A. Weiss, *Identifying reactive peptides from phage-displayed libraries*, in *Peptide Libraries*. 2015, Springer. p. 189-199.

213. Bakhshinejad, B., H.M. Zade, H.S. Shekarabi, and S. Neman, *Phage display biopanning and isolation of target-unrelated peptides: in search of nonspecific binders hidden in a combinatorial library.* Amino Acids, 2016. **48**(12): p. 2699-2716.10.1007/s00726-016-2329-6

214. Even-Desrumeaux, K. and P. Chames, *Phage display and selections on cells*, in *Antibody Engineering*. 2012, Springer. p. 225-235.

215. Hyvönen, M. and P. Laakkonen, *Identification and characterization of homing peptides using in vivo peptide phage display*, in *Cell-Penetrating Peptides*. 2015, Springer. p. 205-222.

216. Funke, S.A. and D. Willbold, *Mirror image phage display--a method to generate D-peptide ligands for use in diagnostic or therapeutical applications.* Mol Biosyst, 2009. **5**(8): p. 783-6.10.1039/b904138a

217. Wiesehan, K. and D. Willbold, *Mirror-image phage display: aiming at the mirror.* Chembiochem, 2003. **4**(9): p. 811-5.10.1002/cbic.200300570

218. Krüger, A., *Selektion von D-Peptidliganden des humanen Androgenrezeptorszur Behandlung der Spinobulbären Muskelatrophie Typ Kennedy.* 2019, Heinrich-Heine-Universität Düsseldorf: Düsseldorf. p. 91

219. Chen, S. and R. Wetzel, *Solubilization and disaggregation of polyglutamine peptides.* Protein Sci, 2001. **10**(4): p. 887-91.10.1110/ps.42301

220. Hironobu Naiki, K.H., Masanori Hosokawa, and Toshio Takeda, *Fluorometric Determination of Amyloid Fibrils in vitro Using the Fluorescent Dye, Thioflavine T.* Analytical biochemistry, 1989. **177**: p. 244-249

221. Kolkwitz, P.E., J. Mohrlüder, and D. Willbold, *Inhibition of Polyglutamine Misfolding with D-Enantiomeric Peptides Identified by Mirror Image Phage Display Selection.* Biomolecules, 2022. **12**(2).10.3390/biom12020157

222. Liedberg, B., Nylander, C., & Lundström, I., *Biosensing with surface plasmon resonance—how it all started.* Biosensors and Bioelectronics,, 1995. **10(8),**: p. i-ix.

223. Stenberg, E., Persson, B., Roos, H., & Urbaniczky, C., *Quantitative determination of surface concentration of protein with surface plasmon resonance using radiolabeled proteins.* Journal of colloid and interface science,, 1991. **143(2),**: p. 513-526.

224. Pain, R., *Determining the CD spectrum of a protein. .* Current protocols in protein science,, 2004. **38(1),**: p. 7-6.

225. Santur, K., E. Reinartz, Y. Lien, M. Tusche, T. Altendorf, M. Sevenich, G. Tamguney, J. Mohrluder, and D. Willbold, *Ligand-Induced Stabilization of the Native Human Superoxide Dismutase 1.* ACS Chem Neurosci, 2021. **12**(13): p. 2520-2528.10.1021/acschemneuro.1c00253

226. Krejci, A., T.R. Hupp, M. Lexa, B. Vojtesek, and P. Muller, *Hammock: a hidden Markov model-based peptide clustering algorithm to identify protein-interaction consensus motifs in large datasets.* Bioinformatics, 2016. **32**(1): p. 9-16.10.1093/bioinformatics/btv522

227. De Genst, E., D.Y. Chirgadze, F.A. Klein, D.C. Butler, D. Matak-Vinkovic, Y. Trottier, J.S. Huston, A. Messer, and C.M. Dobson, *Structure of a single-chain Fv bound to the 17 N-terminal residues of huntingtin provides insights into pathogenic amyloid formation and suppression.* J Mol Biol, 2015. **427**(12): p. 2166-78.10.1016/j.jmb.2015.03.021

228. Minakawa, E.N. and Y. Nagai, *Protein Aggregation Inhibitors as Disease-Modifying Therapies for Polyglutamine Diseases.* Front Neurosci, 2021. **15**: p. 621996.10.3389/fnins.2021.621996

229. Simon, R.J., Kania, R. S., Zuckermann, R. N., Huebner, V. D., Jewell, D. A., Banville, S., ... & Marlowe, C. K., *Peptoids: a modular approach to drug discovery.* Proceedings of the National Academy of Sciences, 1992. **89(20)**: p. 9367-9371

230. Elfgen, A., *Untersuchungen zur Metabolisierung therapeutisch aktiver D-Peptide.* Diss., 2019.

231. He, R.Y., X.M. Lai, C.S. Sun, T.S. Kung, J.Y. Hong, Y.S. Jheng, W.N. Liao, J.K. Chen, Y.F. Liao, P.H. Tu, and J.J. Huang, *Nanoscopic Insights of Amphiphilic Peptide against the Oligomer Assembly Process to Treat Huntington's Disease.* Adv Sci (Weinh), 2020. **7**(2): p. 1901165.10.1002/advs.201901165

232. Cortez, L. and V. Sim, *The therapeutic potential of chemical chaperones in protein folding diseases.* Prion, 2014. **8**(2).10.4161/pri.28938

233. Minakawa, E.N., H.A. Popiel, M. Tada, T. Takahashi, H. Yamane, Y. Saitoh, Y. Takahashi, D. Ozawa, A. Takeda, T. Takeuchi, Y. Okamoto, K. Yamamoto, M. Suzuki, H. Fujita, C. Ito, H. Yagihara, Y. Saito, K. Watase, H. Adachi, M. Katsuno, H. Mochizuki, K. Shiraki, G. Sobue, T. Toda, K. Wada, O. Onodera, and Y. Nagai, *Arginine is a disease modifier for polyQ disease models that stabilizes polyQ protein conformation.* Brain, 2020. **143**(6): p. 1811-1825.10.1093/brain/awaa115

234.   Tabrizi, S.J., B.R. Leavitt, G.B. Landwehrmeyer, E.J. Wild, C. Saft, R.A. Barker, N.F. Blair, D. Craufurd, J. Priller, H. Rickards, A. Rosser, H.B. Kordasiewicz, C. Czech, E.E. Swayze, D.A. Norris, T. Baumann, I. Gerlach, S.A. Schobel, E. Paz, A.V. Smith, C.F. Bennett, R.M. Lane, and I.-H.S.S.T. Phase 1-2a, *Targeting Huntingtin Expression in Patients with Huntington's Disease.* N Engl J Med, 2019. **380**(24): p. 2307-2316.10.1056/NEJMoa1900907

APPENDIX

Publication: Inhibition of Polyglutamine Misfolding with D-Enantiomeric Peptides Identified by Mirror Image Phage Display Selection [221]

My contribution:

- execution of experiments
- evaluation of experiments
- data analysis
- visualization of results
- writing original draft

CONFERENCE PRESENTATIONS AND POSTERS

<u>Pauline Elisabeth Kolkwitz</u>, Jeannine Mohrlüder, Dieter Willbold „Stabilization of monomeric polyglutamine proteins by all-D-enantiomeric peptide ligands as therapeutic strategy for polyglutamine diseases" **conference prion 2018** (Santiago di compostella 05.2018) poster presentation

Pauline Elisabeth Kolkwitz, „ Characterisation of D-enantiomeric peptide ligands of polyglutamine-proteins with therapeutic potential for polyglutamine misfolding diseases" **user meeting dynamic biosensors** (Munich 06.2018) lecture

<u>Pauline Elisabeth Kolkwitz</u>, Jeannine Mohrlüder, Dieter Willbold „Selection and characterization of D-enantiomeric peptide ligands for polyglutamine proteins with therapeutic potential for polyglutamine misfolding diseases" **2021 Düsseldorf-Jülich Symposium on Neurodegenerative Diseases** (Düsseldorf 10.2021) poster

Verwendung von D-enantiomeren Peptidliganden von monomeren polyQ-haltigen Proteinen für die Therapie verschiedener Polyglutamin-Erkrankungen

Pauline Elisabeth Kolkwitz, Jeannine Mohrlüder, Dieter Willbold

Anmeldung eingegangen: 18.01.2022

Amtliches Aktenzeichen: 10 2022 101 090.2

90

Eidesstattliche Erklärung

Ich versichere an Eides Statt, dass die Dissertation von mir selbständig und ohne unzulässige fremde Hilfe unter Beachtung der „Grundsätze zur Sicherung guter wissenschaftlicher Praxis an der Heinrich-Heine-Universität Düsseldorf " erstellt worden ist.

Ferner erkläre ich, dass ich in keinem anderen Dissertationsverfahren mit oder ohne Erfolg versucht habe, diese Dissertation einzureichen.

_____   _____

Ort, Datum   Pauline Elisabeth Kolkwitz